Cape Peninsula
University of Technology

MODELLING AND CONTROL OF HYBRID PHOTOVOLTAIC AND MICRO-HYDRO SYSTEM

By

MOTEANE THABO MELAMU

Thesis submitted in partial fulfilment of the requirements for the degree of:

Master of Engineering in Energy (MEng Energy)

Department of Electrical, Electronic, and Computer Engineering

Faculty of Engineering and the Built Environment

Cape Peninsula University of Technology

Supervisor: Prof. Khaled Aboalez

Bellville
November 2021

DECLARATION

I, Moteane Thabo Melamu, declare that the contents of this thesis represent my own unaided work, and that the thesis has not previously been submitted for academic examination towards any qualification. Furthermore, it represents my own opinions and not necessarily those of the Cape Peninsula University of Technology.

Signed   **Date**

ABSTRACT

The increase in population growth increased standard of living, and the advancement of technologies has resulted in exponential growth in electrical consumption. Reduction in fossil fuel reserves is therefore diminishing due to the energy demand increase. The combustion of fossil fuels as energy sources leads to pervasive environmental degradation especially the global climate change that is caused by greenhouse gas emissions. As a result, there is an urgency to curb carbon emissions without compromising universal access to modern energy, socio-economic development, employment creation, poverty reduction which are all in pursuit of realizing sustainable development goals. The deficiency in access to energy is linked to a lack of socio-economic development and this is one of the factors that lead to poverty. Globally there are approximately 1.4 billion people who lack access to electricity, 85% reside in rural areas and the majority are in Sub-Saharan Africa.

The power plants utilize fossil fuels and nuclear energy sources which for most of the 20th century was less expensive and in abundance. These are certainly reliable ways of providing energy however they are located closer to the load which implies the rural population is often not connected to the national electricity network. These are some of several reasons why there is an increased interest in a microgrid that utilizes renewable energy sources. However, renewable resources are volatile since they are mostly dependent on weather conditions. To circumvent this, more than one energy source for continuous power flow to meet the load is required. This too requires additional energy storage devices with quick responses to mitigate against disturbances. The inclusion of multitudes of sources requires energy management control for energy flow among the sources to secure reliable and optimal use of the system. The research aims to develop energy management for the system so to maintain power imbalance and mitigate the fluctuation of power that is fed to the load.

The system is designed as a standalone hybrid microgrid system on the Matlab/Simulink environment which comprises of Photovoltaic (PV) array, Lithium-ion (Li-ion) battery storage device Microhydropower (MHP) system. All the sources are supplying the AC load through a three-phase inverter. The DC-DC bidirectional converter interfaces the renewable resources and a battery bank to allow power going in both directions to absorb excess and dispatch power to prevent mismatch due to variation of power from PV array and micro-hydro plant.

The load considered in this research is of 50 remote households amounting to 180kW. The PV account for about 102.2kW and Micro-hydropower contributes around 96.18kW. The weather conditions in terms of irradiance will be considered to mimic real-life situations for the analysis of the power system. The mathematical modeling of components energy management algorithms to prioritize energy demand with regards to the demand is implemented.

The system provides quick response time where PV power transient time is 15ms to stabilize and the MHP takes 0.8s to reach a steady state. This is because of the high mechanical torque on turbine blades due to water kinetic energy that impacts the blades. The fuzzy logic control provides smooth system operation as the energy management system where there is a continuous power flow provided to the load and voltage. This is only true if SOC is neither bigger than SOC_{max}(80%) nor smaller than SOC_{min}(20%). This is to protect the lifespan of the battery. The system provides over 99.4% of accuracy with calculated values compared to the ones generated by Matlab/Simulink. The battery response time to any mismatches is 5ms before it dispatches power or before it can absorb excess power.

Keywords: Energy management, PV system, Micro-hydro system, Battery storage

ACKNOWLEDGEMENTS

DEDICATION

This work is dedicated to my parents, Mrs. 'Marethabile Melamu and my late dad, Mr. Mokhatla Melamu, I am because you sacrificed so much to give me the best. To my sisters Dr. Rethabile, Kefiloe, Rebohile, and my brother Melamu you are the best! My cousins and everyone dear to me this are fruits of your love,encouragement and support.

Table of contents

Table of figures

Tables

Glossary	
AC	Alternating Current
Automatic Voltage Regulator	AVR
DC	Direct Current
DG	Distributed generators
DOD	Depth of Discharge
Li-ion	Lithium ion battery
LV	Low Voltage
PCC	Point of Common Coupling
MHP	Micro hydropower
MPPT	Maximum Power Point Tracker
SOS	State Of Charge
ESS	Energy Storage Systems
SA	South Africa
Wp	Watt power
Hz	Hertz
HRES	Hybrid Renewable Energy System
FC	Fuel Cell
PV	Photovoltaic
P&O	Portubation and Observation
USA	United States of America
FACTS	Flexible AC Transmission Systems
PVC	Polyvinyl Choride
PID	Proportional, Integral and Derivative
SMES	Superconducting Magnetic Energy Storage
CAES	Compressed Air Energy Storage
EMF	Electromotive Force
InCond	Incremental Conductance
Li-ion	Lithium ion battery
PWM	Pulse width modulation
FES	Flywheel Energy Storage
GW	Gigawatt
I_{ph}	Photovoltaic current
R_{sh}	Shunt resistance
V_{mp}	Voltage at maximum power point
VOC	Open Circiut Voltage
RT	Real Time

1 CHAPTER ONE: INTRODUCTION

1.1 Background

The rapid growth in the world's population has resulted in a subsequent rise in energy demand. The global energy demand is projected to grow by 40% by 2035, in particular, oil demand will increase by 0.8% annually(García Vera et al., 2019). Moreover, technological advances made by nations and their people have resulted in an increase in electricity consumption to levels in which may not be manageable(Tuballa & Abundo, 2016). This is the case in Southern Africa, which has experienced an increase in economic growth due to the natural resource-based commodities and facilitated good governance. The Southern African Development Community (SADC) is slowly being industrialized and the standard of living is being improved. As a result, energy demand has increased dramatically. South Africa (SA) is no different as there has been significant growth in the energy sector and this is due to the positive development in the residential, commercial, and industrial sectors. SA gets most of its energy through the combustion of fossil fuels and that accounts for 90% of the total energy produced. The country has had the growth in terms of the generation capacity but there are still major challenges of the high cost of electricity especially during peak periods where prices shoot to almost four times than that of off-peak periods and load shedding due to lack of maintenance(Kusakana, 2018).

To generally address the increased global energy demand and the electricity demand specifically, alternative ways of energy generation, especially from renewable energy (RE) resources are increasingly being sought. RE contributed only 16% to global energy consumption but it can substitute fossil fuels in four specific areas of water and space heating, electricity production, motor fuels, and rural electrification where there is no grid network (Badal et al., 2019). The RE resources also contribute to the reduction of greenhouse gas emissions and improved air quality, and as such, are becoming the most preferred form of electrical energy production, to curb greenhouse emissions from the use of conventional energy resources.

Over 1.6 billion people globally are without access to electricity, the majority of which are in Sub-Sahara Africa. Majority resite in remote villages where power grid expansion is not economically feasible because of dispersion of households, distance from power plants to the load, and the rural settlement terrain which makes it extra challenging. This is despite electrification being the engine that drives both integration and economic growth as energy

security is critical for continued development(Spalding-Fecher et al., 2017; Zanarini & Ragazzini, 2005).

The projected electricity demand, which according to Curley (2014), would double by the year 2050 requires the "rethinking" of the power systems. There is a challenge of aging electrical power system infrastructure that is inefficient and requires a lot of maintenance. To circumvent this, penetration of renewable energy sources is crucial, these oughts to be anchored on their technical and financial feasibility. Despite the advantages, RE power generation is often viewed as unreliable and unable to meet the load. This is because they are highly dependent on weather patterns which fluctuate. To augment these fluctuations, a backup in form of energy storage systems is often required. However, the type of storage employed is dependent on the topology of the area, this storage would be required at unreliable times when there is a mismatch in supply and load. For these reasons, utilization of more than one source of RE energy helps with system stability, reliability, and would decrease generation fluctuations (Amrollahi & Bathaee, 2017).

A hybrid system employing different generating units forms a microgrid. The microgrid that comprises of several RE sources requires a battery bank to improve reliability of the system. The battery bank will determine how long the electric power is being used depending on the state of charge (SOC) and if the battery SOC level drops to a depth of discharge(DOD)(Vosloo & Raji, 2015). Energy storage plays a pivotal role in renewable energy generation due to its intermittent nature. It mitigates against fluctuations of the output and provides reliable and good power quality to the consumer. The life cycle analysis between the battery bank and the combination of the battery bank and pumped storage showed that the combination is less expensive to work with but pumped storage alone has the best economic benefits when compared to the other two scenarios (Mahmoudimehr & Shabani, 2018).

The microgrid (MG) are small-scale grids that enable vast penetration of distributed generation and RE source to the grid or as standalone systems. They contain several energy resources and the customer operates as a single entity and can produce electric and thermal energies simultaneously. Microgrids diversify energy resources and improve system reliability, reduce capital investment, and also reduce the carbon footprint (Mortezapour & Lesani, 2017). The microgrid can have either conventional power generators or renewable energy resources. There has been an increased focus on optimizing the operation and control of the microgrids to have a reduced cost and be stable and this is known as the energy management of microgrids(Nwulu & Xia, 2017).

1.2 Problem Statement

Recent technological advances and the increase in population growth have resulted in the increasing demand for energy which gives rise to greenhouse gas emissions due to the combustion of fossil fuels to meet the load demand (Ghorbani et al., 2017). Energy access helps in the socio-economic development of any country and there is an increase globally in the quest to harness more renewable energy (Kumar & Singal, 2015). In the world, almost 1.6 billion people do not have access to electrical power of which 85% of them are from rural areas and the majority comes from Sub-Saharan Africa. Rural area electrification is a challenge through grid networks because of the high cost of generation, transmission, and distribution, it has a low return on investment for investors due to the high operation and maintenance cost of the grid, voltage loss through long distance transmissions(Longe et al., 2014).

The electrical energy infrastructure concerning transmission and distribution networks is aging and they pose a challenge since the entire system has a centralized common grid control system. The non-renewable energy sources are getting costly, so the integration of renewable energy sources proposes a realistic solution for future generations. The volatile nature of most renewable energy sources makes energy storage systems and control very critical for smooth operation. The problem is, therefore, lack of rural electrification which results to poverty due to lack of economic activities in those areas.

1.3 Aims and objectives

The aim is to model a standalone hybrid system on the Matlab/Simulink environment which comprises Photovoltaic, micro-hydropower plants to supply residents in rural areas with 180kW of power and a lithium-ion battery as back up. The energy management algorithm will be developed to cater for fluctuating weather conditions, allow the switching off and on of the battery depending on power fluctuation and maintain the voltage at required specifications and the state of charge (SOC) to manage the storage system.

Objectives

- To develop an energy management control system that supervises power flow in the hybrid renewable energy sources between the micro-hydro system, solar PV, and battery storage system.

- To include an energy management system that determines when the load switching can be activated, sensing, and control of components through signals. The micro

hydropower system and solar photovoltaic are used to produce electrical energy to cater to the load.

- To include measuring components and control units as part of the energy management system which will help execute necessary functions and have controls the charge share objectives.

- To have a system that can allow the change of different parameters on the Simulink for flexibility of the microgrid and consider future expansion of the load.

- To implement and analyze the hybrid system with varying scenarios to assess the robustness.

1.4 Significance of the research

In the quest to improve rural electrification where the majority lack access to electrical energy which is linked to poverty due to a lack of socio-economic development. If implemented such projects would lead to :

- It will trigger economic activities in rural areas thus mitigating severe poverty by creating jobs,

- Reduce greenhouse emissions caused by combustion of fossil fuel such as wood and cow dung while to cooking and heating. This leads to the reduction in health problems related to smoke inhalation during indoor cooking where biomass is prominent.

1.5 Thesis outline

This thesis will be divided into five chapters:

Chapter 1: Provides an overview of the topic and what the study entails. The chapter also provides the significance and contribution of the research.

Chapter 2: This chapter offers a literature survey on different types of microgrids, microgrid control, factors to consider for microgrids development. Also, it includes types of hydropower plants, types of turbines, and state of hydropower in South Africa (SA), and further deals with the state of photovoltaic contribution in SA and types of energy storage systems (ESS) and their characteristics.

Chapter 3: In this chapter, an extensive literature review on power electronics and power converters, mathematical modelling of PV, and micro-hydropower was carried out.

Chapter 4: Presents the model that is developed comprising PV array, power electronic converter, battery storage systems, and MHP with the hydraulic turbine and governor, and excitation system using Matlab/Simulink.

Chapter 5: Presents the results of the simulation and discussion

Chapter 6: Conclusions are drawn and future work proposed

1.6 Publications

Melamu, M., Khaled A. 2019.Modelling and control of a hybrid PV and Micro-Hydropower System. Cape Peninsula University of Technology annual postgraduate conference, Cape Town: South Africa, 7 November 2019 (Poster).

Melamu M., Orumwense E., Aboalez K. 2020. Simulation of a hybrid PV system and micro-hydropower using Matlab/Simulink.*AIUEproceedings of the 18th Industrial and Commercial Use of Energy Conference 2020.*

Melamu, M., Khaled A. 2021. Energy management system for PV, Micro-Hydropower with battery storage using Matlab/Simulink. Cape Peninsula University of Technology annual postgraduate conference, Cape Town: South Africa, 23 February 2021 (Oral).

Melamu M., Orumwense E., Aboalez K. 2021. Energy management system for PV, Micro-Hydropower with battery storage using Matlab/Simulink.*ARPN Journal of Engineering and Science(Manuscriptsubmitted).*

2 CHAPTER TWO: LITERATURE REVIEW

2.1 Introduction

This chapter explores the level of electrification in SA and the factors that constitute low electrification in remote areas. It further presents the literature survey on microgrids and different types of them. The microgrid concept is also been articulated, first by outlining their benefits, how they are controlled, and operated. Hydropower plants, categorization of different hydropower turbines concerning the available hydraulic head, types of generators, governing system, and excitation systems are reviewed. The state of hydropower in SA has been presented too.

Several energy storage technologies characteristics are presented such as electrical, mechanical, thermochemical, chemical, electrochemical, and thermal. In addition, the photovoltaic principle of operation, state of PV in SA, and different MPPT to help extract maximum power from the photovoltaic systems. Lastly, energy management control of nonconventional power sources and their challenges are discussed. Related work on energy management on renewable energy microgrid has been reviewed

2.2 Electrification in SA

South Africa produces a total of 51309 MW of power through local production of which 46776 MW is through thermal stations while 4533 MW is through renewable energy sources(Rousselot, 2015). The power produced by the combustion of coal is and will be the major contribution for a foreseeable future but that will decrease gradually due to the introduction of renewable energy. A total of 27 power purchase contracts were signed in June 2018 to provide an additional 19400 MW in 2030 of South Africa's Renewable Energy Independent Power Producer Procurement Programme(REIPPPP)(USAID, 2018).

SA is the seventh-largest coal producer globally and 77% of the electricity produced is through coal combustion. This leads to environmental degradation through greenhouse emissions and coal mining which leads to both water and air pollution. National power utility struggling to meet the load by employing load shedding on and off since 2007 on a national level. The load shedding is due to lack of government investment for maintenance of aging power stations, increase in demand by a spike in housing for underprivileged communities. This energy crisis can be mitigated by employing alternative energy sources as ways to provide additional electrical energy to the grid (Jain & Jain, 2017).

In the South African context, urban areas are 80% electrified while only 45% of rural areas are electrified. Several factors are contributing to the low state of electrification in rural areas.

Firstly, is the network costs, secondly, and equally important, is the difficult terrain and the dispersed settlements. The South African government has a goal or policies developed by the Department of Energy to provide universal access to energy and electricity to all citizens. These policies with regards to RE technologies are 1998 White Paper on Energy(WPEP),2003 White Paper on Renewable Energy(WPRE), and 2011 National Development Plan(NDP 2011). As a result of these policies deployment of alternative energy technologies in the least electrified remote areas are gradually being implemented. In rural households, the use of traditional forms of energy such as paraffin, wood, dung, and kerosene is still prominent. These forms of energy hazardous to one's health more to the respiratory system because of carbon dioxide and monoxide produced during combustion (Jain & Jain, 2017; Bonthuys, 2016).

2.3 Microgrids Systems

Microgrid is a combination of controllable loads, distributed generation(DG) units, and energy storage systems(ESS). DG is made up of several prime mover technologies such as microturbines, solar power systems, gas turbines, fuel cells, wind power, and internal combustion engines(Piagi & Lasseter, 2006). DG units in the form of renewable energy have become a very important player in both electrification and reduction of carbon emissions. A single system with power electronic interfaces used can be formed between different energy sources and the load to ensure smooth and efficient power generation of the supply to the load (Moussavou, 2014).

2.3.1 Types of Microgrids

There are three main types of microgrids, which are AC microgrid, DC microgrids, and hybrid microgrids and they differ according to their application in different contexts. These microgrids can be employed in various applications either autonomous or in parallel to the grid. The autonomous system can either be AC or DC distributed networks which can include energy storage. (Mariam et al., 2016)
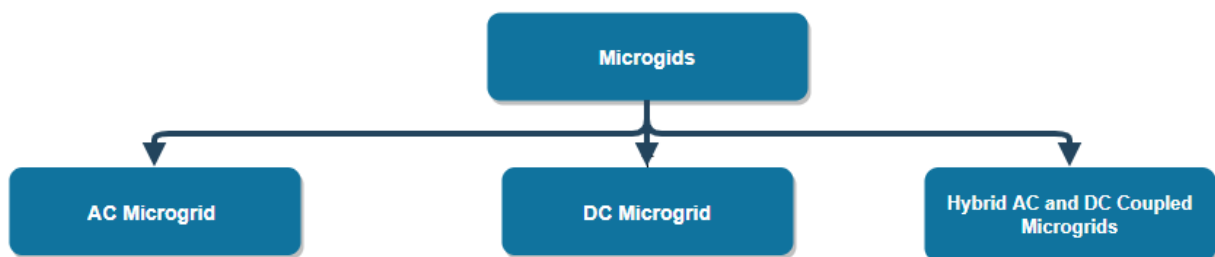
Figure 2-1: Classification of microgrids

2.3.1.1   AC Microgrid

Firstly, AC microgrid is the most preferred microgrid due to the simplicity to connect to the existing infrastructure from the grid without power converters. Secondly, loads need not be reconfigured but distributed generators require power converters to be linked to the AC bus.AC microgrids contribute to the stability of the grid by providing reactive power support for balancing and ancillary services(Moussavou, 2014).

2.3.1.2   DC Microgrid

Although AC microgrids are more preferred than DC microgrids, DC microgrids are beginning to gather momentum since most DG sources produce DC power which also has little power quality challenges. This is also beneficial because most electronic devices like computers, industrial appliances, household appliances employ DC power and this will lead to a reduction in power electronic devices ultimately resulting in a less expensive system. The setback for DC microgrids is the lack of maturity of the system and there is a dearth of protection equipment(Moussavou, 2014).

2.3.1.3   Hybrid Microgrid

Hybrid systems combine both the DC and AC microgrid and they are interfaced by power electronics devices to attain proper operation of the hybrid system. The DC loads can be supplied by the DC source and the same for AC loads for AC source making it a more reliable and flexible system (Moussavou, 2014).

2.4 Microgrid Control

The stabilization of both voltage and frequency forms the core of the problem in the low AC islanded microgrids without the main grid which provides infinite power which helps in maintaining the frequency. In the islanded microgrids the control of voltage and frequency are in a form of local controllers of voltage source inverter which interfaces power sources(Tucci & Ferrari-trecate, 2017). Microgrids operate in two phases, the grid-connected and the standalone where on grid-connected the DG is connected to the point of common coupling (PCC). In the case of the grid-connected, the grid determines the frequency, and the voltage and microgrids either absorb or dispatch power to the main grid. When providing power to the AC load, there must be an inverter to interface as most DG cannot generate 50 Hz and stable voltage. The voltage source inverter(VSI) is one power electronic interface whose control forms the core of the microgrid operation(Tucci & Ferrari-trecate, 2017). The inverter control is executed by two control loops. The voltage and current double closed-loop are employed to maintain the frequency and voltage stability using the PI controller. The outer loop

determines the set values and those set values are used to control voltage in the inner loop due to high bandwidth concerning the outer one. There are several methods used to control the voltage of standalone microgrid and one of the ways is employing conventional stationary frame regulators in the time domain such as Linear-quadratic regulator (LQR). In this operation mode, the islanded microgrid regulates active and reactive power to control the frequency and voltage hence providing power in acceptable specifications(Tu et al., 2018; Vandoorn et al., 2010).

The operation of the microgrid depends on the control scheme of the generators. The employment of the inverter is to control the frequency, voltage of the microgrid, and assist in the accurate power share. The challenge between the standalone and grid-connected is such that the grid-connected inverter cannot provide instantaneous power due to the absence of the large rotor. In standalone microgrids, there is a challenge in load tracking due to the delay in response to signals by microturbines and they are inertialess (Piagi & Lasseter, 2006).

Figure 1.2 illustrates a structure of several DG that form a grid-tied hybrid microgrid. The DG has power electronic interfaces and microgeneration control to provide the required voltage and frequency. The DG's are connected to the PCC with the grid where there is a microgrid system central control that supervises the input generation to required specifications.
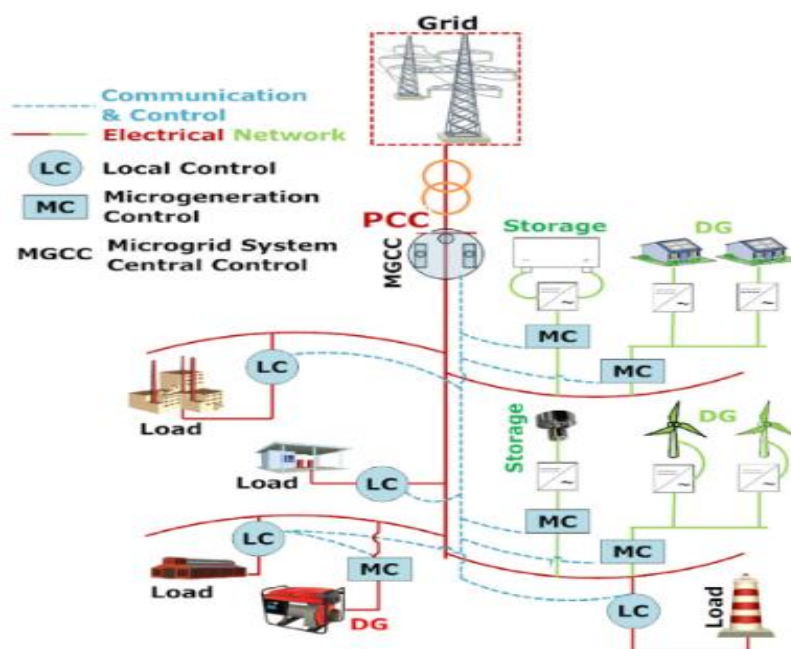
Figure 2-2:Microgrid structure(Mariam et al., 2016)

2.4.1 Factors to consider for microgrids

The primary consideration is to determine if the microgrid energy supply could meet the local loads. The determination of that helps in establishing the configuration of the microgrid, and if it is to be connected to the main grid or it can operate as a standalone system. The microgrid before operation must solve the following issues: (Abu-sharkh et al., 2006).

Precise energy and power balance within the microgrid: This must show how the microgrid will operate on a time scale that ranges from milliseconds to years. The power balance refers to the control over longer periods, consideration of how the supply will meet the demand as time goes by, and what type of storage should be employed.

Grid connection or standalone: the nature topology of the microgrid whether the operator is grid-connected or is operating as the standalone system is an unresolved issue that poses problems technically and on the regulation level.

Energy Storage: Electricity is usually produced when needed but the storage system provides different dimensions in the utility supply and the design criteria. This storage system provides energy security and the size of the storage translates to energy balance.

Demand Management: The difference between supply and demand can be reduced by the management of demand. The shifting of the load helps in energy balance and reduces the size of the storage.

The operational infrastructure of the grid is very complex, it relies on advanced information and communication technologies which makes it pregnable to cyber-attack. The smart grid is made up of seven logical domains: Bulk Generation, Transmission, Distribution, Customer, Markets, service providers, and operations. The first four include two-way power and information flow and This network is very pivotal in information exchange in power infrastructures because cypher attacks mainly come via communication (Wang & Lu, 2013).The last three consist of information collection and power management. The communication network of these domains must be highly distributed and hierarchical.
Microgrids are not only employed in an area without electrical energy or those that are connected to the national grid. The factors that trigger the development of microgrids where there is a national grid are classified into three groups which are energy security, economic benefits, and clean energy (Hirsch et al., 2018).

2.5 Driving factors of microgrids development

2.5.1   Energy Security

Energy security is being influenced by the prevalence of severe weather conditions which are the result of climate change which causes disruptions that lessen the grid reliance. Cascading outages are but some of the contributing factors, these could lead to system failure, which could be catastrophic due to the domino effect that may be a result of operating a system to near-critical capacity(Hirsch et al., 2018).

2.5.2   Economic Benefits

The increase in population growth, the low investment is done on the conventional power systems and the aging electrical infrastructure means the electricity demand is slowly outpacing the supply. Microgrids can help in the mitigation of these issues by assisting in additional capacity so to deter investment for replacement or expansion which results in infrastructure cost savings. It also reduces fuel savings by reducing line losses as they are closer to the load as compared to the conventional power plants, it helps in meeting peak electrical demand (Hirsch et al., 2018). Ancillary services will be supplied depending on the market signals and supplying the service locally if efficient than them from a distant power plant(Lopes et al., 2013).

2.5.3   Clean Energy

The mitigation of climate change by curbing carbon emissions is done by the employment of green energy such as solar PV, wind energy, and hydroelectric power. Clean energy has challenges such as over generation, steep ramping, and voltage control. The storage systems are very critical in microgrids to locally balance the generation and load(Hirsch et al., 2018).

2.6 Hydropower Systems

The sun is still the primary source of energy and is responsible for the water cycle. The sun during the hydrologic cycle heats the water from the earth's surface including land and water bodies so moist air rises in a process known as evaporation, as that most air rises it cools and condenses to form clouds. The next process is precipitation where the water comes down from the atmosphere due to coalescence which is a process whereby tiny droplets merge with a big droplet and that heavier droplet drops due to its weight. The water while reaching the earth's surface is absorbed by the soil while some form surface run-off enters water bodies as underground water. This process is always happening and it is also known as the water cycle (USBR, 2005).
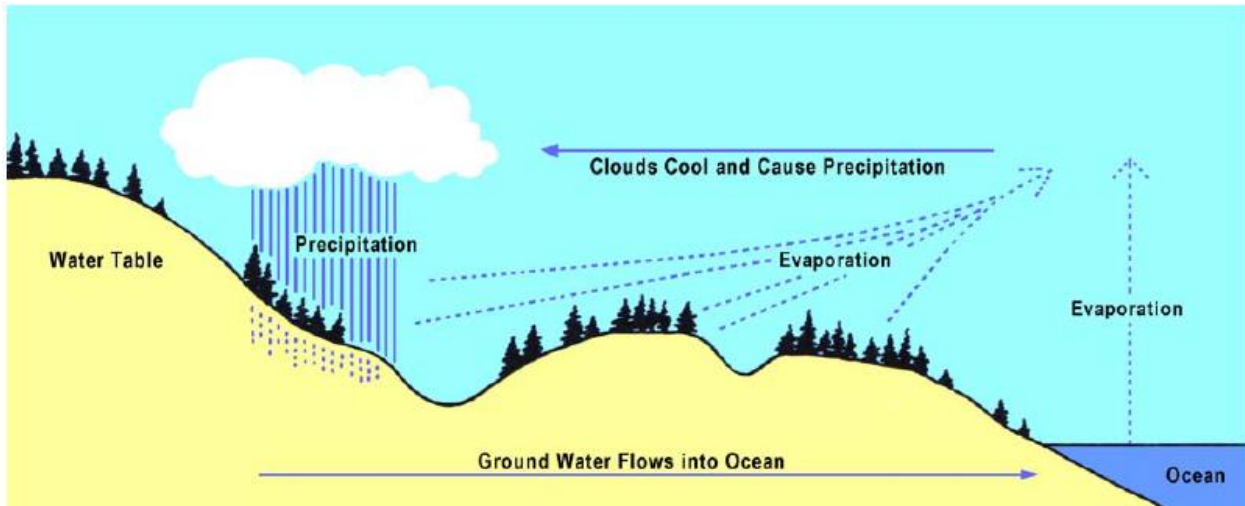
Figure 2-3: Water Cycle(USBR, 2005).

Hydro is derived from the Greek name for water and it is one of the non-polluting sources of energy. The earliest innovation of hydroelectric power has been in existence during the Han Dynasty between 202 BC and 9 AD by the Chinese. The vertical-set of a water wheel used to power trip hammers to pound and hull grain, break ore, and in the early papermaking. The economic growth and waterpower complement one another and in 1771 in Cromford Mill in England's Derwent valley the first world's factory system was set up. This was done by Richard Arkwright to spin cotton and it was powered hydropower and he believed in hydropower to a level that he used the steam engine to pump water into the mill instead of powering the machinery. The key developments in hydropower technology were the design of the turbines in 1827 Benoit Fourneyron developed a turbine capable of producing 6 horsepower(4.5KW). In 1849 James Francis developed the first modern turbine by 1870 and in the 20th century Allan Pelton and Viktor Kaplan followed suit with Pelton Wheel and Kaplan turbine(iha, 2018). In 1878, the first hydroelectric project was implemented to provide power to a single lamp in Gragside in Northumberland, England. In 1882 in Wisconsin, United States of America (USA) the first plant that powered the private and commercial customers then ten years later several hydropower plants were in operation. At the beginning of the 20th century, the USA and Canada were at the forefront of hydropower engineering. In the 1960s -1980s, Latin America and the Union of Soviet Socialist Republics (USSR) developed the largest hydropower plants. In the past few years, Brazil and China surpassed other nations in the developments of hydropower (iha, 2018).

Hydropower is relatively cheap, reliable, sustainable, and renewable energy that does not produce toxic waste. The world is moving away from the reliance on fossil fuel, the production of green energy is of paramount importance to reduce carbon footprint. Hydropower plays a major role in providing clean energy with a 20% contribution to the global electricity need.

Furthermore, it is projected that over sixty (60) countries will get over half of their electrical energy from hydropower plants. Micro hydropower plants are becoming more important not only for rural electrification in less developed countries but also to Europe where large hydropower plants have been exhausted. Micro hydropower(MHP) plants are the more realistic solution because of their low operation expenses, low maintenance costs, they have a long life span, and have minimal socio-economic impacts(Yildiz & Vrugt, 2019).

MHP plants produce electrical energy by converting the kinetic energy of the falling water which translates to the rotation of the shaft and this mechanical energy is the one which is transformed into electrical energy by the generator. MHP systems are such that water is diverted from the mainstream then returned to the stream after turning the turbines without being polluted. The water flows day and night so the use of MHP requires little storage than other technologies. The two of the most important factors to consider while dealing with hydropower is the water flow rate and the hydraulic head which is the elevation between the entrance of the penstock and the turbine (Iemsomboon et al., 2013).

Four basic components that make hydropower plants are the penstock, generator, turbine, and wicket gates. The water would flow due to gravity because of the hydraulic head and it flows through the penstock to the turbine. The regulation of water to the turbine is done by the wicket gates which control the volume flow rate of the water into the turbine. The adjustments made to the wicket gate are done by servo-actuators which are controlled by the governor(Acakpovi et al., 2015).
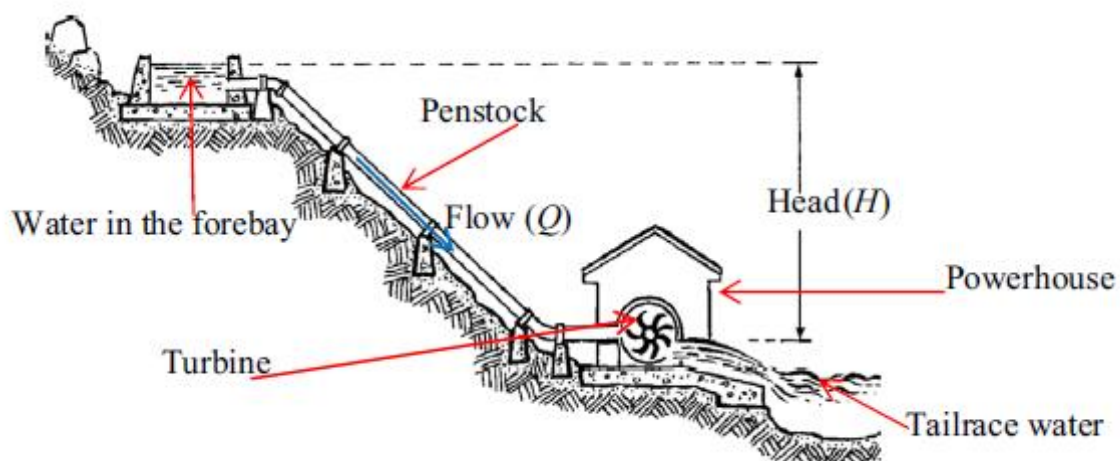
Figure 2-4: MicroHydropower plant Schematic(Kaunda et al., 2014).

Hydropower plays a major role in terms of electrical power production by renewables which accounts for 19% of the global energy (Sultan, 2016). Hydropower is made up of different

arms of power production which are categorized based on their installed capacity. The MHP has numerous advantages such as a lack of emissions that are associated with the production of electrical energy by fossil fuels. There is also less damage to the environment due to the less construction relative to large hydropower plants and this plays a huge role to yield better ecological civilization. The set-up of the MHP has been less expensive due to the low-cost electronic load controllers, cheap Polyvinyl chloride (PVC) penstock, low-cost turbines, and this translate to low investment cost (Kaunda et al., 2014).

In the 20th century, there has been a spring up of large dams with the plan was to provide a reliable power supply. This has come at a cost such as flooding of large fertile land, destroying natural vegetation, the ecosystem upstream and downstream, and displacing people from their natural inhabitants.MHP electrical production is reliant mostly on the run-of-river which means no reservoir or dam is used as storage and in cases that there is a dam it is very small and its purpose is to regulate the water at the intake to the turbines. This translates to less costly and does not cause environmental degradation as water is just diverted from the mainstream to the turbine and water goes back to the river unpolluted. This is essential mostly for rural electrification especially in the less developed countries(Sultan, 2016).
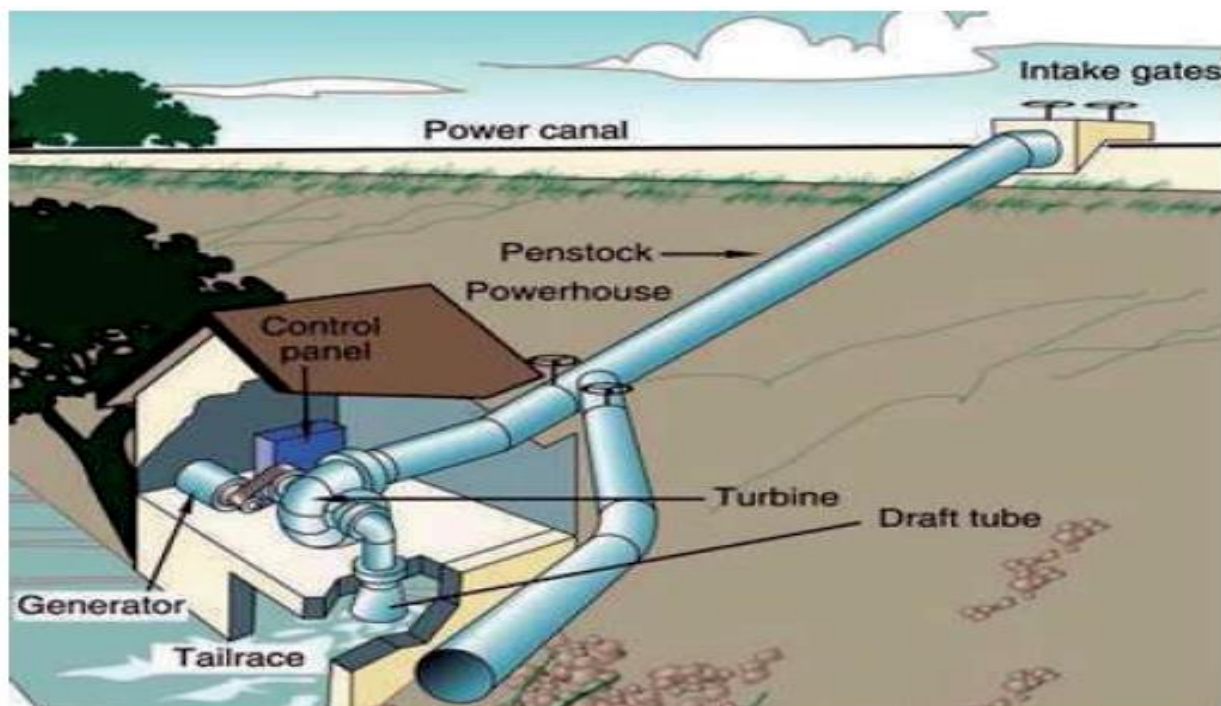
Figure 2-5: Run of river Micro hydropower plant (Sultan, 2016)

It is hard to classify the hydropower system from pico to large hydropower because of developmental policies and populations in different countries. The MHP is considered to be a plant that produces 15 kilowatts annually(Yildiz & Vrugt, 2019).

2.6.1 Design considerations: of MHP

Flow duration curve*:* This is a curve plotted based on the discharge data at a point in the river. The mean annual flow gives the idea of a stream power potential. This can be done periodically either annually or seasonally. This is critical because the choice of the turbine type, size, and speed depend on the net head and water flow rate.

Flow rate measurement*:* The measurement of the discharge is made based on the cross-sectional area which is achieved by dividing it into a series of trapezoids and a mean velocity through it.

Weir and open channel: This is for a low water flow rate set up where water is collected and directed by a notch to the penstock.

Penstock design: These are pipes or a pipe that takes water to the powerhouse to turn the turbine blades and they depend on the nature of the ground, material, and the environment that it will be employed on(Nasir, 2014).

The penstock is the pathway of the water from the source, either a reservoir or a canal to the turbine inlet. They are made up of various materials such as steel pipes, fiberglass, concrete, etc. The decision of which material to choose in the design of the penstock relies on four main factors which are:

- Head loss due to the material
- The thickness of the penstock shell
- Economical size of the penstock
- The geographical route where it will be installed.

The head losses through the penstock are the major losses in the transportation of water from the canal or reservoir as compared to the fitting's losses or the inlet or outlet losses. The head loss in the penstock is mainly due to friction which is proportional to the length and the type of the material the penstock is made up with the equation for that loss is given by:

$$h_f = \frac{fLV^2}{2gD}$$

(2.1)

Where:

h_f =Head loss due to friction (m)

f =Friction factor

L =Length of the penstock (m)

V =Water velocity $\left(\frac{m}{s}\right)$

g =Gravitational acceleration $\left(\frac{m}{s^2}\right)$

D =Pipe internal diameter (m)

It is very critical to design the penstock to reduce the head losses that are on the system due to friction. The net losses on the system reduce the potential of the water as some of the water energy is used to overcome friction. The bigger the diameter the low the losses, this is because while calculating the Reynolds number, having a bigger diameter increases the inertia forces and this helps in having a huge Reynolds number. Reynolds number is the ratio of inertia force to the viscous force of the flowing fluid. Its significance is to determine the type of flow through the pipeline or penstock (Bonthuys, 2016).

$$Re = \frac{Inertia\ Force}{Viscous\ Force} = \frac{\rho \times V \times D}{\mu} \qquad (2.2)$$

$$H_f = \frac{0.3164}{Re^{0.25}} \qquad (2.3)$$

Where ρ is the density of the water (kg/m^3), V is the velocity of the water (m/s), D is the diameter of the penstock (m), μ is the dynamic viscosity of the water $\left(N.\frac{s}{m^2}\right)$ and H_f is the head loss due to friction(Varughese & Michael, 2013).

When the water flows from a higher elevation the potential energy is transferred from potential energy to pressure energy. The efficiency of the conversion energy depends on friction losses which are dependent on the length of the penstock and its roughness which is based on the material that is made of. The other losses are due to the connections made on the penstock like elbows, reducers, and losses at the intake. The penstock is best designed such that there are a minimum length and fewer connections(Tapia et al., 2018).

2.7 Hydropower Classifications

In hydroelectric plants, turbines are the prime movers that are core to the production of electricity by turning the generator in which to harness water energy to produce a rotational motion of the shaft. A turbine is a rotating mechanical device that extracts the energy from a flowing fluid and transforms it into useful work. This is a turbomachine that is made of rotating blades that converts the kinetic energy or remove the angular momentum of the fluid to mechanical energy so to induce torque which is turned into another form of energy like electrical or perform work. Hydropower turbines are classified into two categories, namely, impulse turbines and reaction turbines. The classification is based on both the water flow and the different hydraulic heads. Hydropower is named based on capacity and it differs from country to country(Nababan et al., 2012)

Table 2-1:Classification of Turbine used according to hydraulic head (Dijk et al., 2016)

Classification	Head	Turbine type
High head	>100	Pelton, Francis, etc.
Medium head	30-100	Francis, Kaplan, etc.
Low head	2-30	Pelton, crossflow, hydro engine, hydraulic screw, waterwheel, hydrokinetic, vortex, and siphon

Table 2-2: Hydropower classification based on capacity (Nababan et al., 2012)

Type of hydropower	Power output
Pico	<5kW
Micro	5kW-100kW
Small	101kW-2000kW
Mini	2001kW-25000kW
Large	>25000kW

Hydropower is also divided into four categories based on how the installation is done which are:

Impoundment type: The dam is used to store water and this is mostly on large hydropower plants,

Diverse type: This where the river is diverted to turn turbines and water flows downstream,

Run of the river: This where the natural flow of the river is used and no impoundment,

Pump storage: When the demand is low the water is pumped to a higher reservoir and when the demand is higher the water is released (Nababan et al., 2012).

Modern hydraulic turbines are the output of several years of developments, larger turbines have efficiencies of 96% which are relatively cost-effective as compared to smaller ones based on the cost per installed capacity of a turbine. The focus is shifting from the manufacturing of large turbines to medium and small turbines because of the advances in technology and computer-aided designs which have played a major role in the improvement and customization of small turbines for design flow and head requirements for a site. It is therefore important to understand the basic hydrodynamics of turbines for the selection of a proper one. The energy from the flowing water will result in the twisting force known as torque and its impact on the runner is the difference between the rate of angular momentum at the inlet of the runner and at the exit of that runner, this is called the conservation of radial momentum(Gulliver & Arndt, 1991):

$$T = \rho Q(r_1 V_1 \cos\alpha_1 - r_2 V_2 \cos\alpha_2) \qquad (2.4)$$

$T =$ Touque on the runner $(N.m)$

$\rho =$ Density of the fluid $\left(\frac{Kg}{m^3}\right)$

$Q =$ Volumetric flow rate (m^3/s)

$r_1 =$ Outer radius of the runner (m)

$r_2 =$ Inner radius of the runner (m)

$V_1 =$ Velocity entering (m/s)

$V_2 =$ Velocity exciting (m/s)

Hydro turbines are classified into two categories which are impulse turbines and reaction turbines.

2.7.1 Impulse turbines

The water from the penstock is pressurized by reducing the area and this results in increased velocity of the water that goes through the jet. The high-velocity water from the jets impacts the turbine blades or cups which then rotates. The impulse turbines are usually applied where there is a high head and low volume flow rate. Impulse turbine has three common types which are Pelton, cross flow, and turgo turbine (Sangal et al., 2013).

Pelton Turbines

The water from higher elevation is directed to the turbine inlet through the penstock. The nozzle is fitted where the jet of water coming out is directed to strike the cupped buckets

which are assembled on the circumference of the runner and the force due to the impact causes turning moment and results in high-speed rotation of the runner. In Pelton turbines, either a single jet or multi-free jets are used depending on the application that will be employed and they are mostly used for small hydropower plants(Transport et al., 2015).

2.7.2 **Reaction Turbines**

The mechanical power produced is the result of a pressure difference which creates the lift force to rotate the blades like the aircraft wings. The reaction turbine work when the rotor is fully covered by water and covered by the pressure casing. The reaction turbines are best operated where there are low head and higher flows. The reaction turbine types are Propeller, Francis, and Kinetic(Kilama, 2013).
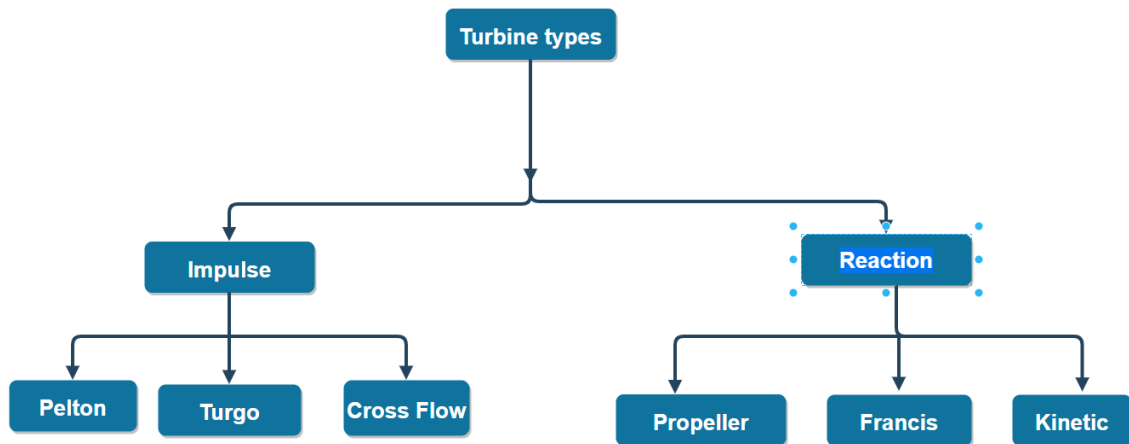
Figure 2-6: Classification of hydro turbines (Kilama, 2013)

Table 2-3: Types of hydropower turbines
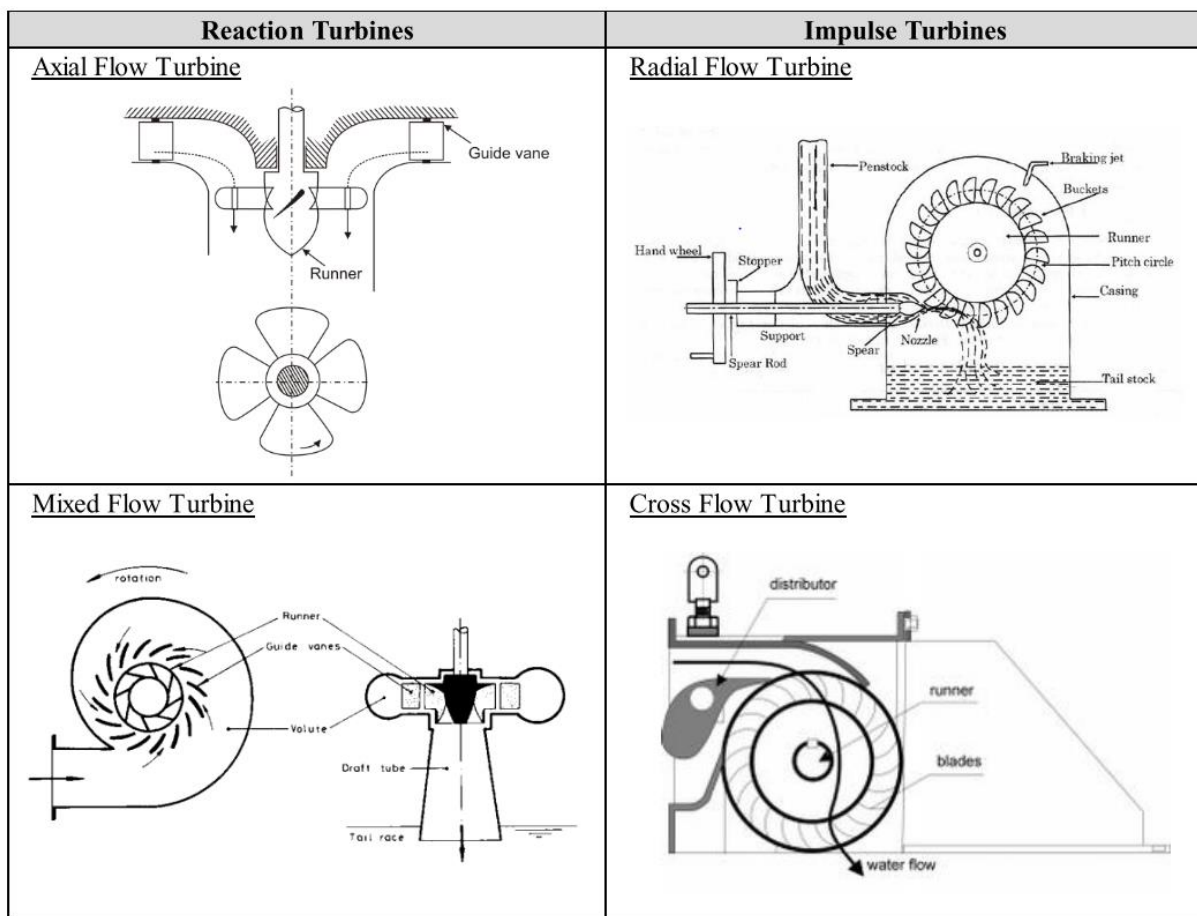
Figure 2-7: Types of hydropower turbines (Bonthuys, 2016)

2.7.3 Power Extraction and Head losses

The power that can be extracted from the MHP is dependent on the flow rate and the net head. Net head(H) is the available head at the inlet of the turbine which is the difference between gross head(H_g) and head loss(h_f) due to friction (Tapia et al., 2018).

$$H = H_g - h_f \qquad (2.5)$$

The power generated by the water from a higher elevation until the production of electrical energy will not be the same as this is not an ideal machine so there will be losses. The energy though will not be lost it will the transformed from one form to another form of which

is not going to impact the power output positively. This means there are inefficiencies concerning the turbine which are

Table 2-4: Efficiencies of a turbine (Upadhyay, 2012)

Hydraulic efficiency (η_h)	This is a ratio of power delivered to the runner by water to power at the inlet of the turbine
Volumetric efficiency (η_v)	It is the ratio of the volume of water that strikes the bucket to the volume of water supplied by the jet to the turbine
Mechanical efficiency (η_m)	This is a ratio of the power available at the turbine shaft to the power delivered by the runner
Overall efficiency (η_o)	This is the ratio of the power available at the turbine shaft to power supplied at the inlet

$$P = \eta \rho Q g H \tag{2.5}$$

Where:

$P =$ Mechanical power

$\eta =$ Efficiency

$g =$ Gravitational accelerations

2.8 Generators

The principle of operation of the generators is based on Faraday's law of electromagnetic induction which states that electromotive force(e.m.f) will be induced in the conductor coil when a current-carrying conductor is placed in a rotating field which is due to the angular velocity(ω) caused by the prime mover and cuts the fluxes(Ashraf & Mallick, 2009).

Electrical machines work on a principle known as Electro-Mechanical energy conversion which converts electrical energy to mechanical energy and vice versa. Generators change the mechanical energy which is produced by a prime mover such as a turbine due to moving water, high-pressure superheated steam or saturated steam, or even nuclear energy resources depending on the plant. The conversion between those two types of energy is due to electromagnetic torque. The electromagnetic torque yields magnetic flux which is a result of armature current and field current. The generators can be grouped into two types which are synchronous and asynchronous (induction) generators. In terms of hydropower plants especially off-grid the 3-phase synchronous generators are preferred over the asynchronous

ones because asynchronous generators cannot provide high-quality electricity due to the sink of reactive power while in synchronous reactive power flow can be controlled through excitation. The two generators have different characteristics depending on the application intended (Kilimo & Kahn, 2012).

The inputs for a synchronous generator are the torque input which transfers the power from the turbine to the rotor through coupling and the excitation current to the field windings in its rotor. The rotation due to mechanical torque from the turbine results in the rotation of the rotor hence the formation magnetic field in the air gap which cuts the stationary coils in the stator which induces a voltage in the stator windings. The mechanical torque due to flux linkages is converted to electrical torque which is used to cater to the load as voltage and current (Kunjumuhammed, 2013). The electrical torque is due to both the stator and rotor field reaction and the tendency of that field trying to align. The electrical torque seeks to oppose the rotation of the rotor hence the continuous need for mechanical torque from the prime mover to maintain the rotation. This means the power output of the generator is directly proportional to the mechanical torque(Kundur, 1994).

2.8.1   Synchronous Machines

The rotating magnetic field is formed in the air gap between the rotor and stator in an alternating current motor where the speed of that rotating magnetic field is known as synchronous speed. The motor rotates at the same speed as the rotating magnetic field (Du Plooy, 2016). The stable power system is such that the synchronous machine can hop back to the original state amid the disturbance or can acquire a new stable without losing synchronism due to power changes. There are two types of synchronous generators and this is differentiated by the arrangement of field and armature windings which are rotating armature and the rotating field. A synchronous generator under steady-state speed is proportional to the frequency of the AC in its armature. The field and armature are two core elements of the synchronous, the field wingdings give direct current and produce a magnetic field which gives rise to alternative voltage in the armature winding. Three-phase armature windings on a stator are distributed 120° apart in space so that there would a uniform rotation of the magnetic field, voltage displaced by 120° in time will be produced in the windings. When the load is balanced the armature currents will produce a magnetic field rotating at synchronous speed. The field is produced by direct current in the rotor windings, on the other hand, revolves with the rotor(Kilimo & Kahn, 2012).

The synchronous generator used in hydroelectric plant's salient poles is due to the slow speed as compared to high-speed synchronous generators with cylindrical poles like steam turbines. The low speed also means that there will be a higher number of pole pairs to produce the needed frequency. In the quest to understand and identify synchronous machine behavior it is important to be aware that all rotor windings and magnetic circuits are symmetrical on the polar axis and interpolar axis. The two axes are direct (d) axis and the quadrature (q) axis(Kundur, 1994).
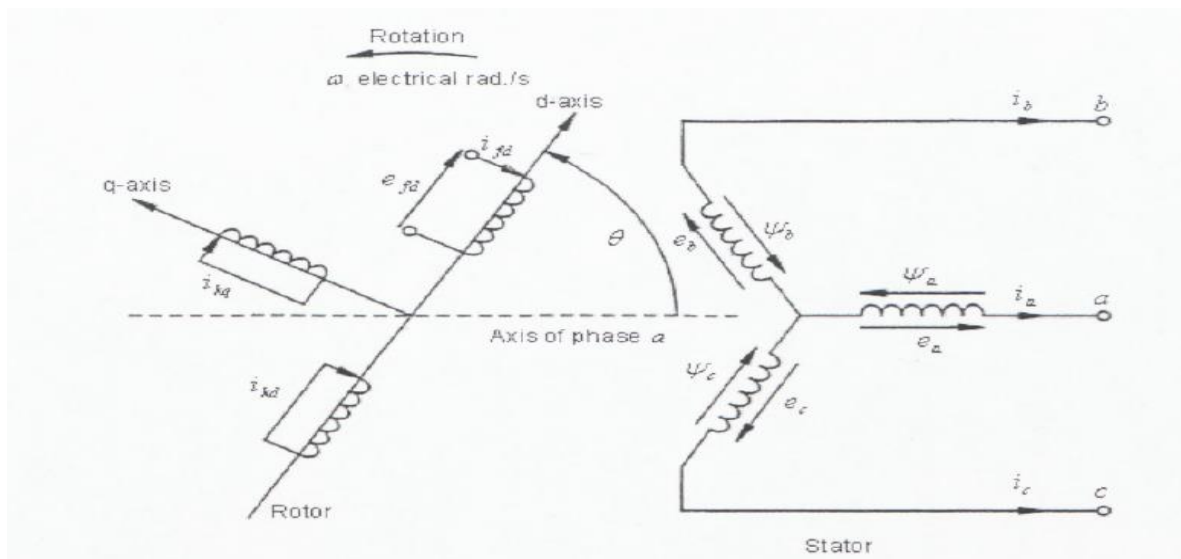
Figure 2-8: Stator and Rotor Circuits of a Synchronous Generator (Kundur, 1994)
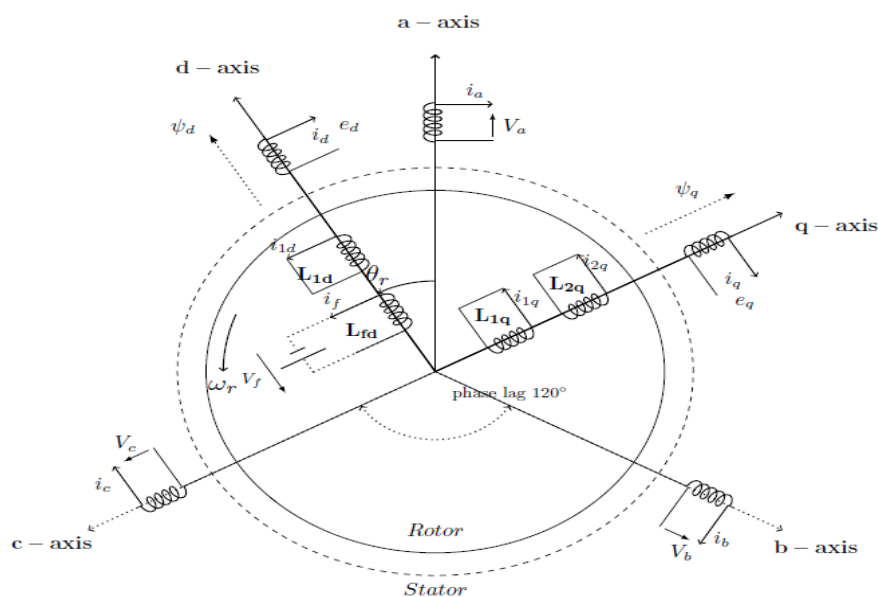
Figure 2-9: Three-Phase Synchronous Machine (Øyvang et al., 2018).

Table 2-5:Synchronous and Induction generators characteristics (Kilimo & Kahn, 2012)

Synchronous Generator	Induction Generator
Efficient	Moderately efficient
Expensive	Less expensive
Requires maintenance	Rugged and robust, little maintenance
Reactive power flow can be controlled through excitation	Sink of excitation
Fixed speed hence very stiff	A small change in speed with torque, hence more compliant
Respond in an oscillatory manner to sudden torque changes	Respond to inputs in no oscillatory way
Suitable for connection to weak networks. Used in autonomous systems	Suitable for weak networks only with power electronics
Requires special synchronization equipment to connect to mains/another generator for parallel operation	Can be simply synchronized to the mains
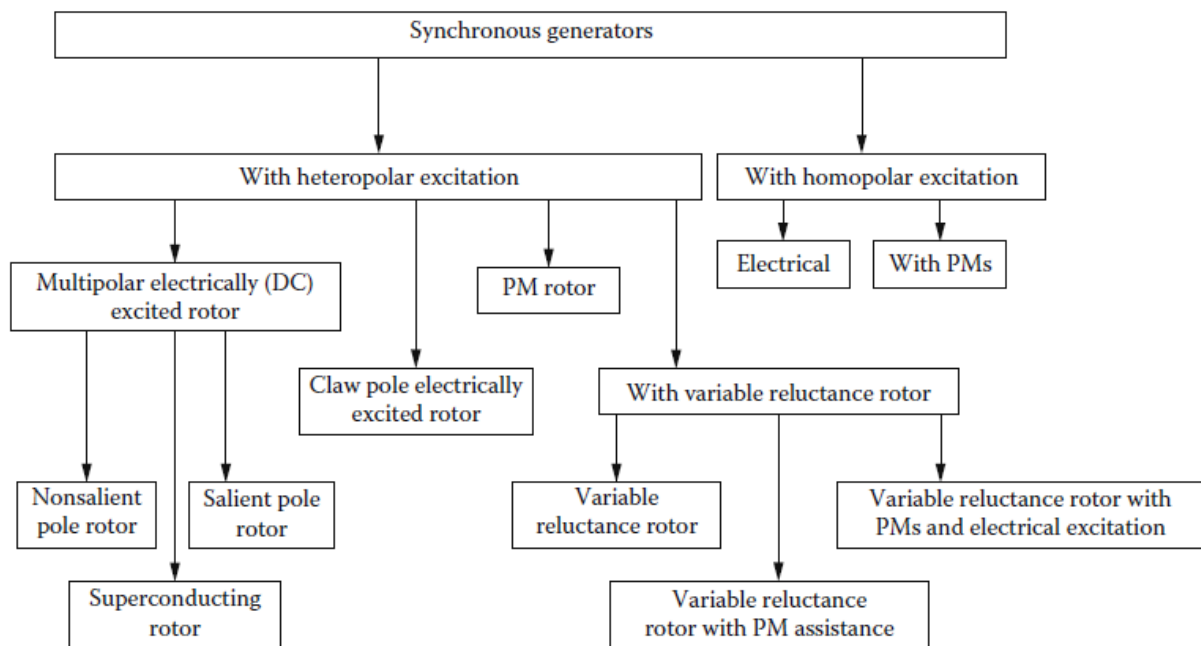
Figure 2-10: Types of synchronous generators (Boldea, 2005)

2.9 Voltage and Frequency Control in hydropower plants

The power quality in the power system is determined by providing among others specific voltage and frequency hence is it paramount to have controls during power generation to maintain those parameters. The voltage control at the generator bus is done by the excitation system of a synchronous generator while the frequency control is done by mitigating the mismatch between generation and load demand and it is dependent on the active power balance. In the power system, generators need to operate at the same speed to produce a

specific frequency(50-Hz) and this is done by governors by regulating the volumetric flow of the water that impacts the turbine blades (Kilimo & Kahn, 2012).

2.9.1 Excitation System

The basic operation of the excitation system is to provide the required magnetic field strength in the rotor windings by feeding the DC supply of which when being cut by conductors induces a voltage. This system helps in the regulation of terminal voltage, to control reactive power flow and in the case of the reactive load. The main function of the excitation system is to improve the stability of synchronous generators by effecting changes that lead to terminal voltage and reactive power supplied by the generator. The excitation system controls the amount of electromotive force (EMF) generated by the generator which therefore regulates terminal voltage, power factor, and the magnitude of the current(Anderson & Fouad, 2002). The excitation control system comprises a regulator, stabilizing transformer, a rectifier, a phasor measurement unit, and the exciter. The exciter injects direct power (DC) to the synchronous generator's field windings(Ayasun et al., 2014).
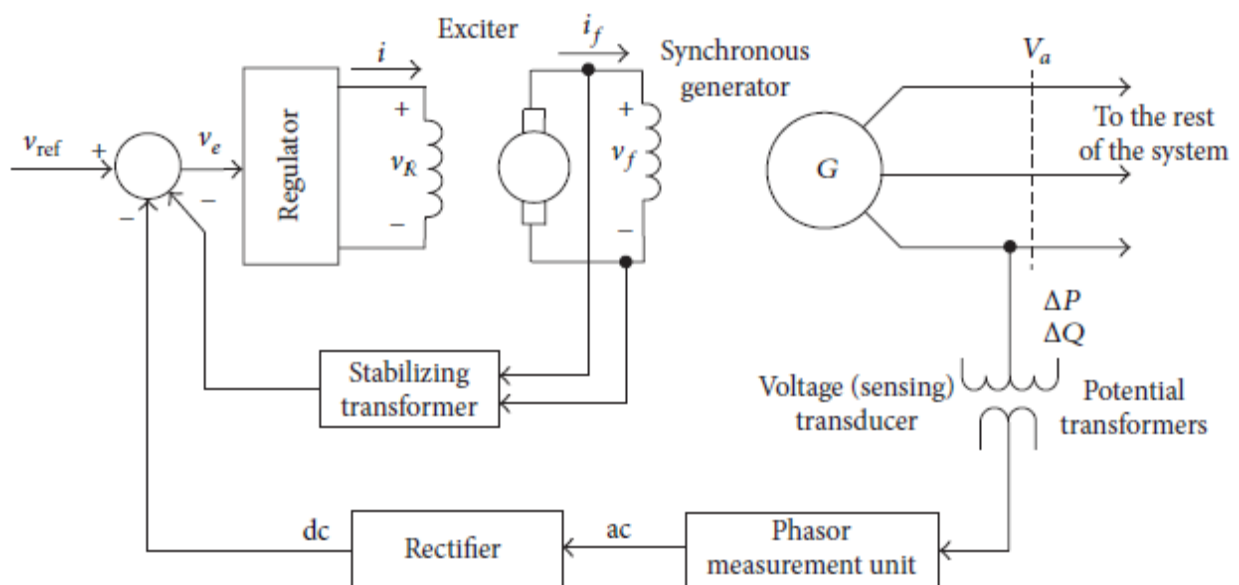
Figure 2-11: Schematic diagram of excitation system control (Ayasun et al., 2014).

The excitation system composes of the summing point where the terminal voltage is compared to the voltage reference where there is a resulting control error. There is also the Automatic Voltage regulator which is the brain of the system that dictates how much the exciter output must provide in order to acquire a required terminal voltage and reactive power. It uses the proportional character which is either lead or lag compensator or proportional, integral, and

derivative (PID) control(Máslo et al., 2016). The frequency of the power system is maintained by regulation of the feed input to turn the turbine blades. In steam turbine is the control of the amount of steam to the blades while in hydropower systems is the volumetric flow rate of the water and this is done by governors. The governing system will then be analyzed below.
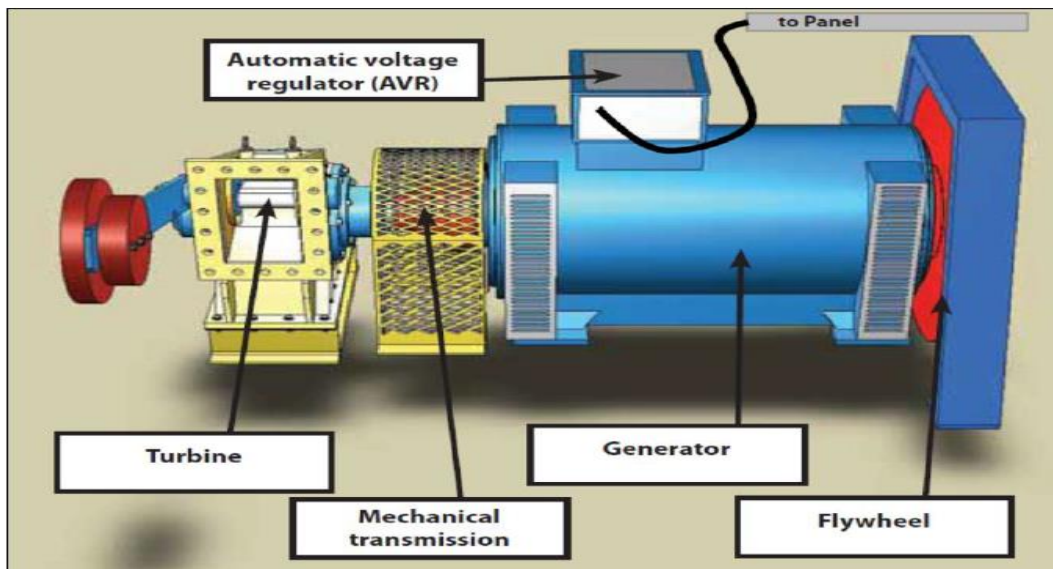
Figure 2-12: Electro-mechanical components of MHP plant (Jorde & Hartmann, 2009)

2.9.1.1   Governing System

The prime mover governors have been utilized since the late 1700s and the most common is the centrifugal flyball governors. The first centrifugal governor was applied by James Watt on a steam turbine in 1788. The use of flywheel governors gathered momentum in the 19th century eliminating the use of float valves which were the competing devices at the time(Anderson & Fouad, 2002). The change in load during the day causes the frequency variation and since the speed of the prime mover is dependent on the load fluctuation. Governors have been utilized for the control of turbine speed or power output. The turbine governor determines the amount of water input to the turbine of which its energy is used to rotate the generator(Abdulkadir, 2015). The design of governors is forever changing due to the nonlinearity of the system, be load changes or disturbances. This has undoubtedly made governors very crucial in the operation of the synchronous generator. "The continuous interconnections, the evolution of generating units, increased voltage transmissions, and power requires continuous improvement in governor design to cope with the new dynamics of systems". This designs entails advanced control techniques and structure for the allowance of the plant to be flexible and operate in different conditions(Eker, 2004).

The hydraulic turbines are coupled to the generator which must run at the synchronous speed to generate the power required at a constant frequency. Generator frequency control is accomplished by the engine governor sensing speed changes from the desired speed set point. The governors are fitted on the turbine for the water flow rate control depending on load changes to maintain synchronous speed. The governing system has three main components which are the actuator, servomotor, and relay valve. The actuator is at times made up of flyball for the centrifugal governor which senses speed change of the turbine shaft because it is merged by the gears and the actuation happens on the main leaver. The relay valve is the piston slide valve. The speed variation of speed causes the main leaver to move up or down whose results in the piston sleeve to allow the oil to be distributed to the servomotor. The servomotor is made up of the piston-cylinder that depends on the oil distribution line the hydraulic pressure will either force the turbine mechanism to reduce or increase the water flow rate to the turbine to increase speed or lower that is based on the load variation. In a Pelton turbine, the turbine mechanism is the spear rod while in Kaplan turbine is the guide vanes and runner vanes and for both the Francis and Propeller turbine the guide mechanism is the guide vanes(Signal et al., 2010).

When there is a steady load on a turbine, the electrical torque is constant so, there is no incremental speed ($\Delta\omega(s)$) meaning the speed is the same as the setpoint speed $\Delta\omega^{ref}$.This is only true for a standalone system but in the interconnected system, the speed is controlled by the system frequency. The speed variation is controlled by the speed governor. The difference in the processing speed and the reference setpoint speed results in the error signal ($U(s)$). The signal is then amplified by the servo amplifier proportionally to the error signal. This results in a larger mechanical force that produces a servo stroke to cause displacement or change the gate position $\Delta G(s)$ to allow more fluid to the turbine blades or less depending on the signal (Anderson & Fouad, 2002).
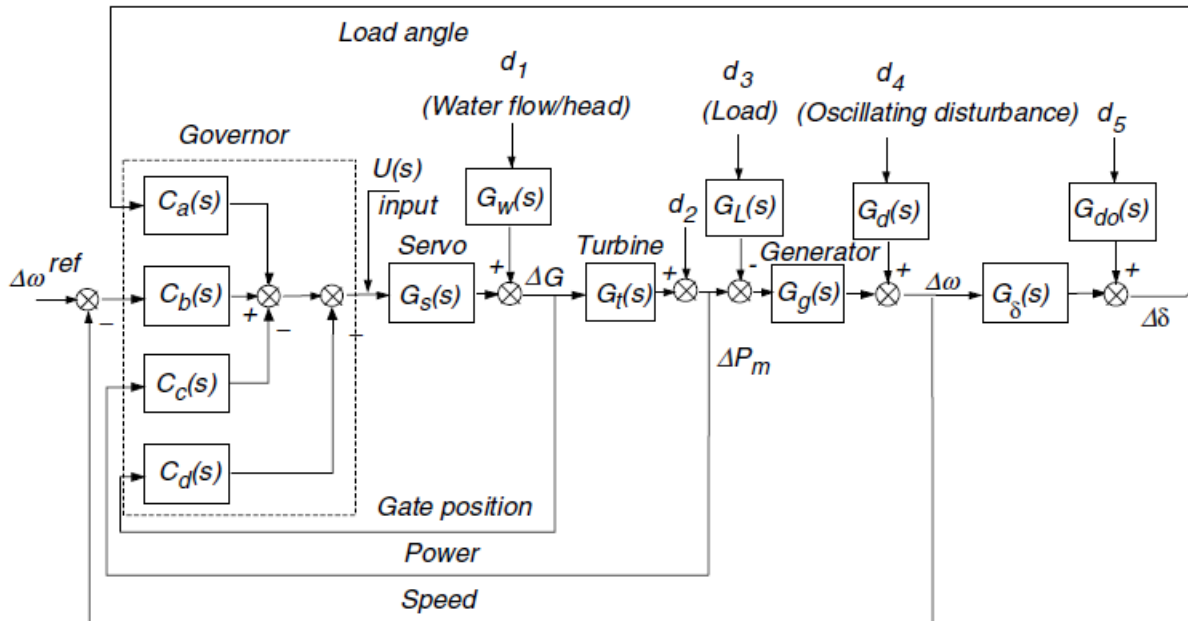
Figure 2-13: Governor control diagram (Eker, 2004).

The following parameters are used as a feedback input signal from the plant to the governor and are deviations from the steady-state. This helps in the improvement of system performance.

Table 2-6: Governors feedback input signals

$U(s)$ =Input signal to the servomotor	$G_g(s)$ =Generator	d_2 =Turbine
$\Delta\omega(s)$ =Incremental speed	$G_\delta(s)$ =Integral speed	d_3 =Load power
$\Delta G(s)$ =Gate position	$G_W(s)$ =Water inflow	d_4 = Speed
$\Delta P_m(s)$ =Turbine power	$G_L(s)$ =Output Load	d_5 =Load angle disturbances
$\Delta\delta(s)$ =Load angle	$G_d(s)$ =Permanent speed	$\Delta\omega^{ref}$ =Set point
$G_s(s)$ =Pilot and gate servo motor model	$G_{do}(s)$ =Load angle disturbances	
$G_t(s)$ =Turbine	d_1 =Water flowrate	
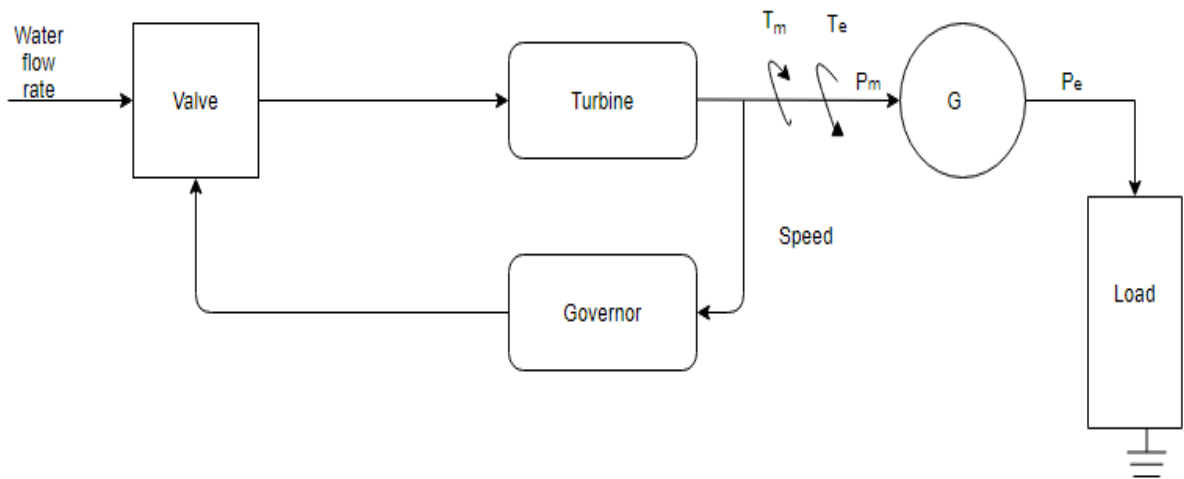
Figure 2-14: Speed governing principle of synchronous unit

The load variation affects the frequency of the machine and this changes the electrical torque output of the generator. When the acceleration torque is zero, the system is operating at a constant speed meaning the same frequency. The difference between the two torques results in speed variation. The unbalance of torques on the rotor and net torque either produce acceleration or deceleration based on the equation below and this needs to be controlled by the governor(Kundur, 1994).

$$T_a = T_m - T_e \qquad (2.6)$$

Where

T_a =Accelarating torque (N.m)

T_m =Mechanical torque (N.m)

T_e =Electromagnetic torque (N.m)

This unbalance due to the torque accelerates the combined rotor mass of the generator and the prime mover and this given by:

$$J \frac{d\omega_m}{dt} = T_a = T_m - T_e \qquad (2.7)$$

Where

28

J = Combined moment of inertia of generator and turbine, kg.m^2

ω_m =Angular velocity of the rotor, mech. rad/s

t =Time, s

T_a =Accelerating torque, N-m

2.10   State of hydropotential in South Africa

South Africa has a low annual rainfall which accounts for only 500mm which makes the country semi-arid which the countries initiated transborder water supply from Lesotho to Johannesburg metropolitan area. This water caters to half of the demand of 12 million residents in the Gauteng administrative district and annually a total of 900 million m^3 of water is transferred from the Katse and Mohale dam(Rousselot, 2015). The lack of sufficient rain in South Africa poses a challenge in prospects of hydropower prospects but small-scale hydropower can be employed using run-off river systems (Bonthuys, 2016).
The dearth of surface water has resulted in only seven dams that provide hydropower and Gariep is the largest with the capacity of 360MW which is situated on the Senqu River. There are approximately 5000 registered dams in South Africa classified in terms of their sizes(Dijk et al., 2016).

Hydropower contributes 661MW which is 14.58% of the total renewable energy production. The hydropower potential has not been fully explored where a huge potential is in the collection area known as catchment which is within the Department of Water and Sanitation(DWS) water management and the water and sanitation infrastructure which is interdepartmental from national to the municipal level and there is no clear line on who has the authority. The lack of rainfall and droughts means SA has a limited hydropower capability. The huge potential is in the Eastern region of the country with between 6000-8000 sites with the potential. The potential of small-scale hydropower in that region can provide a total of 247 MW of power. This input will emerge as a necessary generation as SA has just a total of 38MW installed small-scale hydropower. This could assist massively in rural electrification as these potential sites are found mainly in rural areas of Eastern Cape, Free State, KwaZulu-Natal, and Mpumalanga(Mokveld & Eije, 2018).

The low-head hydropower systems are mostly MHP power plants that are used to power small communities and often use run off the river. This is where there is a diversion of a river and

the water is directed through a weir to keep a constant head then to the pipeline which leads to the turbine. The run of river type of hydropower needs an in-depth understanding of the fluctuation of flow from the river and studies to need to be done and flows need to be calculated on monthly basis and averaged for at least 3-5 years(Dijk et al., 2016).

Table 2-7: Low head hydropower installations in South Africa (Loots et al., 2015)

Existing Infrastructure	Power plant name	Nominal discharge(m^3/s)		Available head(m)	Power Output(kW)	Electrical production(GWh/year	Distance to grid connection(km)
Water treatment works	Wemmershoek	0.9		24	208	1.54	7.2
Water distribution systems	Pierre van Ryneveld	0.16		17	15	0.003	Stand alone
Run-of -river	Merino	29		14.8	3600	24.8	16.4
Dam	Sol Plaatjie	29		10.2	2500	12.2	4.5
Measuring Weir	Neusberg	90		15	10000	71.9	21
Wastewater water treatment	Zeekoegat	0.37		3.6	6.9	0.002	Stand alone
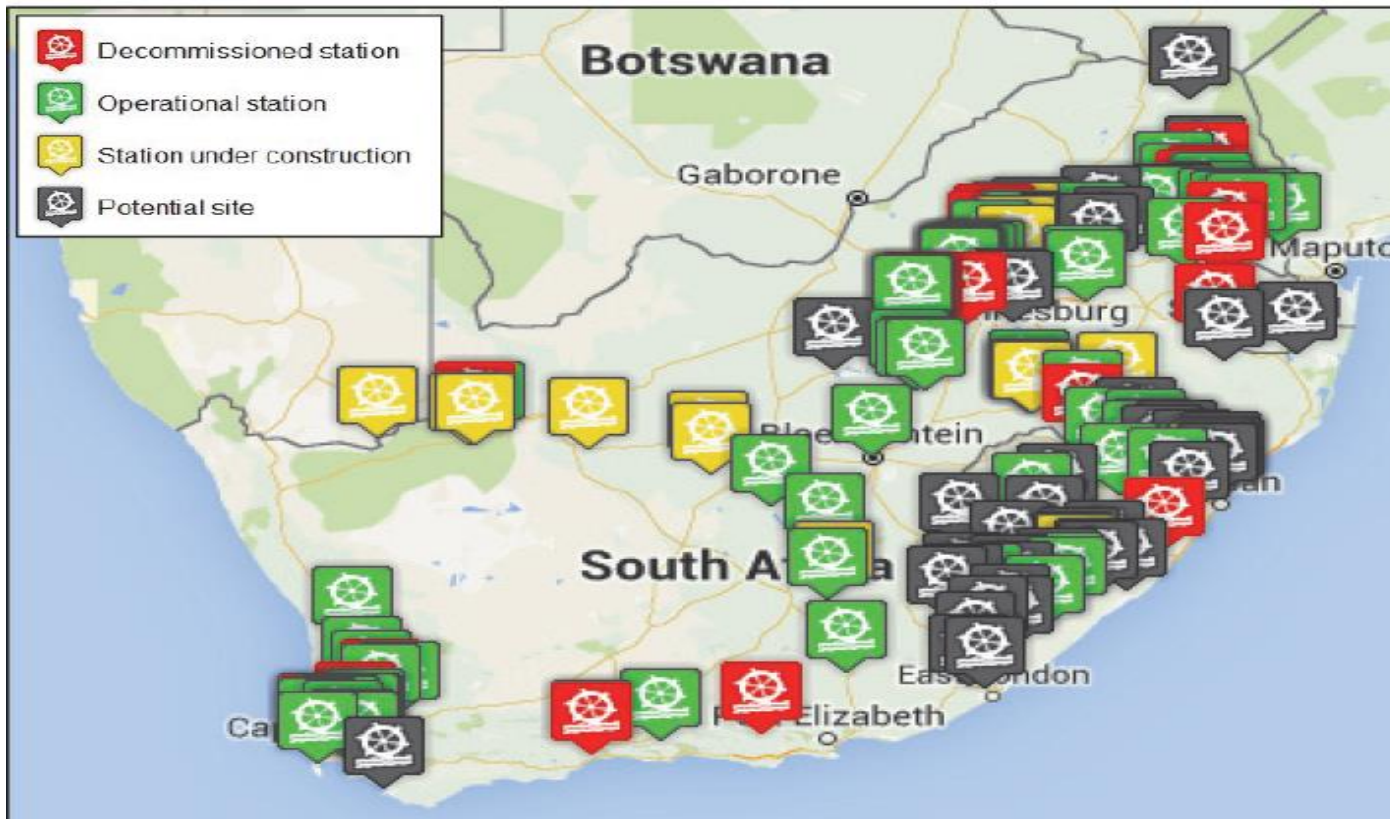
Figure 2-15: Potential, operational, and decommissioned hydropower plants (Klunne, 2012)
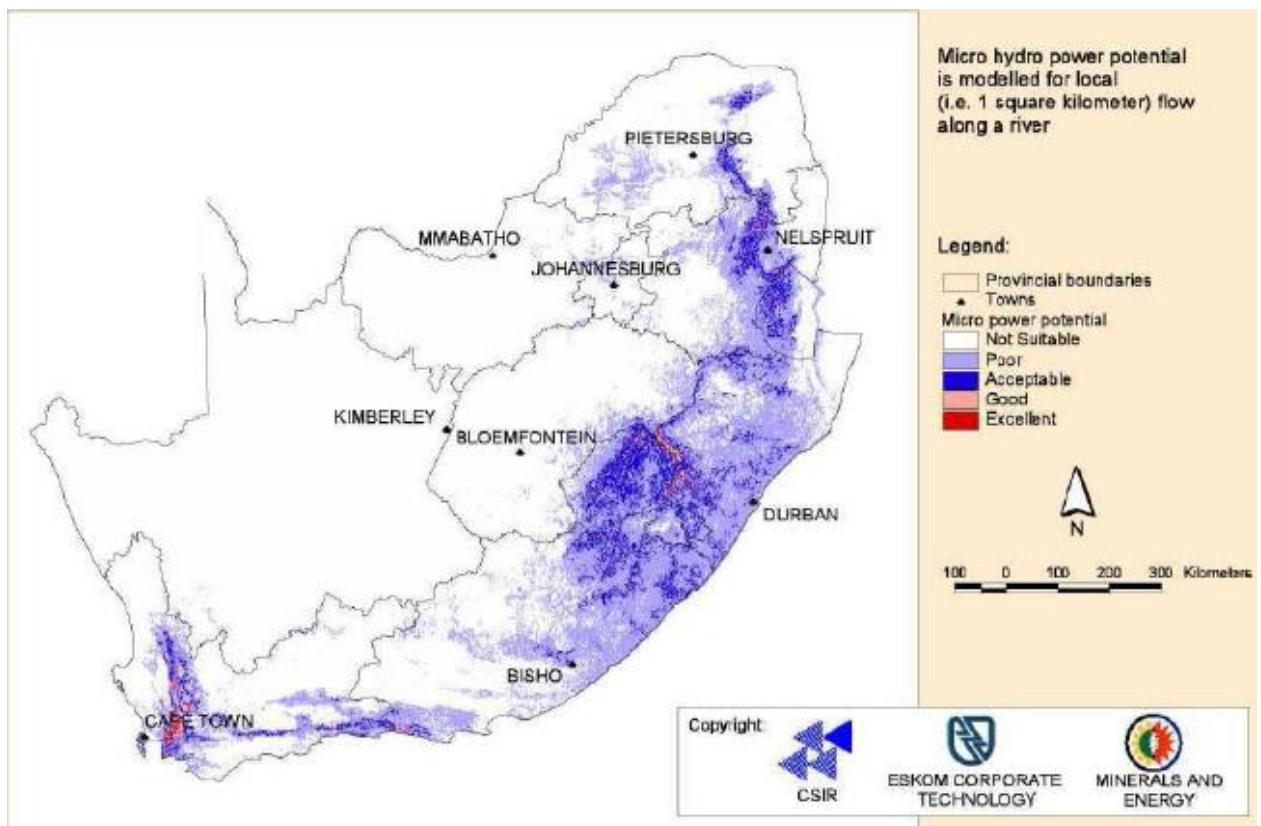
Figure 2-16: Micro-hydro potential (Bonthuys, 2016)

2.11   Photovoltaic

The electrical potential produced when two different materials are hit by photon energy at their common junction is known as a photovoltaic effect. It was in 1839 when the concept of photovoltaic effect was discovered by Antoine-Cesar Becquerel who was a French physicist. In 1877 Adams and Day observed the photovoltaic effect in solid selenium. In 1883 Charles Fritz developed the first photovoltaic cell of which had an efficiency of less than 1%. The development of photovoltaic cells continued wherein 1927 the new photovoltaic cell was developed which was made up of copper and semiconductor copper oxide but it too had an efficiency of less than 1%. Russel Ohl in 1941 developed photovoltaic cells made up of silicon which leads to between 6%-11% in 1954 after more refining by Bell Laboratories. The first practical photovoltaic generator was in 1958 which was producing 1 Watt which was employed in Vanguard satellite and the 1960s when space exploration was in its prime there was more need for improvement on the efficiency of the photovoltaic as more electricity was needed for photovoltaic collectors as the cost was of secondary importance(Singh, 2013).

The sun is the main source of inexhaustible free energy globally and there is a rise in new technologies to harness that solar energy to generate electricity. In a year four million exajoules (1×10^{18}) of the sun's energy reaches the earth's surface. This simply means that the sun's

33

energy that reaches the earth can cater to all global energy needs, but the problem is the technologies that can harvest that energy effectively are not yet available. Despite this huge potential, the contribution of solar energy is still very low but some measures are being taken to reduce carbon emissions, and this shines a huge light on the prospects of solar energy. Furthermore, reduces problems relating to energy security, climate change, unemployment and can also help in the transportation sector (Kabir et al., 2018).

There are two main areas where solar energy is applicable, which are solar thermal and solar electricity. Solar thermal utilizes the direct source of heat energy from the sun while for electricity the sun's energy in a form of sunlight is converted to electrical energy through a process of photovoltaic (Singh, 2013).

There is has been a boom in smart electric grids and at the center of these are renewable energy sources. This quest for green energy is due to the diminishing of fossil fuel reserves, the rise in natural environmental disasters, and the need to reduce pollution that is caused by fossil fuels. The (PV) systems play an essential role mainly because they don't cause environmental degradation and due to their technical merits as they can be used as an energy source in hybrid, standalone, or be grid-connected. PV has several advantages which are the fact that during the production of energy they do not pollute the environment, they have a lifespan of 25-30 years, they have no running cost, and their maintenance is low. PV also has limitations in terms of their conversion efficiencies (12-15%) of PV modules, the PV performances deviate as a result of ambient weather conditions which are wind speed, ambient temperature, relative humidity, and accumulated dust that affects the amount of irradiance to the PV array hence affecting the power output. The increase of surface temperature by $1°C$ of the PV module causes a reduction of 0.5% in efficiency(Kaddah et al., 2018)).

2.11.1 Photovoltaic Cell

Solar energy is the readily available renewable energy that reaches the earth in the form of electromagnetic waves(Keyhani, 2011). Solar Photovoltaic (PV) contribution is gathering momentum in terms of the roles it plays in modern electric power energy. Standalone PV system takes part mostly in the electrification of rural areas where there is no electricity grid. To optimize the size of the PV system there are basic that needs to be followed like knowledge of weather conditions, the satisfaction of load with a certain level of reliability, and all costs that are related to the system (Okoye & Solyalı, 2017).On every material, the sun shines on it either gets reflected, transmitted, or absorbed. The absorption of light means that solar energy is converted to another form of energy as the law of conversion states, energy can neither be formed nor destroyed it can only be changed from one form to another, mostly solar energy is converted to heat energy while being absorbed. The photovoltaic cell is made up of a semiconductor material that converts sunlight into electrical energy in what is referred to as

the photovoltaic effect. The photons are absorbed from the sunlight and generate free electrons. The energy from the sun is adequate while striking the PV excites the electrons and frees them and the built-in barrier in the cell makes these electrons produce a voltage which is used to drive current through the circuit. Silicon is the most used semiconductor material in PV applications which are multi-crystalline silicon and monocrystalline silicon for high-efficiency solar cells(Parida et al., 2011; Singh, 2013).
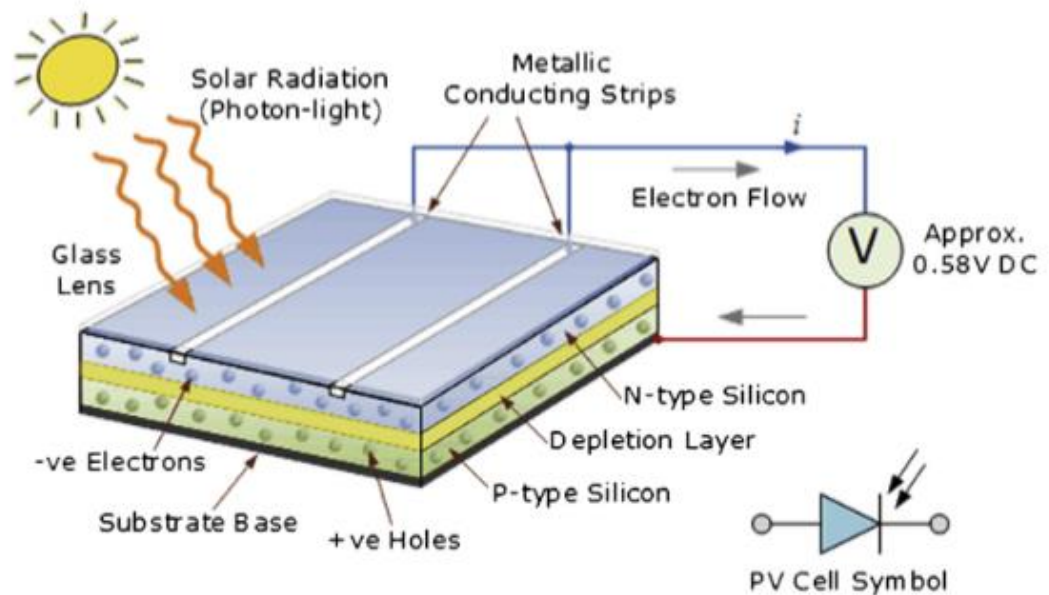
Figure 2-17: Solar cell converting sunlight to electrical energy (Amin et al., 2017)

The PV cell is made with a PN junction and when the sunlight strikes the cells, the energy level of electrons raises then the electron-hole pairs are formed by the interaction of photons with the atoms of the cell. This interaction results in the electric field by the cell junction which leads to photon-generated-electron hole pairs to separate and electrons would move to the n-region of the junction while the holes shift to the p-region of the junction(Messenger & Ventre, 2004). The output of the single cell is not adequate for practicality so for voltage increase the photovoltaic cells are connected in series and for current, they are connected in parallel to make a PV module. The PV modules can be connected both in parallel and in series to form a PV array with a particular rated power(Muaelou et al., 2015). The bigger chunk of power produced by photovoltaic is due to the array set up. The power produced is proportional to the amount of the solar irradiance which is the DC voltage and when it is interfaced in the grid then inverters are employed to produce a 50Hz AC voltage(Moussavou, 2014).
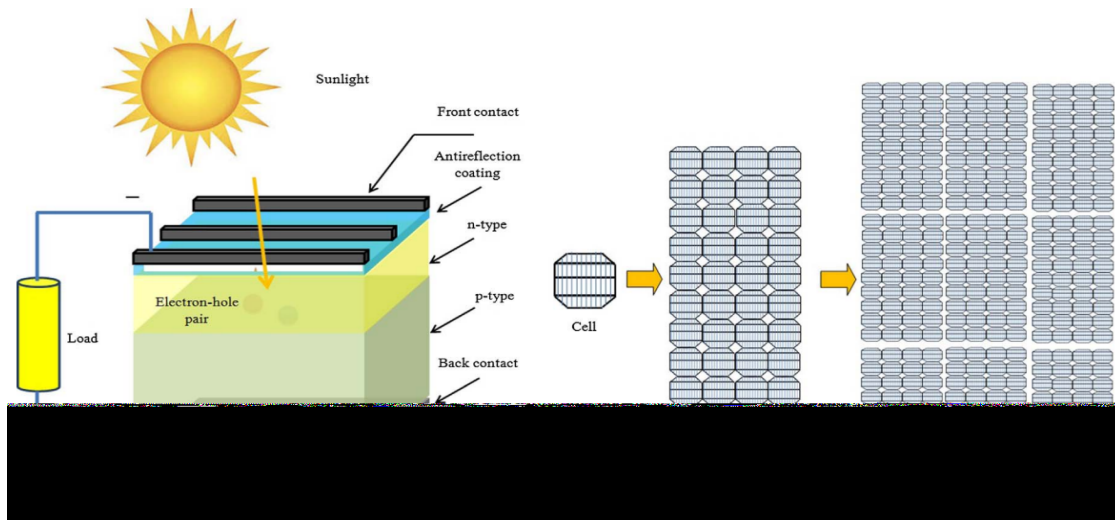
Figure 2-18: Formation of PV array by PV cells

The most critical parameter in the comparisons of power technologies is the cost of energy per kilowatt-hour (kWh) which is the conversion efficiency of the PV and the capital cost per watt capacity. The conversion efficiency of a PV is then given by

$$\eta = \frac{\text{electrical power output}}{\text{solar power impinging the cell}}$$

There has been continued development to improve the efficiency of PV panels at a low cost so as a result there are several different PV panels in the market and they will be discussed how they are manufactured and their efficiencies(Patel, 1999; Battersby, 2019). The USA has 60 gigawatts installed which are expected to double in the coming 5 years while China in 2017 alone installed the equivalent total PV capacity of the USA. Most PV panels have silicon crystals material in them, and they can only convert 15-19% of the irradiance into electrical energy. Stephen Forest who leads research on optoelectronics indicates that organic molecules like polymers and dyes which are synthesized into simple ingredients could be utilized as a light-absorbing layer of a PV cell. This new developments in PV cell which don't use silicon and the reduction in silicon price improves chances of reducing the carbon footprint. This organic cell is very flexible unlike silicon so it can be rolled on rooftops or made on top of surfaces without the thick glass plates. They can be made to make windows as they can be utilized to absorb only infrared light and equally maintain transparency (Battersby, 2019).

2.11.2 Maximum power point tracking (MPPT)

The power output from solar PV relies on atmospheric conditions thus poses a problem of varying power. The solution is MPPT which plays a critical role in the extraction of maximum power from a PV module. Different techniques help in the attainment of the maximum power point(MPP) and if it varies depending on the method, control strategy, and the speed at which

MPP is achieved (Mano & Jeyakumar, 2014). The topology of microgrids relies on the type of power converters which are AC-DC, DC-AC, and DC-DC. The MPPT is made up of a step-up or step-down DC-DC converter to regulate voltage and current at the load. This is attained by a duty-cycle control circuit. There are several MPPT methods which are:

- Perturbation and Observation(P&O)
- Incremental conductance methods (InCond)
- Constant current or constant voltage
- Advanced techniques (fuzzy control, Neural networks, and voltage-based scheme(Prakash et al., 2014).

1.

These techniques have been developed over time and differ in several aspects such as sensors, complexity, cost of effectiveness, convergence speed, correct tracking during variation of weather conditions, hardware needed a lot of other factors. Among the techniques mentioned above two of them which are the P&O and InCond. These methods are the ones that are frequently employed algorithms than other methods. The normal P-V curve has one maximum point, but this is different in the case of partial shading where there are multiple maxima in these curves. P&O and InCond utilize the hill-climbing principle where they move the operating point of the PV array to the direction where power increases. These two techniques are advantageous as they require low computational power and are simple. They, however, have a drawback especially on the rapidly changing weather conditions the oscillations occur on or around the MPP and they get lost which results in the tracking of MPP in the wrong direction (Sumathi et al., 2015).

2.11.3 Perturbation and Observation algorithm

This algorithm employs voltage or current variation to obtain the greatest or smallest value; both voltage and current are directly proportional to power. If the power is increased, the variation continues in the same direction; otherwise, the variation changes direction (Moubayed et al., 2014). The P&O entails the deviation of the power converter's duty cycle and the deviation of the operating voltage of the DC-link between the PV array and the power converter. Varying the duty cycle results in the adjustment of the voltage of the DC-link between the PV array and the boost converter. In the P&O techniques, only one voltage sensor is employed to detect the PV array voltage hence why the cost implications are less (Sumathi et al., 2015).
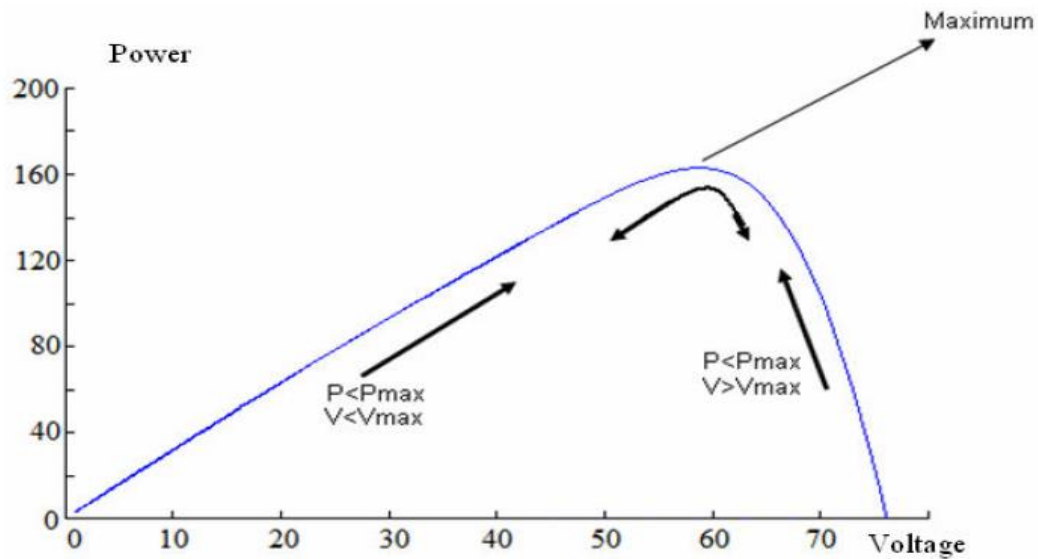
Figure 2-19: P&O P-V curve method (Moubayed et al., 2014)

The steps executed for the P&O technique are:

- Measure current and voltage, calculate power,
- If power is constant, return to take new measurements,
- If power is decreased or increased, test the voltage variation,
- Based on voltage direction then modify current (Moubayed et al., 2014).
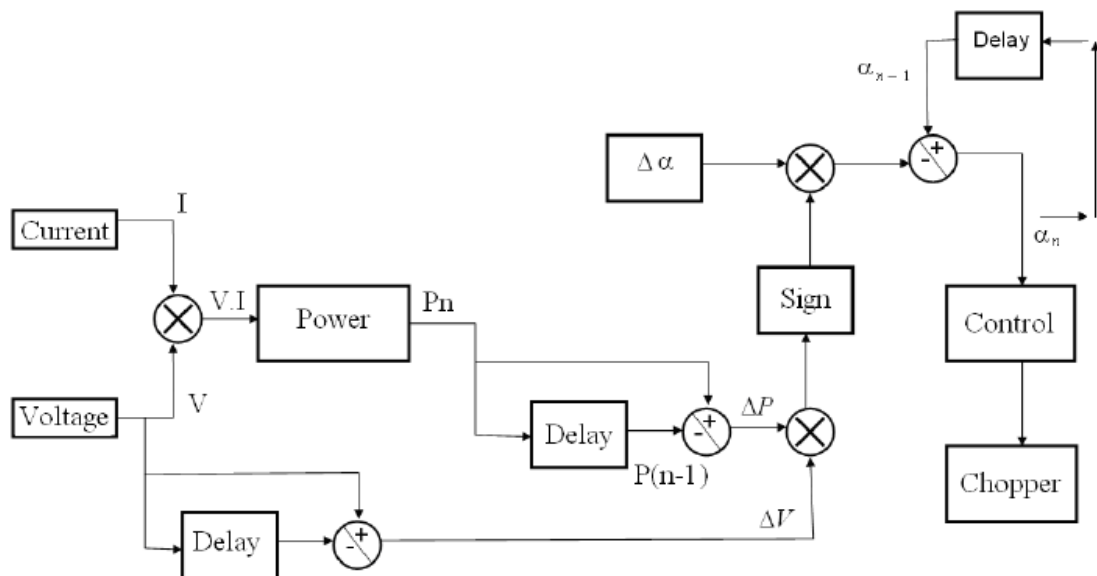
Figure 2-20: Block diagram of P&O (Moubayed et al., 2014)
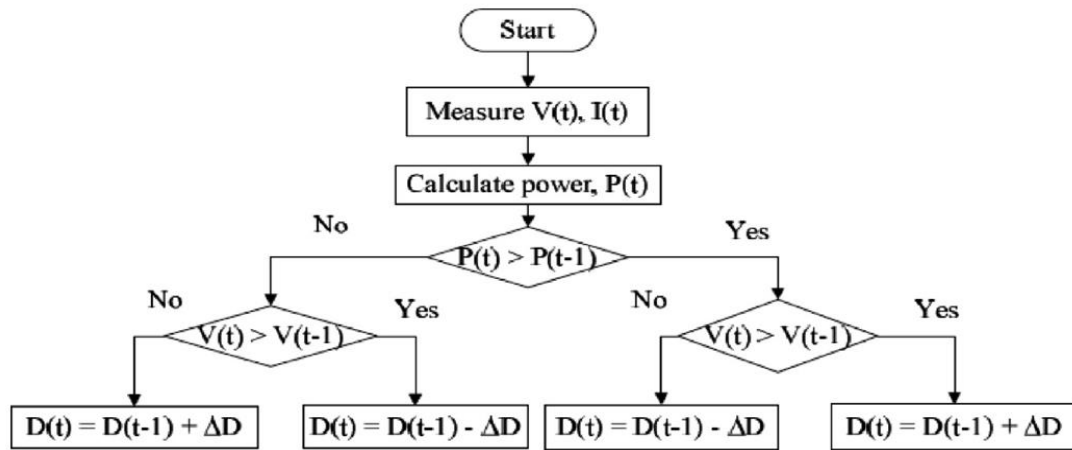
Figure 2-21: Flow chart of perturb and observe method (Eltawil & Zhao, 2013)

In the P&O the PV array voltage is increased slightly and that results in a small change in power. If the power change is positive, meaning it is increasing then the continuous increase of the voltage so the operating point moves closer to MPP. When the small voltage increments lead to a smaller power output than the previous one then the voltage decrease is triggered so to get a higher power output meaning the operating point is closer to the MPP (Eltawil & Zhao, 2013).

Limitations

According to Eltawil & Zhao (2013), the deficiency of P&O is such that when the irradiance decreases the P-V curve flattens out and it becomes tricky to locate the MPP due to the small change in power concerning the perturbation of the voltage. The other limitation for P&O is it can not identify the MPP so it oscillates around the MPP so a higher frequency rate of change of irradiance can provide erratic MPP. Suppose the MPP is at point A in curve 1 and the oscillation is taking place between points A, B, C then there is a sudden increase in the solar irradiance then the P-V curve array moves to curve 2. If during the oscillation, the operating point was supposed to move from A to B then a shift to curve 2 due to change in irradiance happens the MPPT would shift from A to D then the perturbation would go towards F because of the positive change in power relative to the last power measurement of curve 1 and the same scenario would continue if there is still rapid change in the irradiance where there would be a shift from point D in curve 2 to G in curve 3 and this means the MPPT is moving away from the MPP. The scenario is more prevalent on cloudy days where the is a rapid change in solar irradiance.
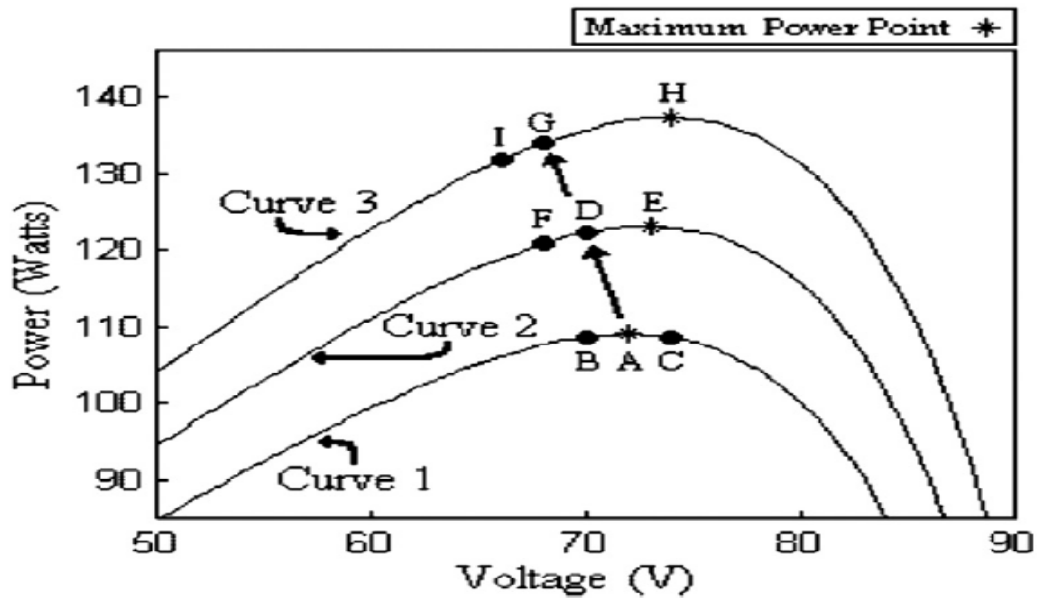
Figure 2-22: Limitations of P&O under the rapid change in irradiance (Eltawil & Zhao, 2013)

2.11.4 Incremental Conductance (InCond)

The InCond algorithm utilizes two sensors for voltage and current to determine the current and voltage of the PV array. The terminal voltage is adjusted towards MPP voltage and it is based on the incremental and instantaneous conductance of the PV module. The gradient of current relative to voltage is employed to reach the MPP. This is the point where the gradient or the derivative is zero (Sumathi et al., 2015). Moussavou (2014)states that to curb the limitations of P&O, the InCond algorithm relies mainly on power variation as compared to the P&O algorithm which is applied on MPPT based on the weather conditions. InCond algorithm is checking the rate of change between voltage and power and setting the result to be equal to zero (Eltawil & Zhao, 2013).

$$\frac{dP}{dV} = \frac{d(VI)}{dV} = I + V\frac{dI}{dV} = 0 \text{ at the MPP}$$

Rearranging the above equation

$$-\frac{I}{V} = \frac{dI}{dV}$$

Where the left side is the instantaneous conductance and on the right side, it is the incremental conductance. This means at MPP both sides must be equal in magnitude but have different signs. If there is a deviation or the result is not zero, the determination of the outcome on whether to increase or reduce the PV voltage to attain the MPP is as follows (Eltawil & Zhao, 2013):

$$\frac{dI}{dV} = -\frac{I}{V}; \quad \left(\frac{dP}{dV} = 0\right), \text{ at MPP}$$

$$\frac{dI}{dV} > -\frac{I}{V}; \quad \left(\frac{dP}{dV} > 0\right), \text{ Left of MPP}$$

$$\frac{dI}{dV} < -\frac{I}{V}; \quad \left(\frac{dP}{dV} < 0\right), \text{ Right of MPP}$$
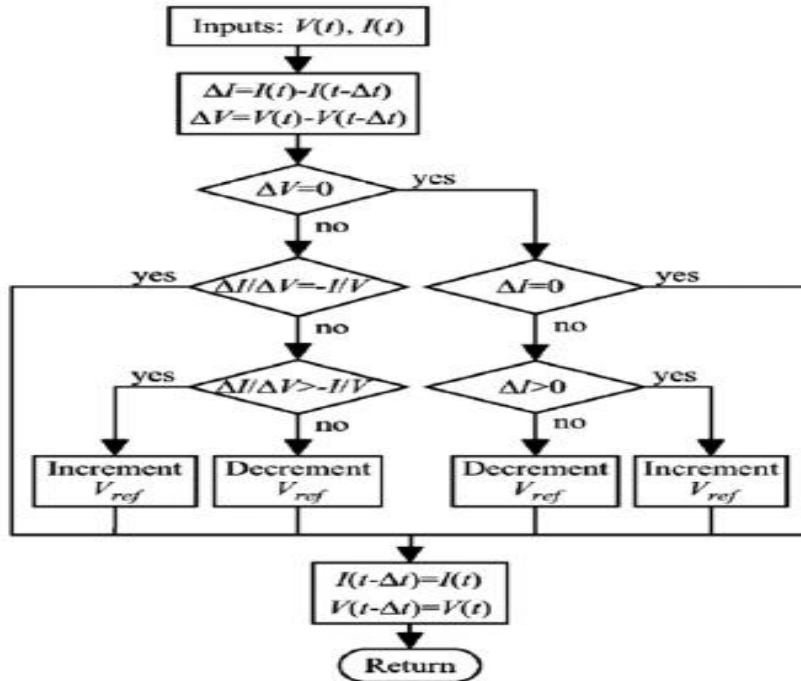
Figure 2-23: Incremental inductance algorithm (Eltawil & Zhao, 2013).
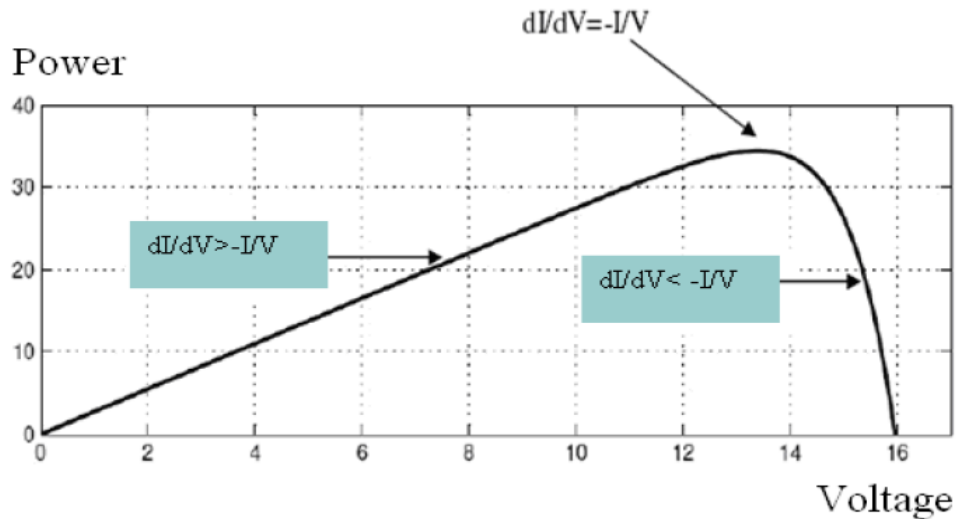
Figure 2-24: Power output using InCond technique (Moubayed et al., 2014)

2.12   The State of PV in South Africa

South Africa has high solar potential where the dominance of high solar irradiance is in the Northern Cape province with better irradiance per square meter. Annually there are over 2500

hours of sunlight with solar irradiance of between 4.2 – 6.5 kWh/m² daily. The total installed capacity of PV is 1.47GW with 509MW was linked to the grid in 2016. The country has been experiencing a power crisis in recent years where load shedding has been implemented to avoid the total blackout of the country and the country continued with the renewable energy independent power producer procurement(REIPPP) program where Eskom signed power purchasing agreements (Bellini, 2017).
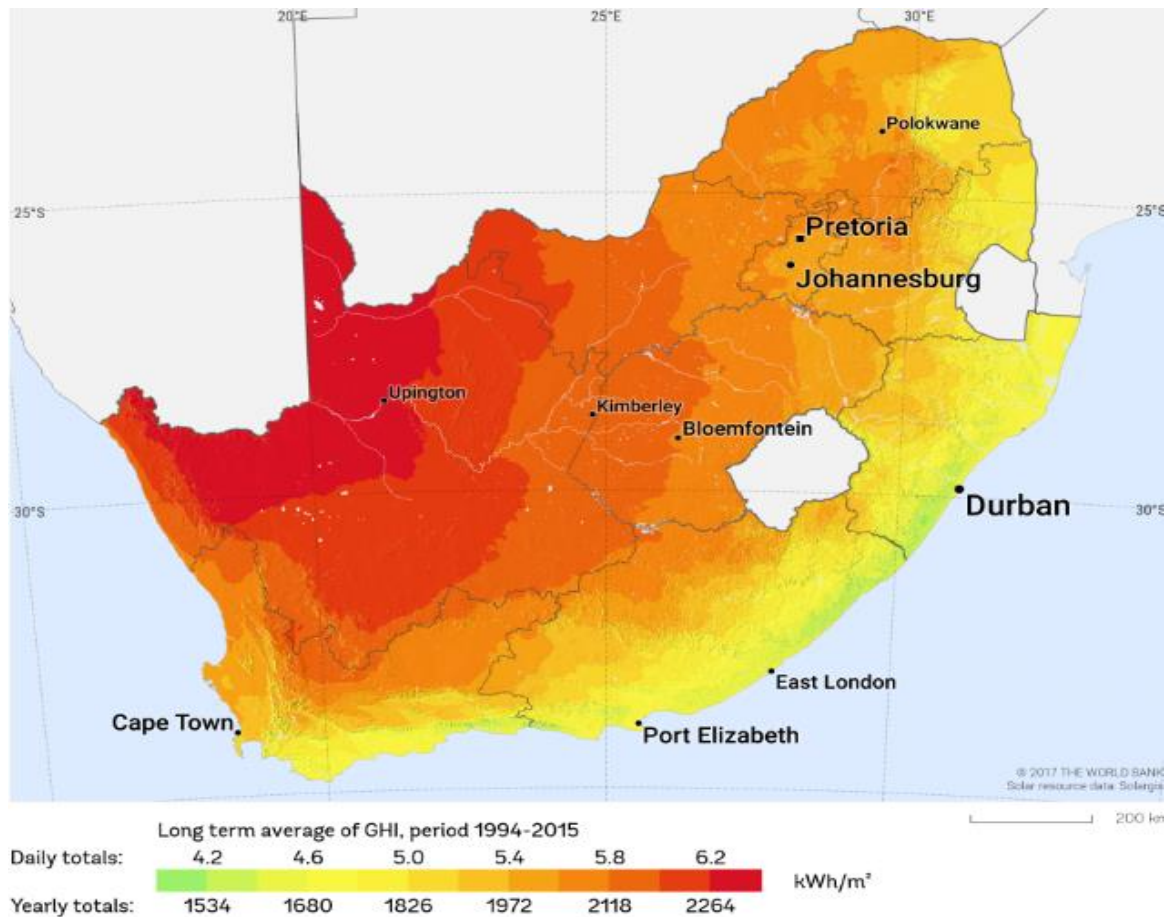
Figure 2-25: South African Global Horizontal Irradiation Data (SOLARGIS, 2019).

2.13 Energy storage systems

There are several energy storage devices and their main task is to balance power and energy demand with the generation. The DG has low inertia, so it becomes challenging to respond to the disturbance that is where the storage systems can mitigate this problem. Renewable sources like wind, solar PV, and hydro in some instances the primary power fluctuates and this results in the provision of variation to power or none at all so the energy storage can dispatch power (Mariam et al., 2016)

The electrical load keeps growing and the power system infrastructure is not able to keep up with to meet the load demand due to the expenses to build new systems, environmental concerns, and the technical aspects which hinder the power system in meeting the load. This

issue has caused major concern in power quality due to the slow response time from synchronous generators during the disturbances to maintain the stability of the system. Devices such as flexible ac transmission systems (FACTS) are perfect measures to control load shedding or drooping from the generator and in the case of high-speed real power the control is done by the power circulation in the converter. The better way to mitigate high-speed real or reactive power control would be the variation of real power at a higher frequency without tampering with the system with power circulation. The energy storage systems then become very important in this regard due to their quick response time in load changes, meeting the load during a power interruption, correction of load voltage profile by injection of reactive power, and can minimize the oscillations(Ribeiro et al., 2001).

Energy storage is defined by the most critical parameter which is the storage capacity which is the amount of stored energy that could be utilized when needed. In comparison with other storage devices that have different capacities, the other term is used is energy density and that is the energy that a device stores per unit volume. There is also the power density which is the amount of energy that could be dispatched to the load. Storage devices such as batteries and fuel cells can store a large quantity of energy but it takes a while for both charging and discharging whereas capacitors can provide a large amount of power in few seconds but have small storage capacity. Supercapacitors employ new technological devices that assist them to have high energy density and high power density (de Villiers, 2009).

The energy stored in electrical systems and electronic devices is in two forms which is the short term where capacitors and inductors form part by storing energy in electrostatic and electromagnetic form respectively. The second is the long-term storage where energy storage devices are employed for either backup system provided that the energy source can not meet the load or it is not producing at all, it is even employed to improve power quality(Nihal, 2015). Electrochemical batteries continue to play a crucial role in day-to-day human activities. They are used in several devices such as mobile phones, laptops to mention a few (Ovali, 2016). Electrical energy must be used immediately after being produced or it will be changed to another un-useful form of energy thus arise the need to store electrical energy especially in the islanded weather-dependent energy sources. Batteries are electrochemical systems devices that change chemical energy to electrical energy and vice versa(Olabi, 2017).

The electricity demand spike in recent years gives rise to supply that is less than the demand. To meet the load means the expansion of existing electricity generators but in developing countries, this is unlikely due to economic, technical, or political reasons. This lead to blackouts so to curb this problem a diesel generator was employed but the reduction in PV-module prices and the anticipated increase in fuel prices means the employment of only diesel generators would be relatively expensive (Alramlawi et al., 2018). The increased penetration by

Renewable energy sources(RES) means there is an interest in energy storage techniques. There are ways in which the energy storage is selected, and the factors as follows:

- Availability of the energy resource,
- Energy requirement and application,
- Energy efficiency storage,
- Energy storage cost,
- Energy storage infrastructure.

Classification of Electrical Energy Storage Technologies

Mechanical	Electrochemical	Electrical
Pumped Hydro-PHS	Secondary battery Lead-acid/NaS/Li-ion	Capacitor Supercapacitor
Compressed Air-CAES	Flow battery Redox flow/Hybrid flow	Superconducting Magnetic-SMES
Flywheel-FES		

Thermochemical	Chemical	Thermal
Solar fuels Solar hydrogen	Hydrogen Fuel cell/Electrolyser	Sensible/latent heat storage

Figure 2-26: Classification of Electrical Energy storage technologies (Luo et al., 2015

2.13.1 Superconducting Magnetic Energy Storage (SMES)

Superconductivity was found in 1911 but only in 1970, it was when it was classified as an energy storage technology. The charge and discharge of efficiency of 95% are but some of the capabilities that have boosted the interest in SMES in electric utilities as well as the military. There are several applications where SMES can be employed such as in voltage stability, frequency regulation, and power quality improvement to mention a few(Ribeiro et al., 2001).

When current flows through the coil the magnetic field will be induced. SMES uses the same principle, when direct current flows in the superconducting coil the DC magnetic field will be formed. Superconductivity is the absence of electrical resistance below a critical temperature. The coil cooled so that the coil material is at low temperature and that helps in the attainment of no resistance in the coil. The outcome of this is the current continues to flow even when the power source is disconnected, this is due to the superconductivity of the coil and this means energy is stored in the magnetic field as it is maintained by the flow of the current. The SMES device has the advantage of being very fast in response and is employed in special circumstances(Nihal, 2015).

The SMES is made up of a superconducting coil of which the temperature is maintained low so there is no resistance by either liquid helium or nitrogen. SMES is connected to the ac power using power converters and it is also to either charge or discharge the coil. Two power converters are employed when the SMES is used and those are namely the current source converter and the voltage source converter. They are both used to interface the superconducting coil to the ac power system. The decision to determine if to discharge/charge/standby is influenced by the control of the made by voltage across the SMES coil, so if there is the positive voltage across the coil it will charge and it will discharge if the negative voltage across the coil(Ribeiro et al., 2001).
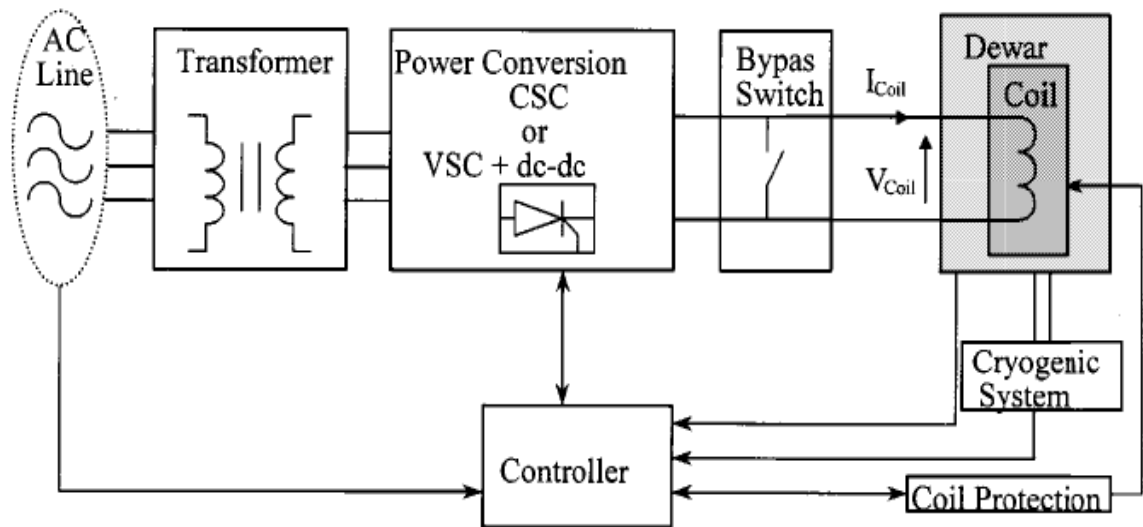
Figure 2-27: SMES layout (Ribeiro et al., 2001)

The energy is stored in the magnetic field generated and it is given by:

$$E = \frac{1}{2}LI^2$$

(2.8)

Where E is the energy (Joules), L is the inductance of a coil and I is the DC flowing in the coil to create a magnetic field (Ribeiro et al., 2001).

2.13.2 Fuel Cell (FC)

This is a device that changes the chemical energy of a fuel to electrical energy by electrochemical technique. This is where the latent chemical energy of a fuel of which hydrogen is mainly employed is used to produce electricity. The hydrogen which is the fuel on the anode is oxidized by oxygen ions so that the molecules are broken down into electrons and protons while oxygen on the cathode reacts with electrons from the outward circuit to produce oxygen ions. The protons move through the electrolyte membrane whereas the electrons are forced through a circuit thus producing electric currents and heat   (Guney & Tepe, 2017).

The fuel cell is made up of several common components. They are anode which is the fuel electrode or the negative side which loses electrons to the outer circuit where hydrogen oxidation materialized. There is the cathode which is the oxidizing electrode that gains electrons from the fuel electrode on the outer circuit while reducing the oxygen. The other component is the membrane electrode assembly is squeezed between two electrodes that have a catalyst in it. There is also a proton exchange membrane which is a polymer film that operates as a filter by blocking gasses and electrons and letting hydrogen ions pass through it and they are known as protons(Jha, 2012).
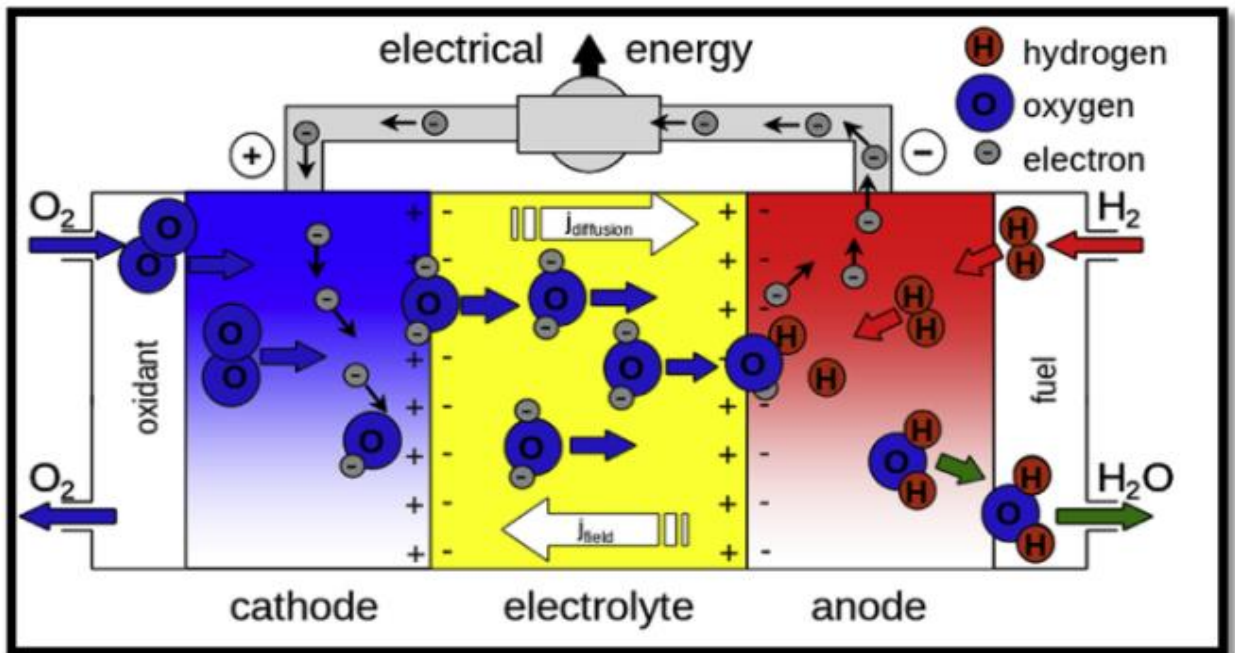
Figure 2-28: Working principle of the fuel cell (Jaiswal et al., 2019)

2.13.3 Mechanical Flywheel

This is a mechanical energy storage system that is at times referred to as a mechanical battery where energy is stored by changing electrical energy into kinetic energy. The flywheel has a mass that is accelerated by the electricity source which is being coupled to it through a shaft. The amount of the kinetic energy stored is dependent on the moment of inertia of the flywheel and the square of the angular velocity.

$$E_k = \frac{1}{2}I\omega^2 \qquad (2.9)$$

Where

$$I = \int r^2 \, dm \qquad (2.10)$$

$$I = \frac{1}{2}r^4\rho\pi h \qquad\qquad (2.11)$$

After integration, substitute for volume and get the value of the second moment of inertia

$$I = mr^2$$

E_k =Kinetic energy

$I =$ Moment of inertia

dm= Small mass which density (ρ) by small volume (v)

r= Radius of the cylinder/flywheel

(Mousavi et al., 2017)

According to Molina, (2017) and Luo *et al.*, (2015), the mechanical flywheel is made up of five basic components namely the magnetically laminated bearings which reduce the friction that results in the wearing of bearings thus improving the efficiency of the storage system, the flywheel, the electric generator/motor, the power electronics unit and the vacuum enclosure. The flywheel is assembled in a vacuum to reduce the drag force which will be caused by the air. When there is a power transmitted from an electric drive and results in positive torque to the flywheel when the motor is spinning at high speeds then electrical energy is stored as kinetic energy and when electrical energy is required then the flywheel is decelerated producing negative torque so electrical energy produced from stored kinetic energy.
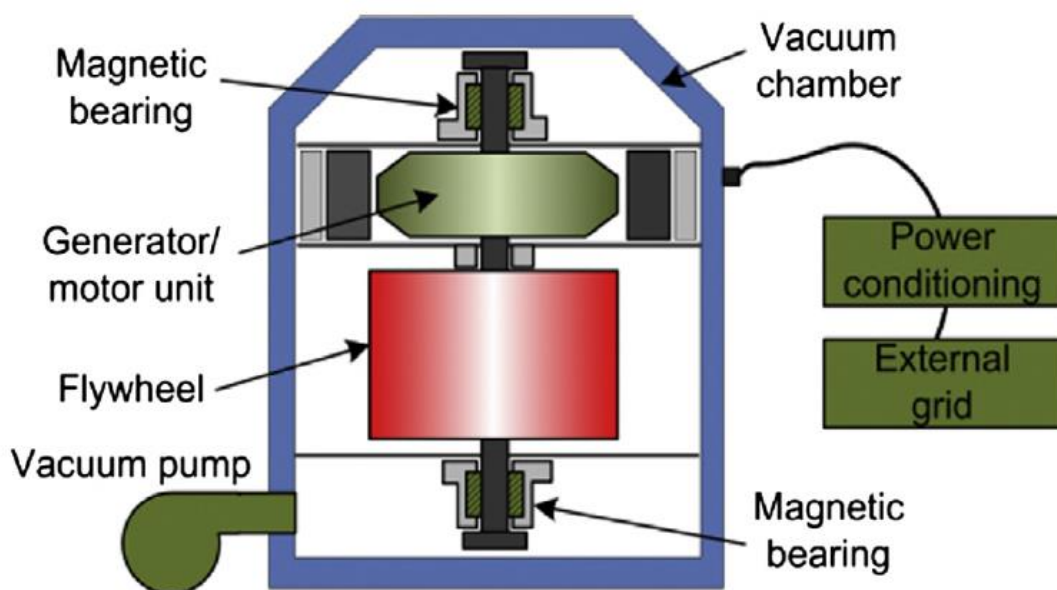
Figure 2-29: Flywheel storage system layout (Luo et al., 2015)

2.13.4 Compressed air energy storage (CAES)

When excess electric power is produced it is then diverted to power a reversible motor/generator unit which is connected to the compressors to pressurize the air. The pressurized air is then stored in mainly underground caves or storage vessels so it could be used when the demand increases. When it is peak time the high-pressure compressed air is freed to the turbine, but it is pre-heated, so it becomes superheated either by heat extracted on the compression process through a heat exchanger or move through a furnace. Once the high-pressure air is heated it is then used to turn the turbine blades of which are connected to a shaft that is coupled to a generating unit that produces electrical power (Luo et al., 2015).
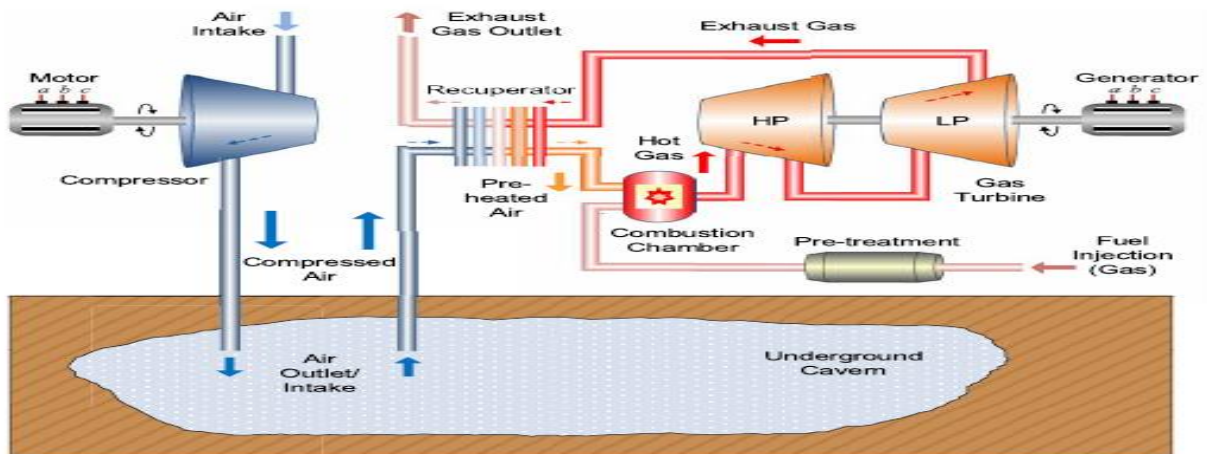
Figure 2-30: Compressed air storage schematic diagram (Ribeiro et al., 2001)

2.13.5 The pumped hydro storage system

This is a storage system where two reservoirs are used, the other one at a higher elevation than the other. When the energy sources mainly the intermittent ones like solar and wind are producing access to electrical energy, the excess energy is used to pump water from the lower reservoir to the higher reservoir. This usually takes place during off-peak hours, when the demand gets high the water is then released. The power produced is dependent on the volumetric flow rate, due to the difference in elevation from the higher reservoir to where the turbines are located. The water will turbine the turbine blades which turn the shaft that is coupled to the generator to produce electricity to cover where the sources could not meet the load(Guney & Tepe, 2017).

2.13.6 Battery Storage Systems

The battery system is employed to maintain the stability of the grid by balancing the power. This is done by the battery becoming the load when there is an excess of energy in the grid or as a voltage source when there is a deficit. There are three major parts in the battery storage system which are the batteries, battery management system(BMS), and power conversion system(PCS).PCS's primary task is to convert the DC power from the battery to AC power and manage power flow during the charging of the battery and discharging. BMS is the control unit for both the battery and the PCS which determines which direction should the power flow(Lindstens, 2017).

Energy storage is the most important component in the microgrid where it is used to store energy especially when access power is produced. The anatomy plays a pivotal role in the running time of the system without generated power and the anatomy determines the capacity of the storage. The proper sizing of the storage must be done in a way that does not comprise the quality of power but also if the anatomy is high the system would be more costly. The other critical matter in the battery bank system is the depth of discharge (DOD) which is the amount of energy the battery delivered. The DOD is calculated by dividing the battery capacity by the anatomy(Mendis et al., 2016).

Factors that influence the performance of the battery are the temperature, the type of the battery, and its age. There is an improvement in the design of deep-cycle lead-acid which is installed where there is a need to discharge or charge rapidly (Keyhani, 2011). The biggest challenge with chemical batteries is that they pose an environmental challenge when they are replaced due to the chemicals in them(Du Plooy, 2016). The construction of the battery bank is based on the capacity, power, response time during fluctuations, and discharge rate. There are several batteries utilized and depending on the application them the choice will differ. Those are lead-acid, lithium-ion, vanadium-based flow, sodium-sulfur, aluminum-ion batteries(Zhang et al., 2018).

Table 2-8: Advantages & Disadvantages of Batteries (Zhang et al., 2018)

Battery Technology	Advantages	Disadvantages	Energy storage applications
Lead-acid	Less expensive	Limited lifespan, long to charge, and high self-discharge Environmental pollution	Frequency control and load adjustment

Lithium-ion	High energy density, great efficiency and have a long lifespan	Expensive production cost needs special charging circuit	Frequency control, load shifting, and power quality
Vanadium based flow	Long life cycle, quick to charge and to discharge	Expensive production cost, need a large area	Load shifting, back-up for emergency and power quality
Sodium-sulfur	Great efficiency, high power, and energy density	It has safety concerns	Load adjustment and backup power
Aluminium-ion	Less expensive, quick to charge and discharge, great efficiency	Not fully developed Low energy densities	N/A

2.13.7 Energy Management Methods in Hybrid

Challenges are being experienced by the conventional way of producing power due to the depletion of fossil fuel, microgrids are gathering momentum to further reduce the carbon footprint globally. Microgrids consists of distributed energy resources with loads.

The increase in the deployment of renewable resources globally in power systems by governments to reduce the carbon footprint and to be energy efficient. These systems are used to supply islanded loads that are far from the grid. Renewable energy sources are intermitted in nature, so they need backup systems in a form of energy storage systems. The improvement of reliability means more than one renewable should be employed which forms a hybrid system and whenever there is a hybrid system there must be an energy management strategy that directs the flow of energy in the system. This strategy for standalone systems ensures that renewable resources always meet the demand. Control system is the core of the hybrid systems so to facilitate the communication between the components and regulates the power from the renewables, the charging, and dispatch of energy storage systems and it also protects them from overcharging or going below the operational limit. The signals are sent to the energy storage if there is access power to charge them and in the case of the battery energy storage it protects from over-discharging. (Olatomiwa et al., 2016).

The energy management of a system is in two phases which are economic and technical. This addresses how the system can operate in a manner to provide optimal return on investment based on several factors such as the type of technology to be employed, sizing of a system to mention a few. These decisions also made to provide good power quality and provide a robust system that consumers can rely on at an optimal price(Marzband et al., 2012).

Operation and Control are the lifeblood of microgrids as two or more distributed generators need to communicate to yield a good operation and provide a good power quality to the load. The challenge facing microgrids is to maintain frequency in their desirable rage by balancing active power.

2.13.8 Related Work

There are several studies conducted to study various ways in which energy can be managed. Authors (Xu et al., 2019) modelled an AC hybrid system power system with wind-solar and pumped storage hydropower. The focus is on the integration of pumped storage to the power system with effects of shaft vibrations and the governing strategies which increase dynamic risk and leads the disturbances. The system is modelled in Matlab/Simulink to mitigate those disturbances by unifying the hydro-turbine governing system and the hydro-turbine generator unit. The three-phase short circuits are mimicked to test the feasibility of the pumped storage when integrated into the hybrid system. The results indicate that the current and voltage of the pumped storage briskly gets to normal operation after the fault has been cleared. Moreover, the results further indicate that the pumped storage can quell fluctuations from solar and wind power

In (Nazir et al., 2014), both the HOMER and Matlab/Simulink are used in a microgrid that is made up of MHP, PV and they are grid-tied. When the author optimizes the system HOMER is utilized using the local renewable energy available of Gunung Nago to check for the combination that would yield the lowest cost and most reduction in carbon dioxide emissions. The baseload profile, availability of water resources, and solar radiation were used to simulate the possible microgrid. The possible solutions from however needed costly initial capital cost and the system was then modelled in Matlab/Simulink. This system however indicates a lot of power fluctuation throughout the simulation from the MHP. The battery power during the load fluctuations is not shown to validate the response time.

 The author Guan *et al.*, (2015) illustrates the combination of several renewable energy sources that helps in the accessibility of electricity, especially in remote areas. Despite that the coexistence of more power sources specifically renewables to form microgrids leads to system instabilities. This is due to different inertias and control strategies. The focus of the research is the hierarchal controller of the hybrid microgrid to accomplish the smooth parallel operation. It further dealt with power-sharing performance and PV and battery being the PQ bus to inject the required active and reactive power to the local grid. The hydropower is operated as the slack bus to regulate the voltage amplitude and the frequency. The system tested different

scenarios where the load is removed from the system or added to test the response to maintain the frequency of the system. In instances where the load is suddenly removed the frequency increases from 49.99Hz to 49.995Hz due to hydraulic power output decrease and experience a 0.001 per unit spike. The different scenarios have tested the robustness of the system and indicate that the system can operate effectively on parallel operations with varying loads.

In this study the research is based is on Mae Sariang microgrid using FLC control on the battery energy storage system (BESS). quest for a quick response from energy storage systems to maintain both the frequency and voltage using energy management techniques is being explored. The system consists of the PV array, diesel generator, hydro generator and, BESS. The system is modelled in DIgSILENT PowerFactory software using FLC to stabilize frequency and voltage fluctuations with BESS. The system is analysed on a standalone microgrid to test how fuzzy logic control performs to control active and reactive power injection from the battery storage system to mitigate the frequency and voltage fluctuations (Tephiruk et al., 2018)

Nowadays there is a significant amount of research conducted on energy management control. Authors Roumila, Rekioua and Rekioua, (2017) modelled a hybrid microgrid system with the wind, photovoltaic (PV) diesel generator with a battery storage system with an intelligent supervisory control based on fuzzy logic control for power balance. Authors Olivier, Abo-al-ez and Kahn, (2020) focusses on energy management on residential load with varying demand using simpower toolbox from Matlab/Simulink also considering wind, PV, and Lithium-ion battery storage. In (Rai & Rai, 2018) the focus is to meet DC loads demand utilizing PV and battery storage to form a standalone hybrid microgrid system and the energy management control is using FLC. Authors in Luta and Raji, (2019) use fuzzy logic for energy management control of a system that comprises a PV array, an electrolyzer, a proton exchange membrane, and a hydrogen tank.

Previous studies have suggested that the combination of PV and Micro-hydropower can help in the stability of the power supply as hydropower and pumped storage has a great regulating ability. However, this too poses a challenge of not meeting the load hence the requirement of a storage system(Fahad et al., 2018; Vera et al., 2019; Nag & Sarkar, 2018; Anitha & Krishma, 2015).

3   CHAPTER THREE: SYSTEM MATHEMATICAL MODELLING

3.1 Introduction

The volatile nature of RE sources relies on weather conditions and most of them produce DC power and this prompts the need for power electronic device as an interface. This chapter presents a literature survey on power electronic devices' history and developments through time. It further presents how those devices are utilised as an interface between two renewable sources producing DC power to AC load. Mathematical modeling of a PV module and MHP as well as the analytical breakdown of inverters, governors, turbine model, and the excitation system are well analysed.

3.2 Power electronics

Power electronic devices are electronic devices utilized to control and convert electric power. This is achieved through switching between different circuit configurations. It can convert power from variable frequency AC to DC or vice versa depending on the application. The power electronic devices are made up of inductors, capacitors, and semiconductor switches. The uncontrolled switches are line commutated such as thyristors instance diode, where the controlled ones employ circuits using control signals (Luta, 2019).

High penetration of distributed generators requires power electronic devices to interface from the generation to a load. They manage power flow, maintain output frequency and voltage in the case of the inverter. High renewable generation leads to reduced inertia which is critical in maintaining the frequency stability of power systems. The virtual inertia generated by DC-link capacitors of power electronics converters is now being employed. The DC-link is also used in supercapacitors and battery storage is also used as an alternative inertia supplier. The technological advances in semiconductors and control will lead power electronics to be matured for inertia control soon (Fang et al., 2018).
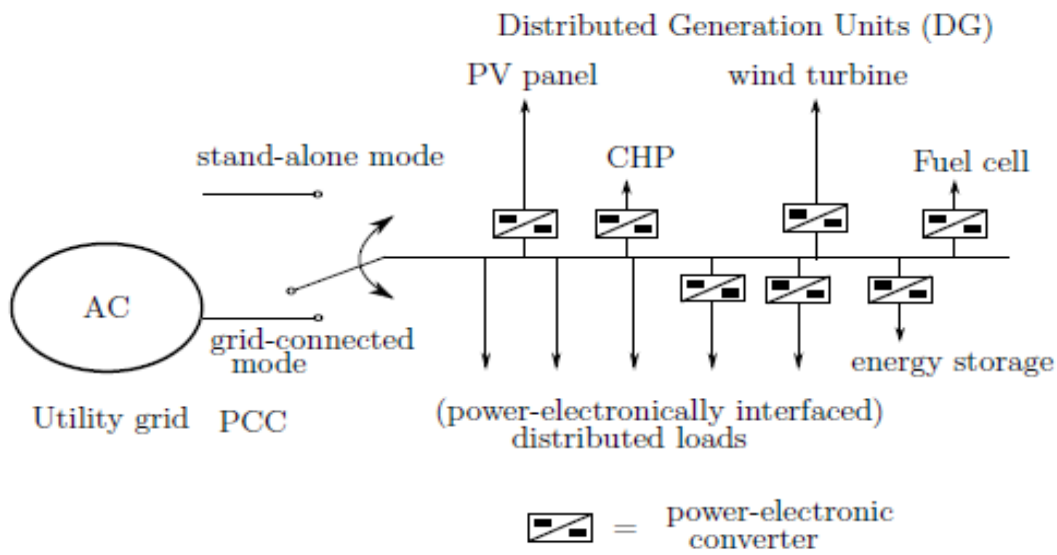
Figure 3-1:Microgrid standalone and grid-connected with power electronics (Vandoorn et al., 2010)

The semiconductor devices were discovered in 1950, and since then huge developmental research around this area has been done. There has been a rapid development of power electronics in the past three decades due to improvements in semiconductor devices and microprocessor technology (Iov et al., 2007).
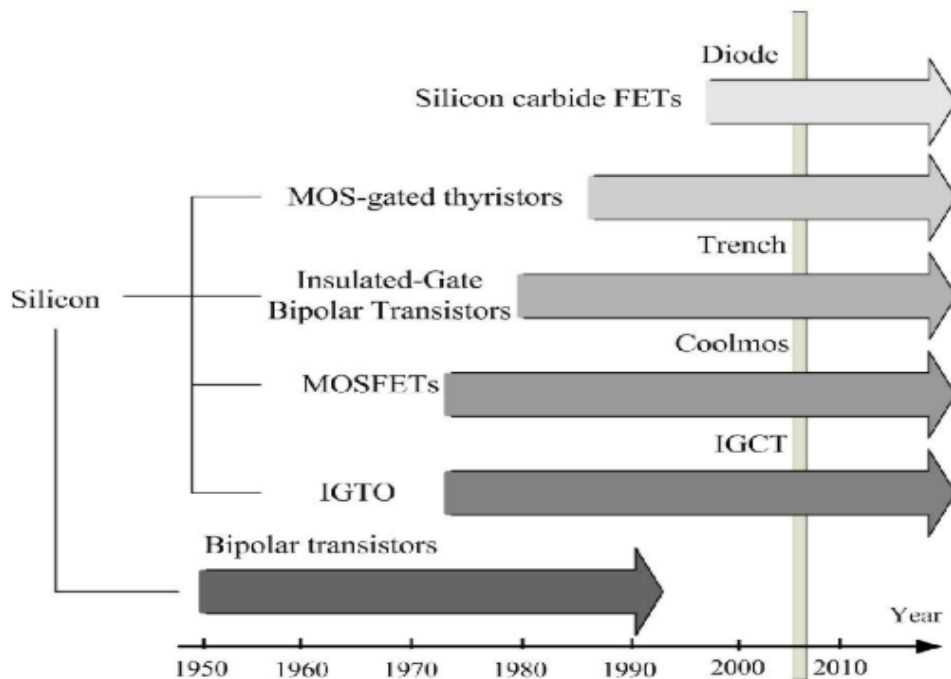

Figure 3-2: Development of power semiconductors (Iov et al., 2007)

The DG such as wind turbine and PV systems that form microgrids leads to system instabilities that do not provide continuous power. This is because of lack of inertia or is less as compared to the generator inertia for energy balance. The solution of making this possible is to be connected to the grid or three-phase source is the use of power electronics devices. This device helps in the interfacing of the DG to the grid by changing the power from the DG source to a fixed frequency AC power, they improve the flexibility and adaptability of the system and provides ancillary services(Mahmoud et al., 2014).

The integration of DC-AC grid or source employs mostly power converters which are conditioning devices that regulate voltage and frequency to make it compatible with grid qualities. The distributed generation such as photovoltaic and fuel cell generates DC power while Wind Energy and microturbines produce AC power with varying frequencies which need the inverter to interface to the grid with voltage and frequency at required standards(Mataifa, 2015)

3.3 Solar PV mathematical modeling

The construction of a PV cell entails a lot of complex physics fundamentals, so the equivalent circuit is shown in figure 3.3 below which shows diode and ground leakage currents.
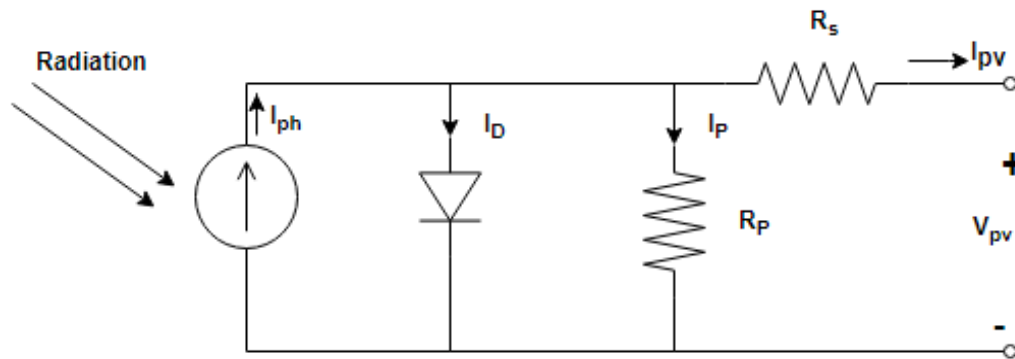

Figure 3-3: PV cell with a single diode (Mataifa, 2015)

The mathematical modeling of a PV cell single diode is based on the following equations;

$$I_{PV} = I_{ph} - I_d - I_p \tag{3.1}$$

$$I_d = I_0(e^{\frac{V_{PV}+IR_S}{V_t}} - 1) \tag{3.2}$$

$$I_0 = I_{RS} \left(\frac{T_G}{T_{ref}}\right)^3 e^{\frac{qE\left(\frac{1}{T_{ref}} - \frac{1}{T_G}\right)}{AK}} \qquad (3.3)$$

$$I_p = \frac{V_{PV} + I_{PV}R_s}{R_p} \qquad (3.4)$$

$$V_t = \frac{nKT}{q} \qquad (3.5)$$

$$V_t = \frac{nKT}{q} \qquad (3.5)$$

$$I_{PV} = I_{ph} - I_0(e^{\frac{V_{PV} + IR_s}{V_t}} - 1) - \frac{V_{PV} + I_{PV}R_s}{R_p} \qquad (3.6)$$

The output terminal current I_{PV} is equal to the current that is produced by photon energy I_{ph}, which is dependent on the cell operating temperature and radiationless diode-current I_d and ground shunt leakage current I_P. The PV cell output current and voltage relationship can be related by combining equations (3.1 - 3.4) which gives equation (5)(Mataifa, 2015)

A =Cell Area

V_{oc} =Open circuit voltage

V_t =Thermal voltage

V_{PV} =Voltage output of the cell

$R_p \& R_s$ = parasitic resistances

I_d =Diode current

I_o = Saturation current of the diode

q =Electron charge=1.6*10[-19] Coulombs

n =ideality factor

K =Boltzmann constant=1.38*10[-23] Joule/°K

T =Temperature on absolute scale °K

The description of cell electrical performance is reliant on the two most critical parameters which are open circuit voltage V_{oc} and short circuit current I_{sc}. The shorting of the output terminals helps in the measurement of short circuit current under full illumination. The ground-leakage current relative to I_d and I_{ph} is small so it can be ignored, so the maximum

photovoltage is attained when loading current $I = 0$ i.e. when there is open-circuit voltage(Muaelou et al., 2015).

When the PV cell is short-circuited the cell output voltage becomes zero ($V_{PV} = 0$) and the cell output current equals the short circuit current ($I_{PV} = I_{sc}$).

$$I_{sc} = I_{ph} - I_0(e^{\frac{I_{sc}R_s}{V_t}} - 1) - \frac{I_{sc}R_s}{R_p} \qquad (3.7)$$

$$V_{oc} = \frac{nkT_c}{e} \ln\left(\frac{I_{ph}}{I_0}\right) = V_t \ln\left(\frac{I_{ph}}{I_0}\right) \qquad (3.8)$$

3.4 Power Converters

3.4.1 DC-DC Bidirectional converter

It is the device that is employed as the interface to control the charging and the discharging of the battery bank. It is used where there are two fixed voltages from a DC source which is from the DC bus and the battery system(Saleh et al., 2016).

3.4.2 Inverter

When there are alternative energy sources that provide electrical energy with voltages that are not in synchronism such as DC voltage generators and AC voltage generators operating at nonsynchronous speed, so there is a need for a power converter to interface for proper interconnection and that is an inverter (Raji, 2012). This is a device that converts DC power to AC power at the required voltage and frequency by controlling the switching device of a semi-conductor (Neacsu, 2006). The inverters are categorized into two groups which are the voltage source inverter (VSI) which regulates the voltage waveform and the current source inverter (CSI) which regulates the current waveform. There are three types of inverter topologies and they are the half-bridge inverter, single-phase inverter, and three-phase voltage source inverters (Moussavou, 2014).

3.4.2.1   Half Bridge Inverter

This is a type of inverter that applies to low voltage applications. It is made up of two controllable switches. The switching is to help to modify the DC voltage source into the AC output voltage and it can be employed as a DC-DC converter or DC-AC converter. The capacitors are in series connection across a DC source. The switches need to alternate so they cannot be on simultaneously or there will be a short circuit that will damage the switches (Moussavou, 2014).
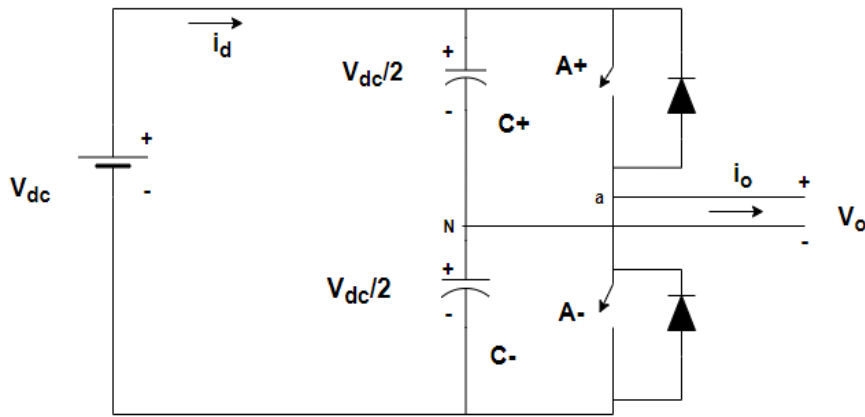
Figure 3-4: Single half-bridge VSI

3.4.2.2   DC-AC Converter (Three-phase inverter)

When converting a DC supply to a three-phase AC supply an inverter is employed with switches and shown in Figure 3.5 below. The switches are set such that they turn on and off at regular periods of 60° to produce the three-phase voltage. The switching is dependent on the modulation scheme and switches on the same leg cannot ON simultaneously as it would short the voltage which is against the Kirchhoff Voltage rule (Luta, 2019).
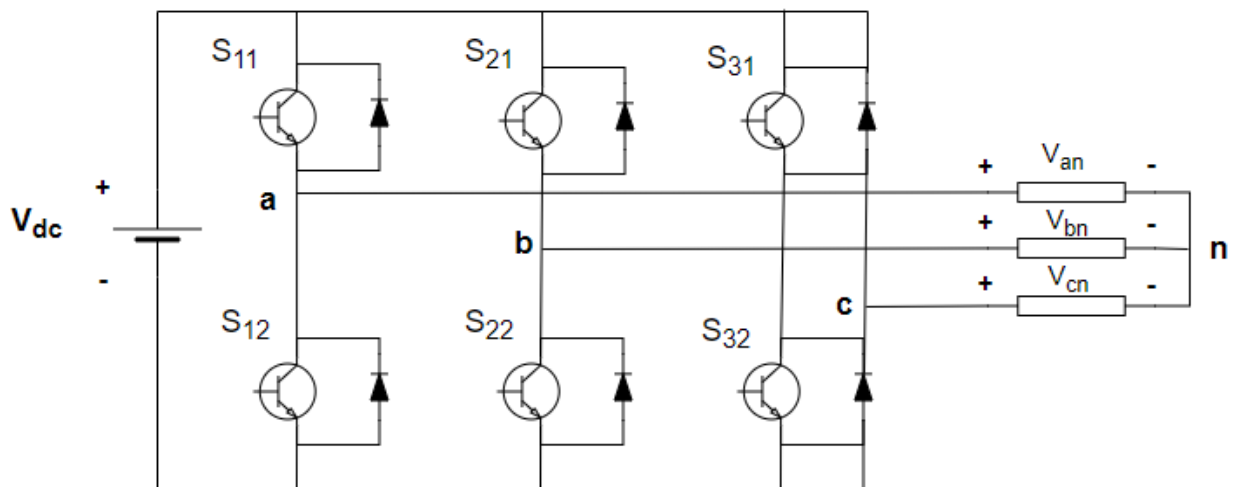

Figure 3-5: Three-phase full bridge inverter

3.5 Micro-hydro mathematical modelling

The MHP power plant is constructed and designed to use by streams of water from the river and it needs a small or no reservoir so to turn the turbine blades to produce power. The MHP plant is made up of three core sections, namely the hydro turbine governor, excitation system,

synchronous generator, and the load. Figure 3.6 depicts the schematic diagram of MHP which consists of the governor, penstock, and generator.
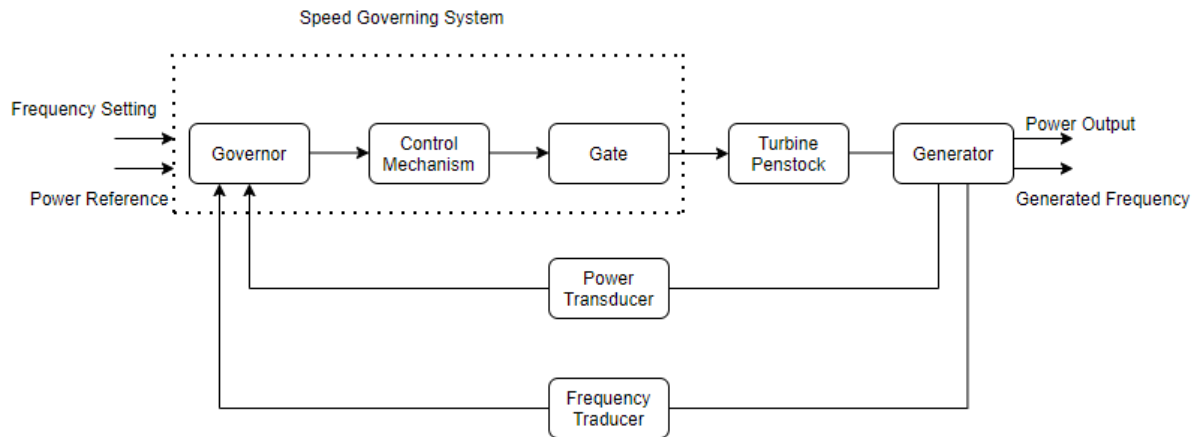

Figure 3-6: MHP schematic diagram

The water moves from a higher elevation and this results in what is referred to as hydraulic pressure due to height difference. The water then impacts the turbine blades with velocity (U). The volumetric flow rate is controlled by the gate driven by a servomotor. The mechanical power is then given by

$$P_m = \eta \rho g Q H \tag{3.9}$$

Where:

P_m = Mechanical power

η = Efficiency

ρ = Density of the water

g = gravitational acceleration

Q = Volumetric flow rate

H = Hydraulic head

The hydraulic turbine transfer function

Some characteristics that determine the hydraulic turbine performance are the impacts of inertia in the water column that channels water to the turbines, the water compressibility, and the elasticity of pipe walls. In the modeling of ideal hydraulic turbine and water column stability studies, some assumptions are considered but not paint a clear picture in mimicking real-life scenarios. The following assumptions are taken into consideration;

- The hydraulic resistance is minimal,
- The penstock pipe is inelastic, and water is incompressible,

- The water velocity is proportional to the gate opening with the square root of the net head,
- The turbine output power is proportional to the product of the head and the volumetric flow rate(Kundur, 1994).

The characteristics of the turbine and penstock are based on the three basic equations which are

- The velocity of water in the penstock
- Turbine mechanical power
- Acceleration of water column

IDEAL TURBINE MODEL

The formula that governs water velocity in the penstock

$$U = K_u G\sqrt{H} \qquad (3.10)$$

Where

U= Water velocity

K_u= A constant of proportionality

G= Gate position

H= Hydraulic head at the gate

Where there is a small deviation about the operating point then change in water velocity becomes,

$$\Delta U = \frac{\partial U}{\partial H}\Delta H + \frac{\partial U}{\partial G}\Delta G \qquad (3.11)$$

Substitute expressions for the partial derivatives and divide through by $U_0 = K_u G_0\sqrt{H_0}$

$$\frac{\Delta U}{U} = \frac{\Delta U}{2H_0} + \frac{\Delta G}{G_0}$$

Or

$$\Delta \overline{U} = \frac{1}{2}\Delta \overline{H} + \Delta \overline{G} \qquad (3.12)$$

"0" indicates initial steady-state values and the "Δ" small change and _ indicates normalized values based on steady-state operations.

Turbine mechanical power

The mechanical power produced by the turbine is dependent on the hydraulic head(H) and the volumetric flow rate(Q) which is a product of area (A) and the water velocity (U).

$$P_m = K_p H U \tag{3.13}$$

Linearizing due to the small deviation and normalizing by dividing both sides by $P_{m0} = K_p H_0 U_0$

$$\frac{\Delta P_m}{P_{m0}} = \frac{\Delta H}{H_0} + \frac{\Delta U}{U_0}$$

Or

$$\Delta \overline{P_m} = \Delta \overline{H} + \Delta \overline{U} \tag{3.14}$$

Substituting $\Delta \overline{U}$ from equation 3.11

$$\Delta \overline{P_m} = 1.5 \Delta \overline{H} + \Delta \overline{G} \tag{3.15}$$

Substituting $\Delta \overline{H}$ from equation 3.11

$$\Delta \overline{P_m} = 3 \Delta \overline{U} - 2 \Delta \overline{G} \tag{3.16}$$

The acceleration of the water column due to the change in the head at the turbine is based on Newton's second law of motion and it is given by

$$(\rho L A) \frac{d \Delta U}{dt} = -A(\rho g) \Delta H \tag{3.17}$$

ρ= Mass density

L= length of conduit

A= Area of a pipe

61

g= Acceleration due to gravity

U=Water velocity

t= time seconds

Newton's second law evident more when the dimensionless analysis is done using fundamental units which are mass, length, and time (MLT) which helps determines relations between several variables.

$$\rho = \frac{Kg}{m^3}$$

$$L\&H = m$$

$$A = m^2$$

$$g = \frac{m}{s^2}$$

$$U = \frac{m}{s}$$

$$t = s$$

Substituting the fundamental units in equation 3.15

$$\frac{Kg}{m^3} \times m \times m^2 \times \frac{m}{s^2} = -m^2 \times \frac{Kg}{m^3} \times \frac{m}{s^2} \times m$$

This holds as Newton's second law states force is the change in mass by the velocity with time. $F = mass \times acceleration$

$$Kg \times \frac{m}{s^2} = -Kg \times \frac{m}{s^2} \quad \gg \frac{ML}{T^2}$$

Divide equation 3.14 into both sides by $A\rho gH_0U_0$ the acceleration then becomes normalized and becomes

$$\frac{LU_0}{a_g H_0} \frac{d}{dt}\left(\frac{\Delta U}{U_0}\right) = -\frac{\Delta H}{H_0}$$

Or

$$T_w \frac{d\Delta\overline{U}}{dt} = -\Delta\overline{H} \tag{3.18}$$

Equation 3.18 indicates that if there is backpressure at the gate position towards the end of the penstock then the water in the penstock will lose energy and start to decelerate.

Where

$$T_w = \frac{LU_0}{a_g H_0} \tag{3.19}$$

T_w is the starting time of the water, it is the time that is needed for hydraulic pressure due to head H_0 to move water in the penstock from a static position. The value is between 0.5s and 4.0s under full load.

Substituting $\Delta\overline{H}$ from equation 11

$$T_w \frac{d\Delta\overline{U}}{dt} = 2(\Delta\overline{G} - \Delta\overline{U}) \tag{3.20}$$

Replacing $\frac{d}{dt}$ with Laplace operator s

$$T_w s \Delta\overline{U} = 2(\Delta\overline{G} - \Delta\overline{U})$$

$$\Delta\overline{U} = \frac{1}{1 + \frac{1}{2}T_w s} \Delta\overline{G} \tag{3.21}$$

Substitute $\Delta\overline{U}$ from equation 3.15

$$\frac{\overline{\Delta P_m}}{\Delta\overline{G}} = \frac{1 - T_w s}{1 + \frac{1}{2}T_w s} \tag{3.22}$$

Equation 3.22 is the transfer function of the hydraulic turbine which shows how the turbine power output changes with the gate opening and this is the case of an ideal turbine without losses.

63

NON-IDEAL TURBINE MODEL

The ideal turbine model is used in small-signal performances of the turbine and paints a picture of the basic principles of the hydraulic system. Previously the turbine's representation stability studies were based on transfer function represented by equation 21 above but this is representation has challenges where the power output and the frequency vary significantly. The nonideal model is employed in time-domain simulations where is a large signal. The assumption for this model is that there are unrestricted head and tailrace, the conduit is rigid and the fluid is incompressible (Kundur, 1994).

The water velocity in the penstock is given by,

$$U = K_u G \sqrt{H} \qquad (3.23)$$

$$P_m = K_p H U \qquad (3.24)$$

The volumetric flow rate in the penstock is given by,

$$Q = AU \qquad (3.25)$$

The rate of change of water velocity in the penstock is given by,

$$\frac{dU}{dt} = -\frac{g}{L}(H - H_0) \qquad (3.26)$$

Where

A=Pipe area

U= Water velocity

G= Ideal gate positioning

L= Length of conduit

H, H_0= hydraulic head at the gate and its initial steady-state value respectively

Q= Volumetric flow rate

g= gravitational acceleration

t= time in seconds

The focus is large signal performances so equation 3.23 & 3.24 are normalized based on rated values and they become

$$\frac{U}{U_r} = \frac{G}{G_r}\left(\frac{H}{H_r}\right)^{\frac{1}{2}} \tag{3.27}$$

$$\frac{P}{P_r} = \frac{U}{U_r}\left(\frac{H}{H_r}\right) \tag{3.28}$$

The "r" indicates rated values in the per unit notation the equations become

$$\overline{U} = \overline{G}(\overline{H})^{\frac{1}{2}} \tag{3.29}$$

$$\overline{P} = \overline{U}\,\overline{H} \tag{3.30}$$

Making $\overline{H}$ the subject of the formula from equation 28

$$\overline{H} = \left(\frac{\overline{U}}{\overline{G}}\right)^2 \tag{3.31}$$

The per-unit form of equation 3.26

$$\frac{dU}{dt}\left(\frac{U}{U_r}\right) = -\frac{g}{L}\frac{H_r}{U_r}\left(\frac{H}{H_r} - \frac{H_0}{H_r}\right) \tag{3.32}$$

Or

$$\frac{d\overline{U}}{dt} = -\frac{1}{T_w}(\overline{H} - \overline{H_0}) \tag{3.33}$$

In Laplace notation

$$\frac{\overline{U}}{(\overline{H} - \overline{H_0})} = -\frac{1}{T_w s} \tag{3.34}$$

T_w is the starting time of the water at the rated load with a fixed value for the turbine-penstock unit and it is given by

$$T_w = \frac{LU_r}{H_r g} = \frac{LQ_r}{gAH_r}$$ (3.35)

The mechanical power is

$$P_m = P - P_L$$ (3.36)

Where P_L is the turbine power loss due to friction

$$P_L = U_{NL}H$$ (3.37)

U_{NL} is the water velocity at no load

The normalized form equation 3.35 gives

$$\overline{P_m} = (\overline{U} - \overline{U_{NL}})\overline{H}$$ (3.38)

Equation 3.38 represents the per-unit value of the power output from the turbine on a base equal to the turbine MW rating. In power systems, it is preferred to represent output power and the mechanical torque of a turbine to the base of generator MVA rating or a common MVA base and it gives

$$\overline{T_m} = \left(\frac{\omega_0}{\omega}\right)\overline{P_m}\left(\frac{P_r}{MVA_{base}}\right) = \frac{1}{\overline{\omega}}(\overline{U} - \overline{U_{NL}})\overline{H}\,\overline{P_r}$$ (3.39)

Where

$\overline{\omega}$= per unit speed

MVA_{base}=Base rating on which turbine torque is made per unit

$\overline{P_r}$= per unit turbine rating

The change from no load to full load without the losses and have 1 per unit is the ideal gate opening whereas in the real gate opening it is the change from the fully closed position to fully open with 1 per unit
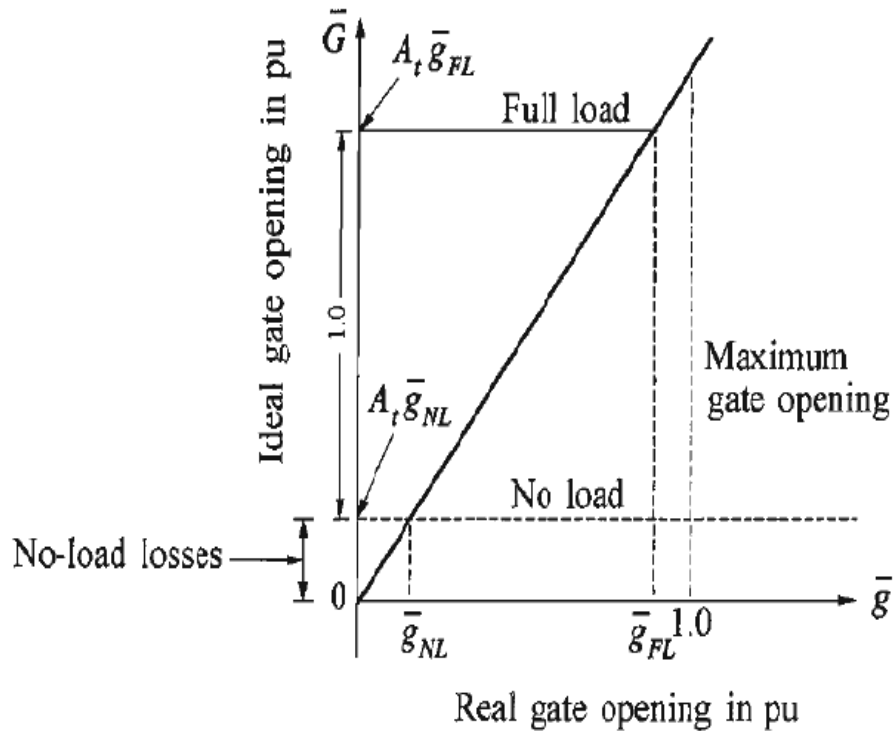
Figure 3-7: Relationship between real and Ideal gate openings (Kundur, 1994)

This relationship is characterized by the following formula

$$\overline{G} = A_t \overline{g} \tag{3.40}$$

Where A_t is the turbine gain

$$A_t = \frac{1}{\overline{g}_{FL} - \overline{g}_{NL}} \tag{3.41}$$

In the modelling of the hydraulic turbine there are assumptions taken to consider which are:

- The blade of a turbine is considered smooth,
- Water hammer is neglected,
- Fluids are compressible which is defined by the Bulk modulus which is the surge of pressure given with a decrease in volume but it wouldn't be considered hence the fluid(water) is considered incompressible,
- The water velocity is proportional to gate opening,
- The power output is due to the hydraulic head and the velocity of the water.
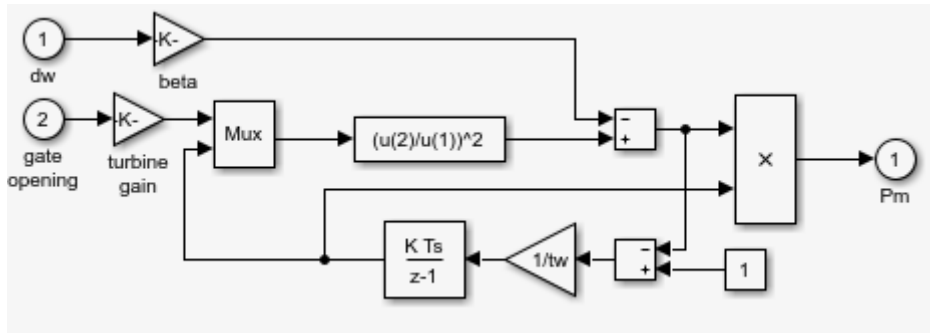
Figure 3-8: Hydraulic turbine in Matlab/Simulink

$$P_m = A_t H(Q - Q_{NL})$$ (3.42)

Where :

P_m: Mechanical power at the shaft

Q: Volumetric flow rate

Q_{NL}: Volumetric flow rate with no load

$$Q = G\sqrt{H}$$ (3.43)

Where :

G: It is the gate opening(rad)

H: Is the net head(m)

3.6 Excitation system model

The excitation system's core function is to supply direct current to the field windings of a synchronous generator. Voltage and reactive power flow control are among the exciter's control functions, which contribute to promoting system stability. The protective function of the exciter is to ensure that the appropriate voltage and reactive power flow do not exceed the capability limits of the synchronous machine, excitation system, and other equipment (Haruni, 2013).
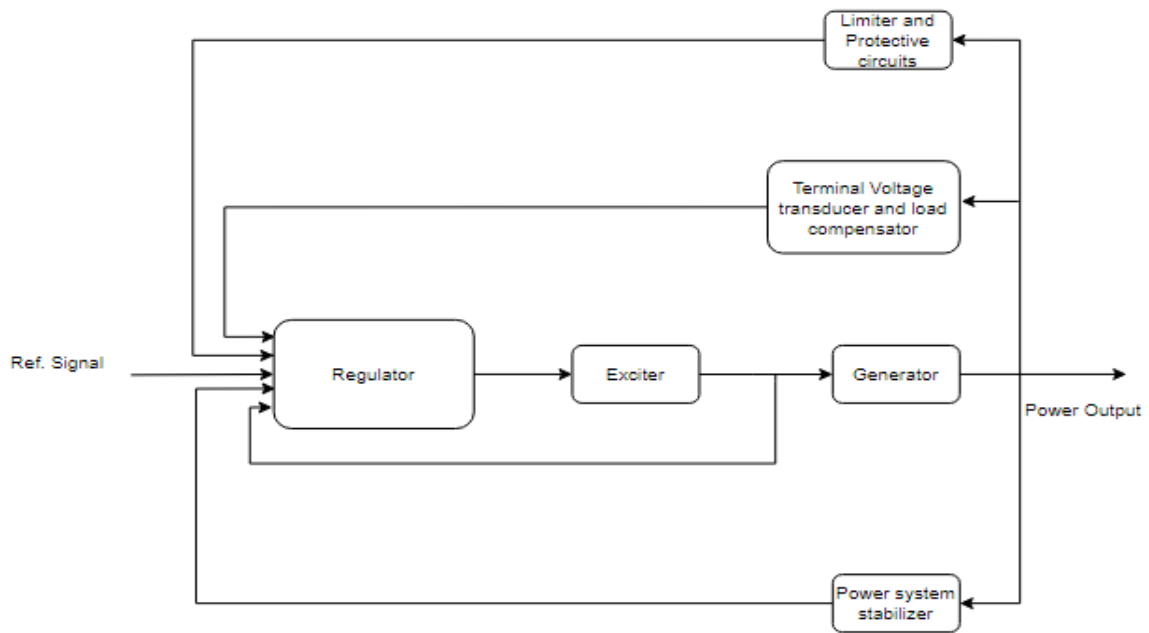
Figure 3-9: Exciter block diagram

3.7 Proposed system operation

The system consists of two power sources which are PV array, MHP, and battery storage systems as the backup system as illustrated in figure 2.10 below. The battery storage system either absorbs excess power or dispatch when the power sources are producing less. The PV system contributes about 102.4kW to the system and consists of the DC-DC boost converter with maximum power point tracking (MPPT) to be able to extract maximum power from the array and voltage source converter. The MHP consists of the excitation system, synchronous generator, turbine, and the governor and will supply a consistent power of 95kW. Furthermore, there is a rectifier as an interface device for the integration of MHP, PV, and Battery storage. The system is connected to the AC load via a voltage source converter(VSC). The inverter uses a phase-locked loop(PLL) to maintain the frequency and phase angle of the voltage. The control scheme is made up of voltage and current regulators using PI control to improve the power factor of the system.

LC filters are used to quell harmonics produced by the inverter. The PV is the primary power source of the system therefore, the irradiance will be varied to mimic real-life scenarios. The Li-ion battery storage with a bidirectional buck-boost converter is employed as a backup system to maintain continuous power to the load and maintaining 750 volts on the DC bus. Insulated-gate bipolar transistors (IGBT) are employed as switching devices to maintain the voltage at the DC link. MHP is producing a constant power with a flow rate of $0.27m^3/s$ and a hydraulic head of 45m.

69

Under IEC/ISO62264 which is an international standard for supplier and manufacturer communications, the microgrid needs to adapt to this standard. There are four levels of control which are the internal control loops, primary control, secondary control, and tertiary control. The two controls that have been utilized in this system are the inner control and the primary control. The internal control loop employs power electronics devices like VSC in managing frequency and voltage inside the microgrid. In primary control, the storage system is controlled by the bidirectional converter based on voltage fluctuation using PI control.
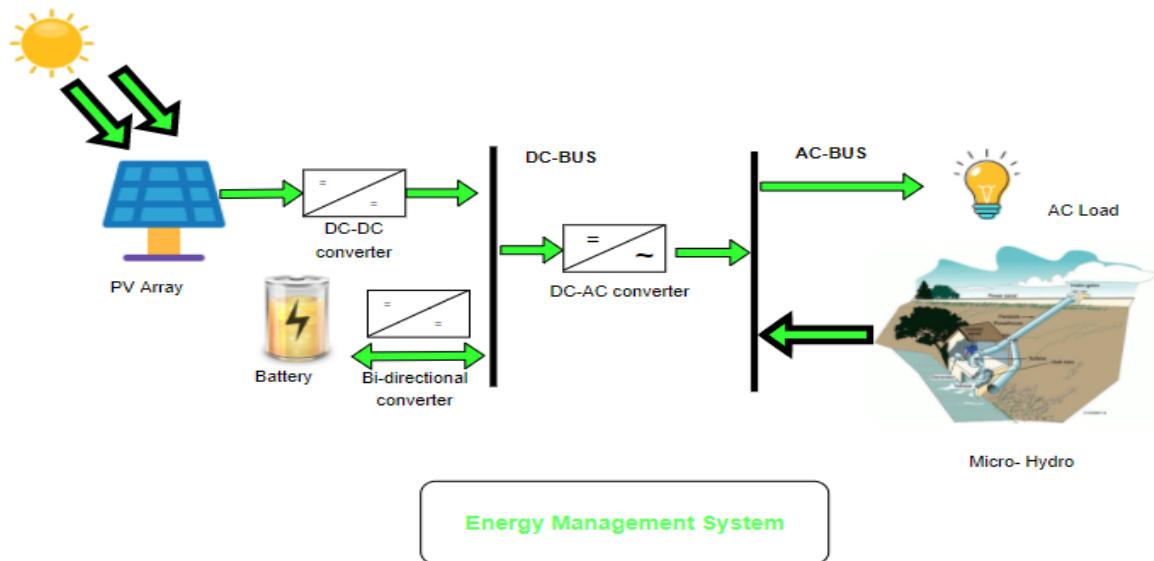
Figure 3-10:Hybrid microgrid system architecture

4 Chapter Four: System Design

4.1 Introduction

This chapter presents the design calculations of a hybrid microgrid system whose components include solar photovoltaic array, DC-DC boost converter, DC-AC inverter, LC filter, MHP(synchronous generator), excitation system, battery bank, and DC-DC bidirectional converter. The system power output is based on electrifying rural households with a 180kW load. A solar photovoltaic array is connected to a DC-DC boost converter and IGBT inverter with LC filter and the capacity bank to filter harmonic from the voltage source inverter, the energy management algorithm to manage power flow and charging and discharging of the battery bank.

4.2 System Modelling
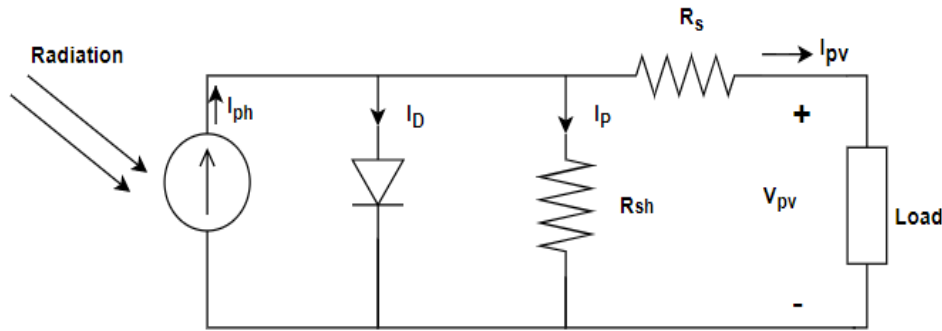
4.2.1   Model of a Photovoltaic cell

Figure 4-1: Equivalent circuit of the PV cell

Figure 4.1 above, the voltage-current characteristic of the PV cell is presented as:

$$I = I_{ph} - I_s \left\{ \exp\left(\frac{V + IR_s}{A}\right) - 1 \right\} - \frac{V + IR_s}{R_{sh}}$$

(4.1)

$$A = \frac{mkT_c}{q}$$

(4.2)

The shunt resistance is far larger than the series resistance so the expression $\frac{V+IR_s}{R_{sh}}$ in equation 4.1 is negligible hence equation 4.3

$$I = I_{ph} - I_s \left\{ \exp\left(\frac{V + IR_s}{A}\right) - 1 \right\}$$

(4.3)

Photocurrent I_{ph} relies on the operating temperature of the solar cell and solar radiation and is determined based on equation 4.4

$$I_{ph} = \frac{(I_{sc} + Ki(T_c - T_{ref}))\lambda}{1000}$$

(4.4)

The cell saturation current is determined by:

71

$$I_s = I_{RS} \left(\frac{T_c}{T_{ref}} \right) \exp \left(\frac{qE \left(\frac{1}{T_{ref}} - \frac{1}{T_c} \right)}{KA} \right) \qquad (4.5)$$

The solar cell is based on the following parameters:

- Open circuit voltage, V_{OC}: It is the maximum voltage from a solar cell
- Short circuit current: It is the greatest current generated by a solar cell when V=0
- The cell voltage with light absence is determined by:

$$V_{OC} = \frac{mkT_c}{q} \ln \left(\frac{I_{ph}}{I_o} \right) = A \ln \left(\frac{I_{ph}}{I_0} \right) \qquad (4.4)$$

Where

T_c= Absolute cell temperature

A= Thermal voltage

 m= Ideality factor

k= Boltzmann's constant

T_c= Cell temperate

V= Voltage

q= electric charge

4.3 Solar Photovoltaic Design

The solar cell is made up of semiconductive material that can convert solar radiation to electrical energy. The photovoltaic array output depends also on the solar cell temperature and radiation. Voltage and current outputs rely on several cells that are connected in series and parallel. The photovoltaic array is modeled using the parameters in Table 4.1 below which corresponds to data of 1 Soltech-1STH-230-P panel. The operating temperatures are 25 and 50°C and irradiance of 1000 Watts per m^2, with current versus voltage and voltage versus power graph which is illustrated in Figure 4.2 shown below. The power from the photovoltaic array is 102.47kW achieved by having 28 parallel stings and 16 series modules

Table 4-1:Technical data of a PV module (1 Soltech-1STH-230-P)

V_{oc} (V)	37.1
I_{sc} (A)	8.18
V_{mp} (V)	29.9
I_{mp} (A)	7.65
R_s (ohms)	0.34833

R_p (ohms)	294.1335
I_{sat}(A)	3.0478e-10
I_{ph}(A)	8.1897
n	1.0028

Table 4-2: PV parameters

PV Type	1 Soltech-1STH-230-P
Cells per module	60
Series connected strings	16
Parallel connected strings	28

Table 4-3: Energy consumption for basic domestic appliances

Item	Power Rating (W)	Daily use(h)	Days used	Monthly energy consumption(kWh)
1x Energy light saver	11	5.0	30	1.7
1x TV	35	6.0	30	7
1x Iron	1000	4.0	6	24
1x Kettle	1000	0.5	30	15
1x Hot plate	1000	1.0	25	25
1x Regular light	100	5	30	15
1x Refrigerator(20L)	250	6.5	30	49

The peak power each household needs is 3396 W and to power 50 households the peak power needs to be approximately 170kW ignoring the transmission and other losses that could be lost due to efficiencies of machines and devices employed. The load is then set at 180kW for this system. The PV will be designed to produce 100kW of power.
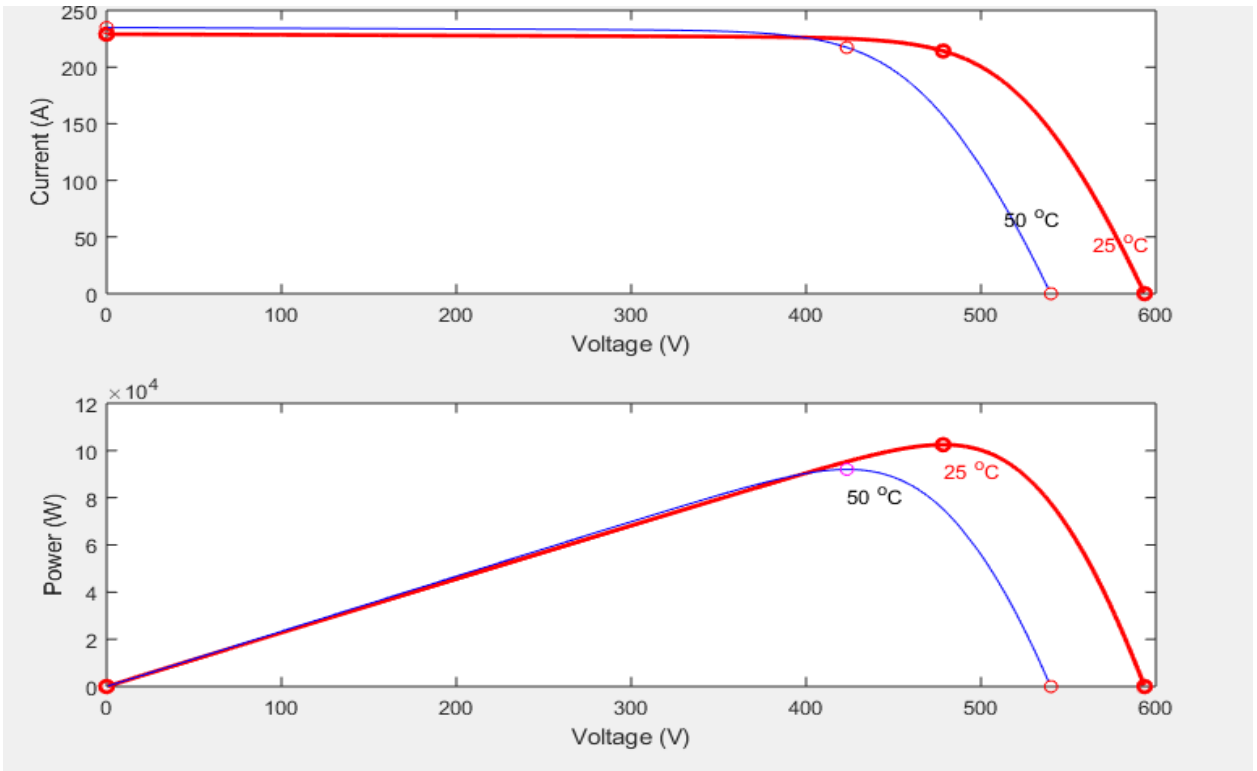
Figure 4-2: Photovoltaic module characteristics Current Vs Voltage and Voltage Vs Power

The number of panels that are in series is obtained by dividing the voltage output expected from the array by the voltage at the maximum power point (V_{mp}) of the panel $\frac{450}{29.9} = 15.05$

The number is rounded up to give 16 panels in series

The output current is calculated based on the power that is accepted from the array divide by the voltage produced by the PV array which is $16 \times 29.9 = 478.40 \, V_{dc}$

$$P = IV \tag{4.2}$$

$$I = \frac{100 \times 10^3}{478.4} = 209.03A$$

The number of panels that are in parallel is obtained by dividing the output current by the current at the maximum PowerPoint

$$I_{mp} = \frac{209.03}{7.65} = 27.32$$

74

The same principle of rounding up is used as it impossible to have a fraction of the panel hence 28 panels in parallel.

The total power produced will be:

$$P_o = 28 \times 7.65 \times 16 \times 29.9 = 102.47 \text{kW}$$

$$C_{DC\ Link} = \frac{V_{pv}D}{\Delta V_{pv}f_s^2 L_{boost}} \tag{4.3}$$

$$C_{DC\ Link} = \frac{0.362 \times 478.4}{4 \times 44.31 \times (5 \times 10^3)^2} = 70.76 \times 10^{-6}$$

This capacitor is to minimize the ripple voltage across the PV terminals (Badran et al., 2016).

4.3.1   DC-DC converter

These are electrical circuits that are employed to play a core role in energy transfer to provide a different voltage than the supplied one. They are used to maintain the required voltage within the required specifications. There are several DC-DC converters namely the buck, boost, buck-boost, full-bridge, and cuk converters but the buck and the boost converter hold the basic topologies of all converters the rest is the modification of those two. The switching regulator is used due to its high efficiencies and capability as compared to the linear converters in the designing of DC-DC converters. The use of pulse width modulation is preferred as it maintains both the switching frequency and varies the duty cycle to get the required voltages (Gebreab, 2013).

4.3.2   Pulse Width Modulation

To maintain the desired voltage output from the DC-DC converter, the switch ON and OFF time must be controlled and be kept at a constant frequency (Gebreab, 2013). The method is known as pulse width modulation (PWM) switching which maintains the switching frequency. This is achieved by generating the dc voltage in a form of pulses that has different width with regards to areas with higher amplitude. The width is indicated by varying the ON time relative to the switching period. (Zacharek & Sundqvist, 2018).

4.3.3   Boost Converter Design

In the quest to increase the voltage from the voltage source to a higher voltage, the boost converter is employed. The boost converter comprises the inductor, capacitor, diode, and

PWM. The size of the inductor L and the capacitor is determined by the required voltage and current outputs. The capacitor is to ensure that the required voltage is continuously provided while the diode prevents the backflow of current back to the source (Gebreab, 2013). The determination of when the switch to be ON or OFF is done by the PWM controller by sensing high or low voltage. When there is a high voltage at the circuit gate the power transistor will be ON and when there is a low voltage then it will be OFF (Moussavou, 2014).
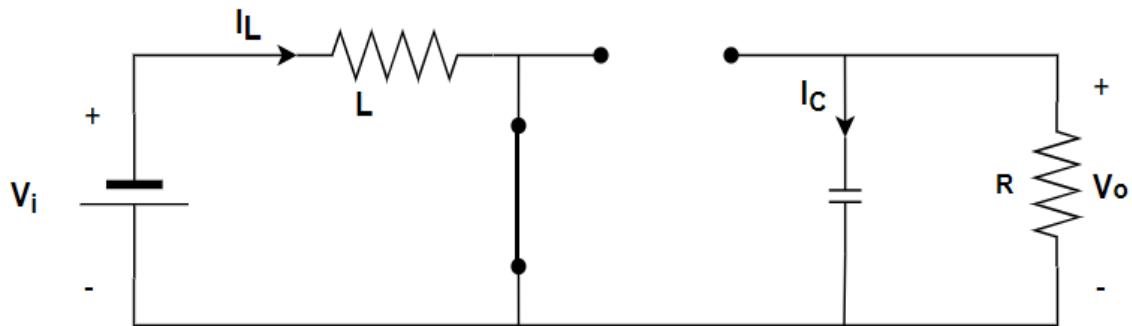
Figure 4-3: Schematic of the boost converter switch ON

When the switch is ON as shown by figure 4.3 above the duty cycle time is on (DT) inductor gets charged and the current I_L increases in a linear pattern while the capacitor is discharged by supplying the load with the current.
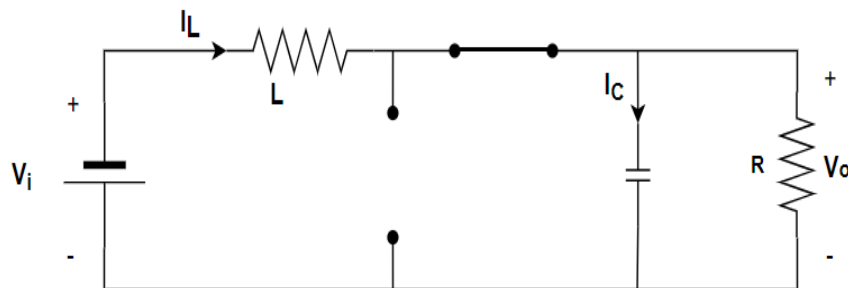
Figure 4-4: Schematic of the boost converter switch OFFs

When the switch OFF the energy stored in the form of the magnetic field is realized, I_L is forced through the diode, and the inductor supplies the load and charges the capacitor simultaneously.
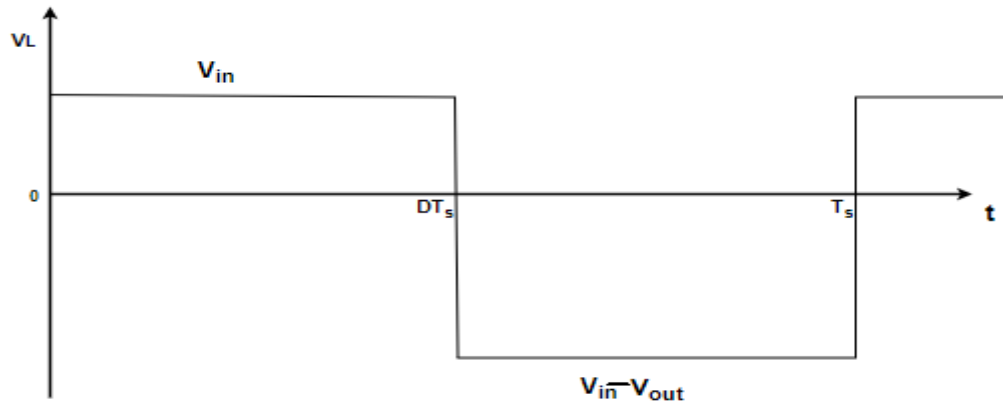
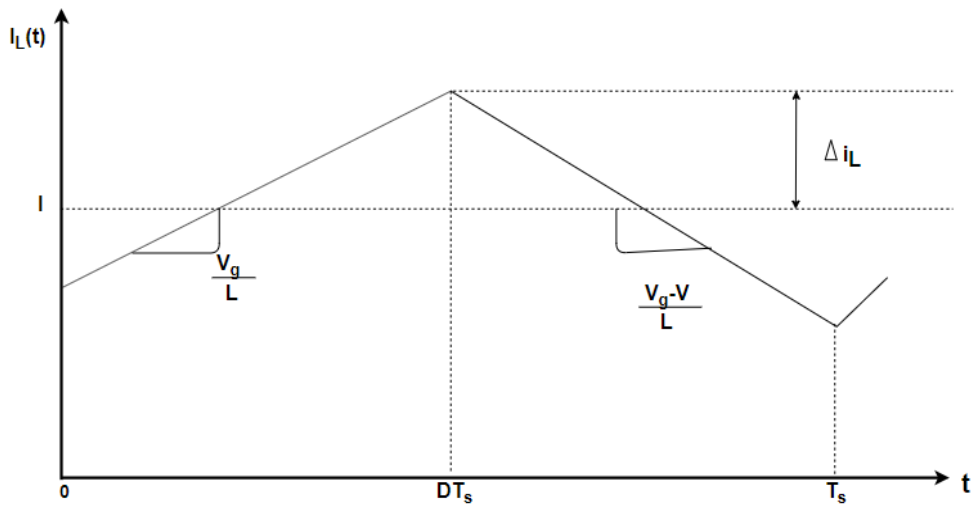Figure 4-5: Inductor voltage (Gebreab, 2013)

Figure 4-6: Inductor ripple current waveform

$$\Delta i_L = \frac{V_i}{L} DT = -\frac{V_i - V_o}{L}(1 - D)T$$

$$V_i D = (-V_i + V_o)(1 - D)$$

$$D = 1 - \frac{V_{in}}{V_{out}} \tag{4.3}$$

$$1 - \frac{478.40}{750} = 0.36$$

$$L = \frac{V_i D}{\Delta I_i f_s}$$ (4.4)

Where D is the duty cycle, V_i is the voltage from the PV array ΔI_i is the inductor ripple current which is 30% of the load current $((I_L)$ and f_s is the switching frequency.

$$I_L = \frac{P_{in}}{V_{in}} = \frac{100 \times 10^3}{478.4} = 209.03 \text{ A}$$

$$\Delta I_i = 0.3 \times 209.03 = 62.71 \text{ A}$$

$$L = \frac{478.4 \times 0.362}{62.71 \times 5 \times 10^3} = 552.32 \text{ μH}$$

The value of the capacitor is given by

$$C_{DC} = \frac{I_o D}{\Delta V_o f_s}$$ (4.5)

$$I_o = \frac{P_o}{V_o} = \frac{102.47 \times 10^3}{750} = 136.63 \text{A}$$

$$C_{DC} = \frac{136.63 \times 0.362}{5 \times 10^3 \times 7.5} = 1.32 \text{ mF}$$

Where ΔV_o is the ripple voltage and is 1% of the desired voltage after boost and I_o is output current. This capacitor stores excess energy when there is more power and dispatches it during insufficient periods to maintain capacitor power flow.

4.4 Inverter (DC-AC)

The inverter employed is the Isolated Gate Bipolar Transistor (IGBT) to convert the DC supply from the solar PV array which has been boosted and MHP to AC supply. The universal bridge is used functions in three levels, three-phase VSC type.
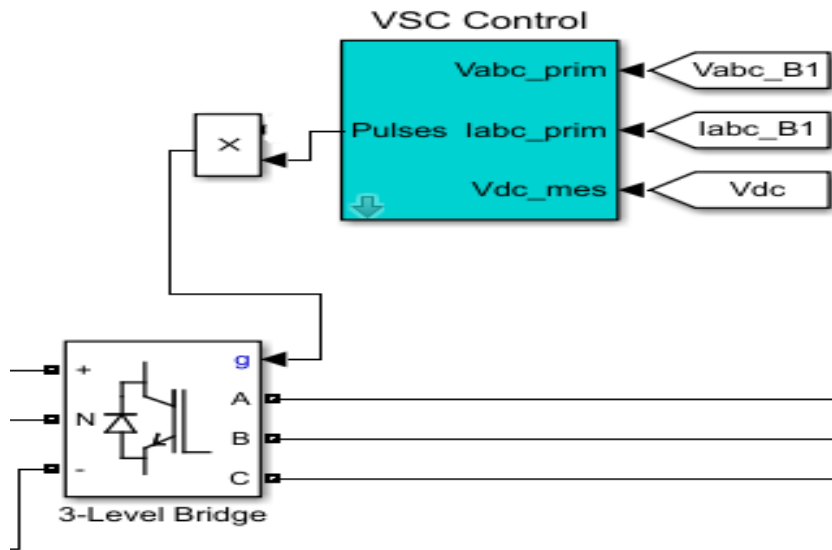
Figure 4-7: DC - AC inverter with VSC control

When the PV system or DC supply is either connected to a grid or a three-phase source operating in a specific voltage and frequency then there is a need to have an inverter control to synchronize the DC power output to that of the three-phase source. Current and voltage from the abc coordinates at the sending side of the transformer are measured and pass through a phased lock loop (PLL). The phase-locked loop is a feedback system that consists of a phase detector, voltage-controlled oscillator (VCO), and filter. The phase detector compares the phase difference from the input reference signal and the output signal from the VCO to produce an error proportional to the phase difference. The feedback loop system locks the input signal and output signal so that the phase difference stays the same and this results in the same frequency. The PLL in a grid-tied is used by power converters for synchronization, it does that by using the grid voltage, frequency, and phase as a baseline and adjusted to grid frequency. The phase angle and three-phase parameters are turned into two-phase parameters from the abc frame to the dq frame which is known as a synchronous frame. These go through the current regulator to attain maximum power input to the grid or a three-phase system (Kumar, 2017 and Moussavou, 2014).
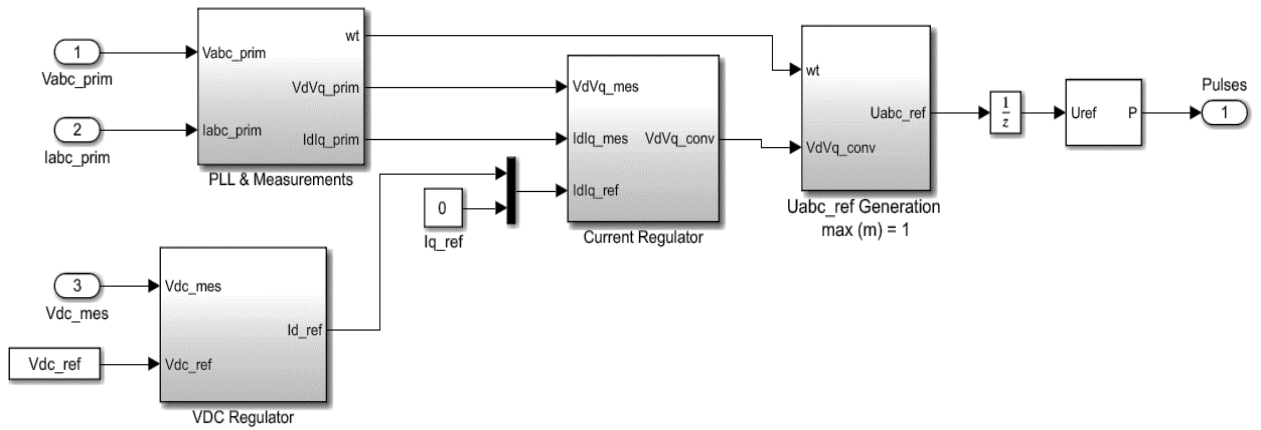
Figure 4-8:Voltage source converter control

Figure 4.8 above depicts VSC with PLL that assists to keep frequency on required specifications and phase angle of the voltage. The control comprises voltage and current regulators to provide a good power factor. The VDC regulator converts DC voltage through a PI controller which produces I_d^* current by comparing DC voltage and the DC voltage reference. The I_q and I_d are generated by PI controllers from the current regulator. The I_q^* is zero to improve the inverter power factor. The change in the I_d signal is refined to reduce the error by the PI controller and generate the V_d signal to compare with ωt to get V_d^*.

The change in I_q is also refined by the PI controller to give V_q and compare with ωt to get V_q^*. The Uabc block represents a dq0 frame for PWM generation.
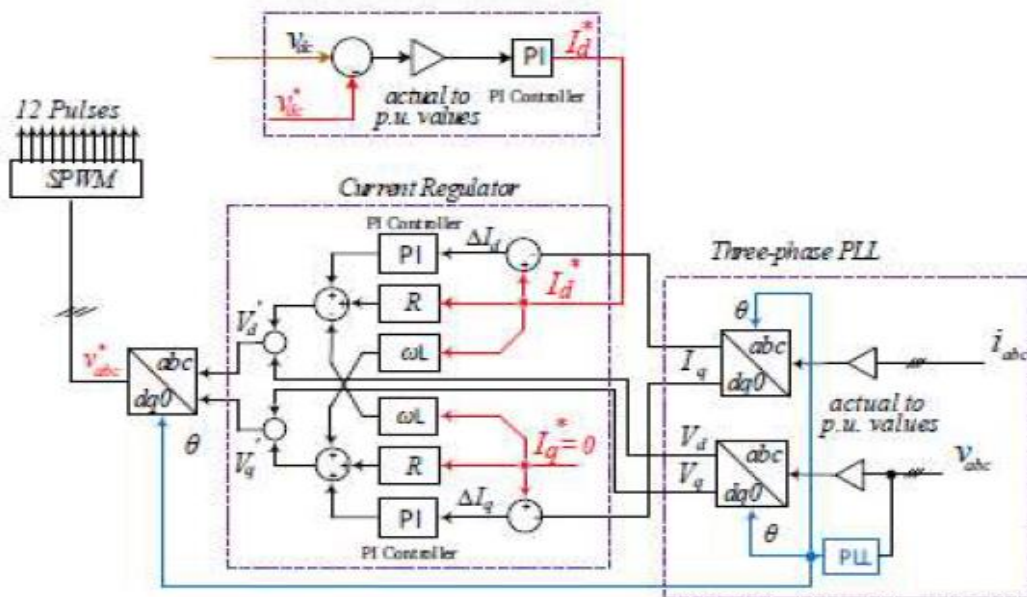
Figure 4-9:Voltage source control scheme

4.5 Filter topologies

The DC power that is supplied to the load is done through a voltage source inverter(VSI). The voltage output from the inverter has harmonics hence a need to be mitigated by the use of filters between the load and VSI for good power quality (Raji, 2012).

4.6 L-Filter

The degree to which the harmonic content is mitigated is determined by the filter used. This is a first-order filter that include one inductor in series with the mains. The L-filter is the most commonly utilized filter due to its ease of manufacture and lack of resonance complications seen in second and third-order filters. Its primary goal is to mitigate the current ripple that is from the inverter switching. It is more efficient while used with a high switching modulation inverter, it can mitigate 20Db per decade over the whole frequency range. The inductance L_f is calculated using equation 4.6 when V_{dc} is 750V, switching frequency of 5kHz, and the inductor ripple current becomes 20% of the maximum peak to peak output current.

$$L_f = \frac{V_{dc}}{4\Delta i f_s}$$

(4.6)

$$I = \frac{P}{V_{dc}} = \frac{102.47 \times 10^3}{750} = 136.63A$$

$$0.2 \times 136.63 = 27.33A$$

$$\frac{750}{4 \times 5 \times 10^3 \times 27.33} = 1.37 \text{ mH}$$

4.7 LC Filter

High-order filters use both inductors and capacitors to reduce harmonics, but the configuration becomes complicated. The LC-filter is a second-order filter that is commonly used in microgrids that operate in islanded mode. The LC filter is rarely used in a grid-connected microgrid because its resonance frequency varies with the grid's inductance value (Moussavou, 2014).Sinusoidal voltage with a small total harmonic distortion the maximum ripple voltage is 1% of the maximum peak to peak output voltage, so the size of the capacitor C_f is given by:

$$C_f = \frac{\Delta i}{8 f_s \Delta V_o}$$

(4.7)

$$\Delta V_o = 0.01 \times 750 = 7.50V$$

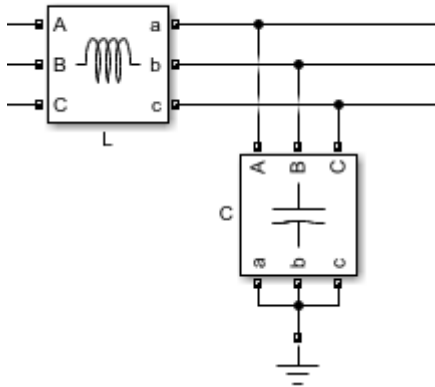$$\frac{27.33}{8 \times 5 \times 10^3 \times 7.5} = 91.10\mu\text{F}$$

Figure 4-10: LC-filter in Simulink

4.8 Micro-hydro plant

The simulation of the MHP model requires steady-state initialization and this was executed by using the machine initialization option in the powergui block which solves load flow and updates voltages and currents phasors of the power system. The synchronous generator is recognized in the powergui as a swing generator hence the active power and terminal voltage are the ones specified. It is during this process of initialising the synchronous generator the powergui also initialise both the hydraulic turbine and updates the adequate field excitation needed by the generator with regards to the load flow.

4.8.1 Excitation System

The excitation system of the generator determines the output value of voltage and reactive power thus regulating energy output from the generator and determines the stability of the whole plant. In the instance where the rotor speed is maintained to provide the required frequency of between 49.5Hz and 50.5 Hz, the automatic voltage regulator (AVR) in the excitation system controls the magnitude of the voltage at the terminals and reactive power output of the machine and that brings about the system stability.

4.8.2 Hydraulic turbine

The mismatch of power supplied by the turbine to the generator and that consumed by the load from the generator leads to either acceleration of the rotor of a synchronous generator or deceleration depending on what type of fluctuation. If more power is generated than what is

demanded by the load the will be a mismatch between the mechanical and electromagnetic torque acting on the rotor leading to rotor acceleration and vice versa. It is crucial to maintain power balance by implementing load frequency control.

The load frequency control is done by electric servomotors for a synchronous generator which is employed to maintain the frequency of the system within set parameters with regards to fluctuation in load demand.

The modelled hydraulic turbine consists of the governor which is a system that regulates the turbine rotating speed using the servomotor. The servomotor determines the opening of the gate using the PID controller to adjust the error due to the difference between the reference rotational speed w_{ref} and the actual turbine speed w_e which is a reflection of load demand changes. The frequency is maintained by either closing or opening the gate of the turbine regulating the volumetric flowrate which ultimately affects the turbine power output. The droop characteristics use two alternatives which are dependent on the binary signal d_{ref} whereby the top position uses negative feedback in the lower position the droop signal is the difference of P_{ref} which is the reference power and the actual measured power P_e.
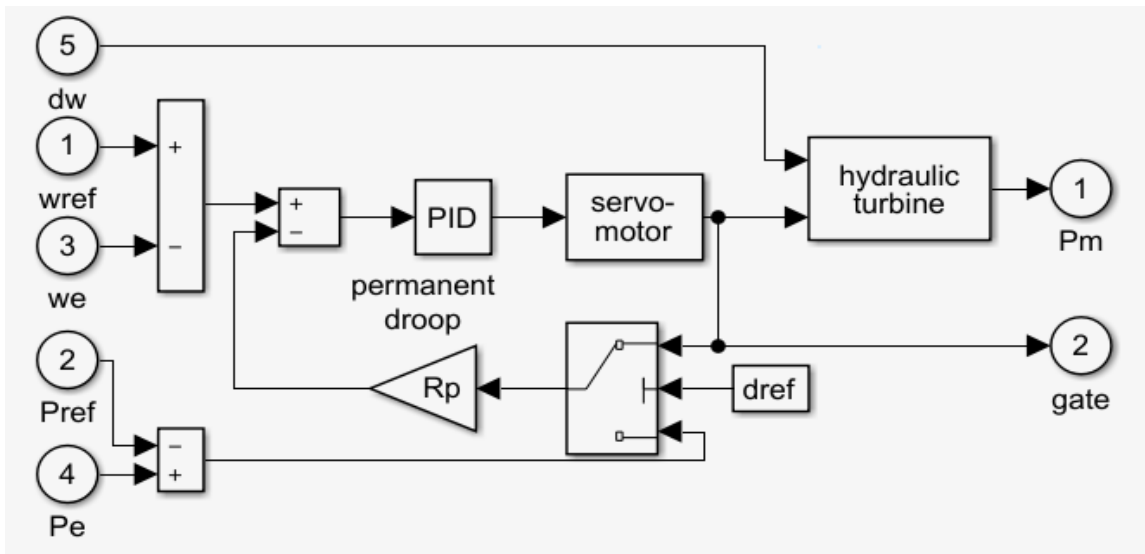

Figure 4-11: Hydraulic turbine with governor block MATLAB/SIMULINK

4.9 Power Calculations

The water power is converted to kinetic energy by the nozzles, the buckets are hit tangentially by water from the jets producing an impulsive force on them. The velocity from the nozzle assuming no friction losses is given by:

$$V_1 = \surd(2gH) \qquad (4.8)$$

Where:

G: Gravitational acceleration

H: Gauge pressure head at the nozzle

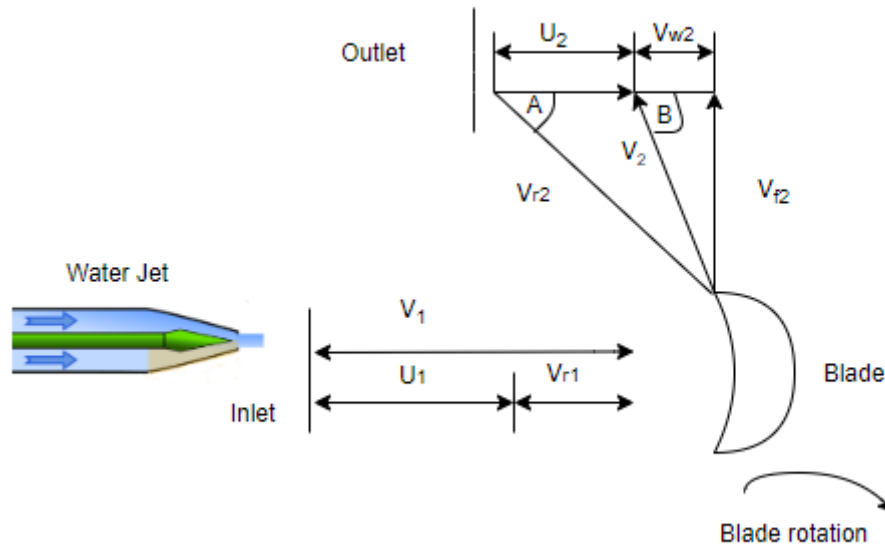V_1: Velocity from the jet

Figure 4-12: Pelton Wheel velocity triangle

The tangential velocity at inlet is given by:

$$V_1 = V_{w1} = V_{r1} + U_1 \qquad (4.9)$$

Where:

V_1 : Absolute fluid velocity at inlet(m/s)

V_{r1}: relative velocity at inlet(m/s)

U_1: Tangential velocity of a blade(m/s)

V_2: Absolute fluid velocity at the outlet(m/s)

V_{r2}: relative velocity at outlet(m/s)

V_{w2}: relative velocity at inlet(m/s)

U_2: Tangential velocity of a blade at the outlet(m/s)

V_{f2}: velocity of flow at the outlet(m/s)

A: Angle made by the relative velocity with blade motion

B: Angle made by the absolute velocity with blade motion

Assumptions:

- No friction loss as water passes through the bucket $V_{w1} = V_{w2}$. Angel A equals zero, $V_2 = V_{r2}$
- The bucket is uniform $U_2 = U_1 = U$
- The speed ratio is 0.5
- Generator efficiency η_{gen} 95%

The tangential velocity at inlet is given by:

$$V_2 = U_1 - V_{w2} \cos B_2 \tag{4.10}$$

The change in tangential fluid velocities are used to come up with shaft torque and power generated and it is given by:

$$V_2 - V_1 = V_{w1}(1 - \cos B_2) = (V_1 - U)(1 - \cos B_2) \tag{4.11}$$

The power is the mass flow rate of the water by the bucket velocity by the change in tangential fluid velocity at inlet and exit.

$$P_{shaft} = \dot{m}U(V_1 - U)(1 - \cos B_2) \tag{4.12}$$

Substituting the mass flow rate with the volumetric flow rate and the density of the water the power becomes:

$$P_{shaft} = \rho Q U(V_1 - U)(1 - \cos B_2) \tag{4.13}$$

$$V_1 = \sqrt{2 \times 9.81 \times 45} = 29.71 \text{m/s}$$

The blade velocity is determined by using the speed ration

$$\frac{U}{V_1} = 0.5 \ggg U = 29.71 \times 0.5 = 14.86 \text{m/s}$$

The volumetric flow rate is considered to be 0.27 m³/s, the density is 1000kg/m³ the blade angle at the outlet is taken to be 133.5º.

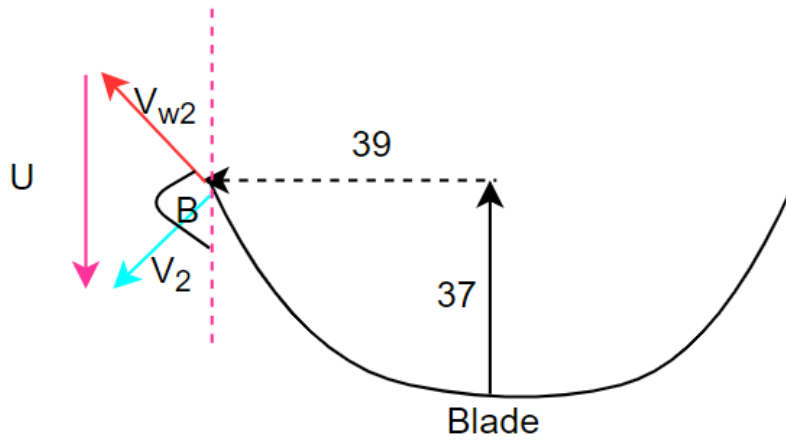Figure 4-13: Blade outlet velocities

$$B = 180 - \theta \ggg \theta = \tan^{-1}\left(\frac{39}{37}\right) = 46.5 \ggg 180 - 46.5 = 133.50$$

$$P_{shaft} = 1000 \times 0.27 \times 14.86(29.71 - 14.86)(1 - \cos 133.5) = 100.69 kW$$

$$\eta_h = \frac{P_{shaft}}{\rho g H Q} = \frac{100.69 \times 10^3}{1000 \times 9.81 \times 45 \times 0.27} = 84.60\%$$

$$\eta_{overall} = \eta_h \times \eta_{gen} \ggg 0.846 \times 0.95 = 80.37\%$$

The generated electric power with the consideration of η_{gen} then becomes

$$P_{electric} = 100.69 \times 0.95 = 95.66 kW$$
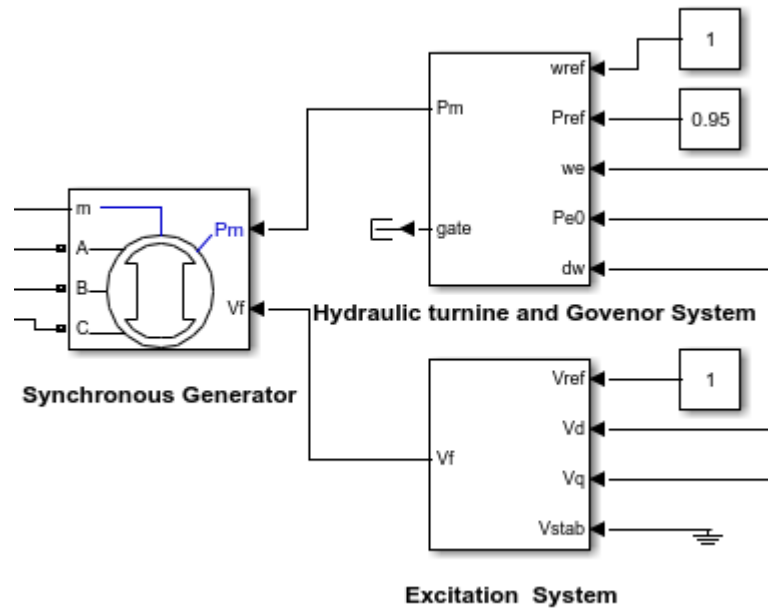
Figure 4-14: Microhydro system MATLA/SIMULINK
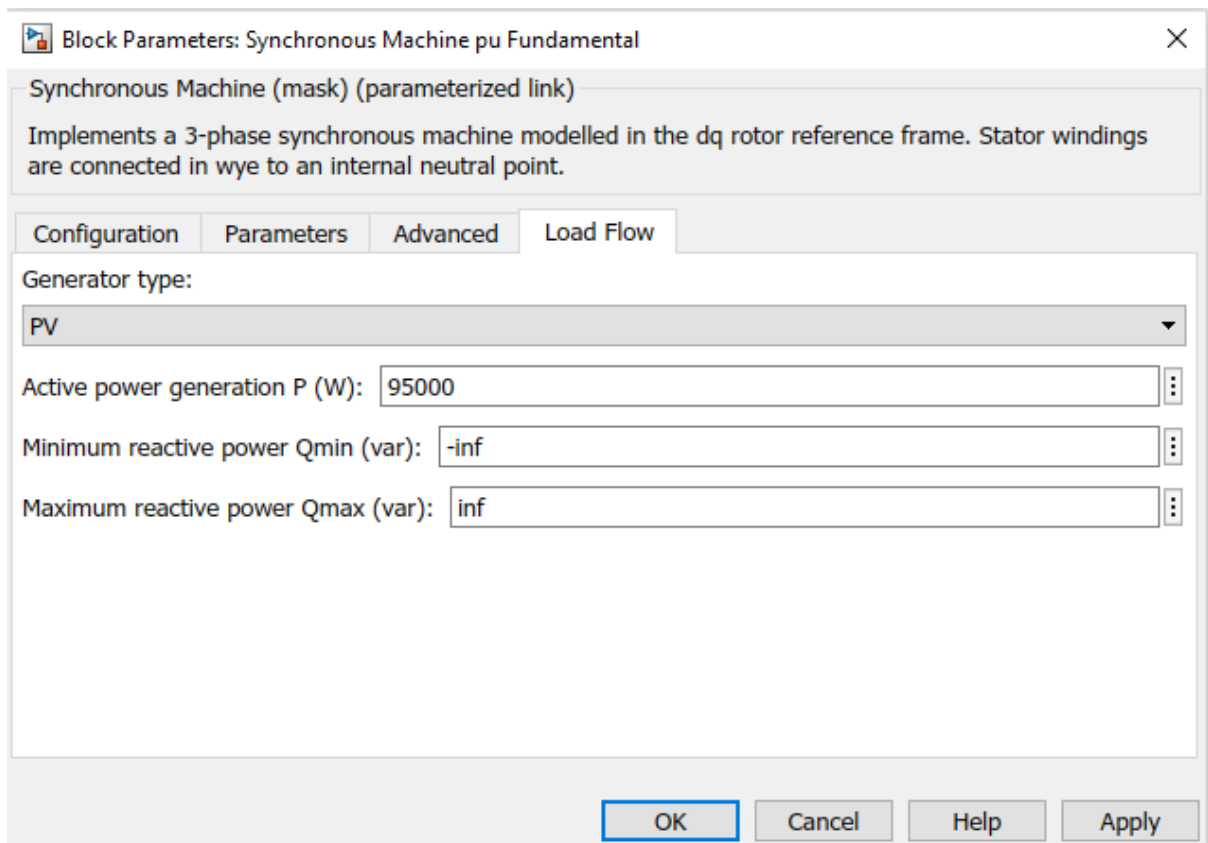

Figure 4-15: Synchronous machine parameters

Figure 4-16: Synchronous machine rated power output

4.10   Battery Bank

Alternative energy sources such as wind turbines and solar PV have intermediate generation due to their reliance on weather conditions. There is a need to mitigate that through storage systems. In this thesis, Lithium-ion batteries are employed so to have a reliable hybrid system due to their high energy efficiency, long lifespan, high power density, and high reliability as compared to other battery types such as lead-acid,nickel-cadmium(NiCD), and nickel-metal hydride(NiMH) batteries. The battery storage system will comprise of two components which are the battery bank and a bi-directional DC-DC(buck/boost) converter with two switches to control power flow(Kumar, 2017; Moubarak et al., 2018; Motapon et al., 2014).

The buck/boost converter assists in matching the voltage from the batteries from the renewable source, it further controls the charging and discharging of the battery (Lindstens, 2017) The batteries need to be kept in good conditions, there needs to be mitigation of over-discharging and charging so to have a longer lifespan. If these conditions are not prevented, it leads to reduce the capacity of the battery. There needs a battery management system that monitors the voltage, current, and temperature to keep the state of the battery in good condition and balancing the charge to the cells to keep the cell voltage consistent. The control of the battery

system can be done by the microcontroller which monitors both voltage and current depending on the SOC and the ambient temperature (Zacharek & Sundqvist, 2018).

4.11 Battery Modelling

The battery system is connected at the output of the DC-DC boost converter from the PV array through the DC-DC bidirectional converter to allow it to either absorb excess energy by acting as a load or dispatch power and operate as a voltage source. The block is found in SimPowerSystems library in Matlab and it has three connecting terminals where two are for physical and "m" terminal is for signals which are SOS, voltage, and current. The physical terminal is connected to the DC link from the PV array. The fluctuation of either MHP and PV array power due to their intermittent nature results in a mismatch between supply and demand, thus the need for a battery bank.
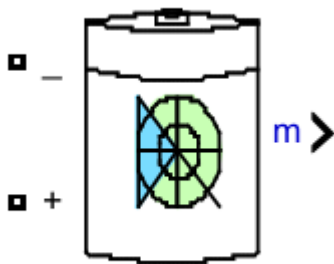

Figure 4-17: Battery bank block

The Lithium-ion battery charging and discharging model is given by the following equations(Motapon et al., 2014; Wang et al., 2014).
Discharge:

$$V_{batt} = E_o - R \times i - K\frac{Q}{Q - it} \times (it + i^*) + A\exp(-B \times it) \qquad (4.14)$$

Charge:

$$V_{batt} = E_o - R \times i - K\frac{Q}{it - 0.1Q} \times i^* - K\frac{Q}{Q - it} \times it + A\exp(-B \times it) \qquad (4.15)$$

Where:

V_{batt}= Voltage battery(V)
E_o= Battery constant voltage(V)

K=Polarisation constant (V/(Ah)) or polarisation resistance (Ω)

Q=Battery Capacity (Ah)

it=Actual battery charge (Ah)

A=Exponential zone amplitude(V)

B=Exponential zone time constant inverse (Ah)$^{-1}$

R=Internal resistance (Ω)

i=Battery current(A)

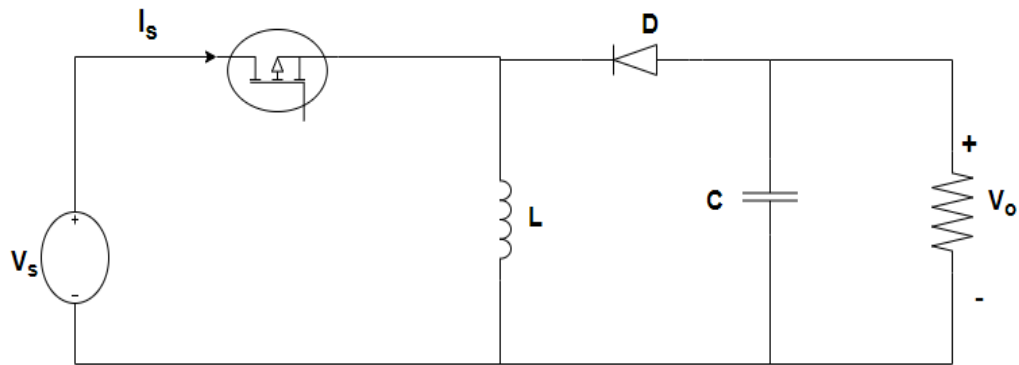i*=Filter current(A)

exp= Expontional zone voltage(V)

Figure 4-18: Bidirectional Converter

There are switches and the diode which is connected in the direction opposite to the power flow from the source, to a capacitor and the load, and those are connected in parallel as shown in figure 4.18 above and this helps to help current flow in one direction. The switch is turned ON and OFF by employing the PWM which is either time-based or frequency-based (Zacharek & Sundqvist, 2018).
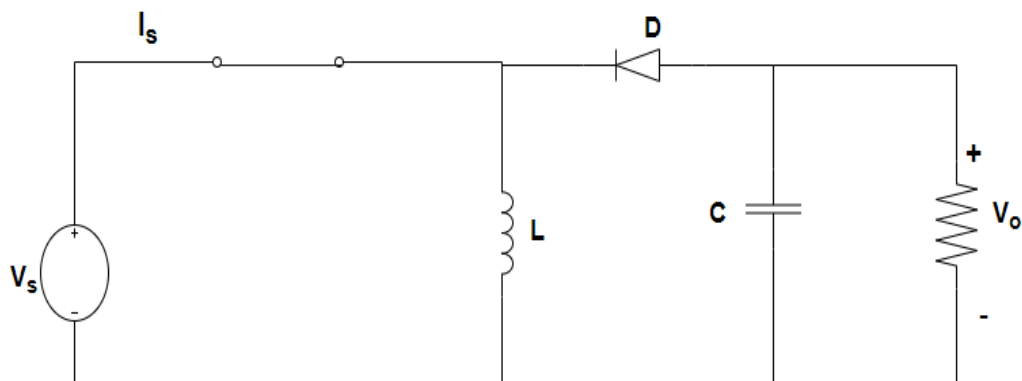

Figure 4-19: Bidirectional converter with Switch ON

When the switch is ON the current flows through the inductor and the voltage across the inductor V_L is equal to the V_s so due to the constant voltage the inductor current increases

90

linearly and the inductor stores charge and results in the inductor having more energy (Zacharek & Sundqvist, 2018).

When the switch is ON which is determined by the duty cycle D where is $D = \frac{T_{ON}}{T}$ and T is the period. The voltage source and the voltage across the inductor are equal;

$$V_s = V_L = L\frac{di}{dt}$$

The increase of current during the ON period results in the following rate of change of the inductor;

$$\frac{\Delta i}{DT} = \frac{V_s}{L}$$
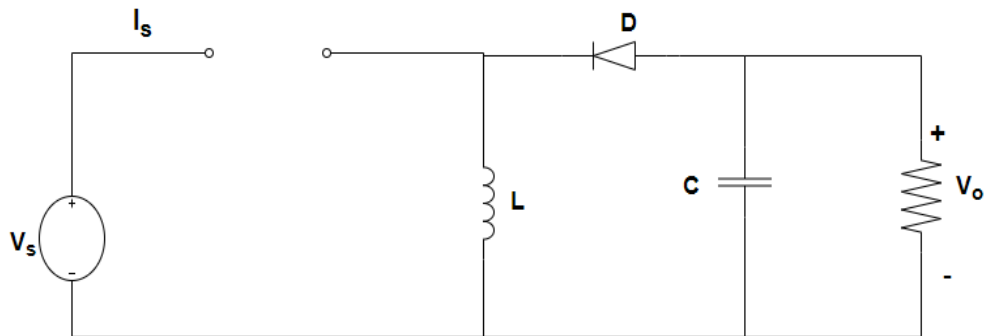
$$\Delta i = \left(\frac{V_s}{L}\right)DT$$

Figure 4-20: Bidirectional converter with Switch OFF

This is the OFF state and in this instance, the polarity of the inductor is reversed and the energy stored in the inductor is then dispatched and dissipated in the load which results in maintaining the flowing current in the same direction and this makes the output voltage because the inductor has now become the source (Zacharek & Sundqvist, 2018).

$$L_{min} = \frac{D(1-D)^2 V_O}{2 \times f \times I_{ccm}} \tag{4.16}$$

$$D = \frac{V_{Bat}}{V_O} \tag{4.16}$$

Where:

V_{Bat} = Battery Voltage (Low Side)

V_O = PV voltage (High Side)

$$D = \frac{400}{750} = 0.53 \tag{4.16}$$

Where:

L_{min}=Inductor value

D= Duty cycle (0.533)

I_{ccm}=10% of I_{Load}

f= Switching frequency (50kHz)

$$L_{min} = \frac{0.533(1 - 0.533)^2 \times 750}{2 \times 50 \times 10^3 \times 13.6} = 6.40 \times 10^{-5} H$$

$$C_{Boost} = \frac{D I_{Load}}{f \times \Delta V_O} \tag{4.17}$$

Where

ΔV_O= 1% of V_O

$$C_{Boost} = \frac{0.533 \times 136.6}{50 \times 10^3 \times 7.5} = 1.94 \times 10^{-4} F$$

This is a DC-DC power electronic device regulator that can either boost or buck the voltage. In this simulation, IGBT switches would be employed and this converter uses the DC link voltage V_{dc}. This is to have a constant DC link voltage. When voltage fluctuates, the instability of the DC link voltage requires a voltage stabilizing controller. The output voltage of the bidirectional converter relies on the ability to correctly detection of the control system so to determine whether buck or boost the voltage. This helps in the improvement of the efficiency and the performance of the system(Karimi, 2014).
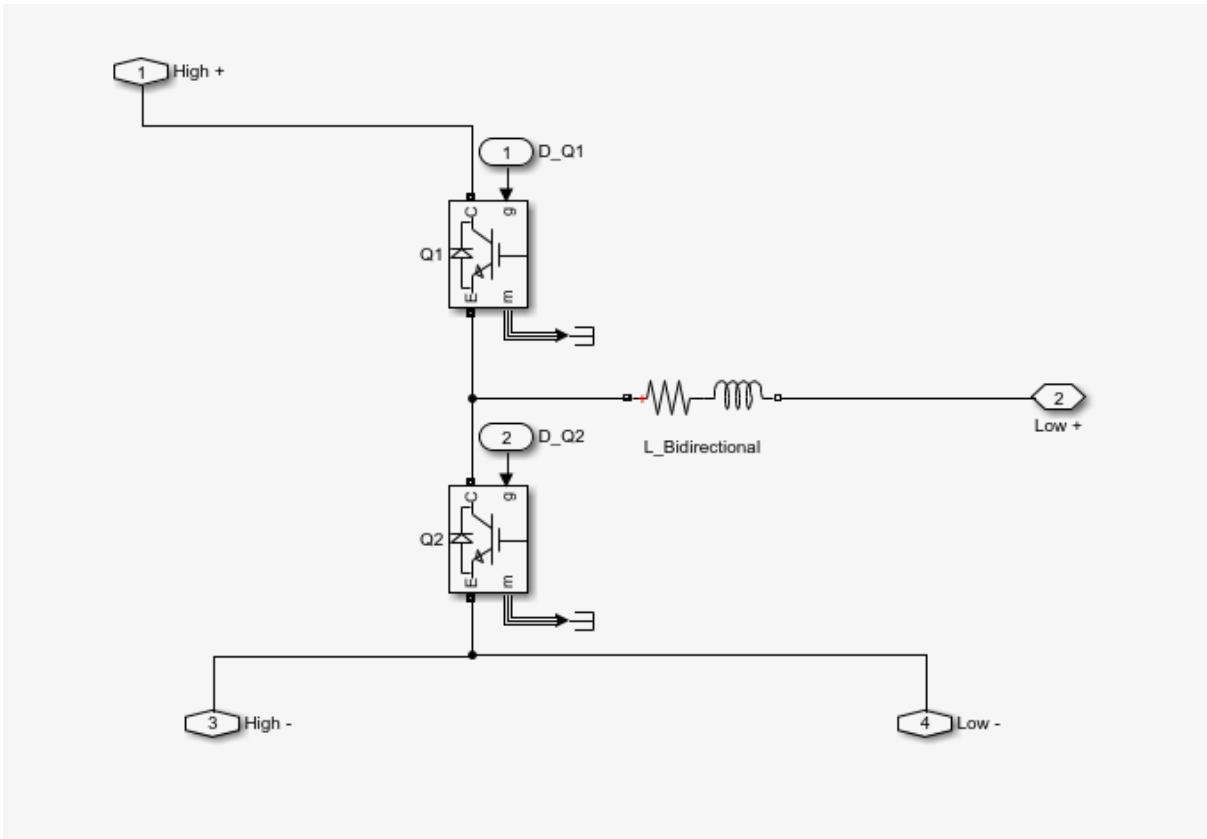
Figure 4-21: Battery Storage bidirectional converter circuit

The battery bidirectional DC_DC converter employs two switches as illustrated in figure 4.1 above. The main purpose is to maintain the required voltage, thus either buck or boost mode will be activated and this relies on the control scheme illustrated in figure 4.22 below.
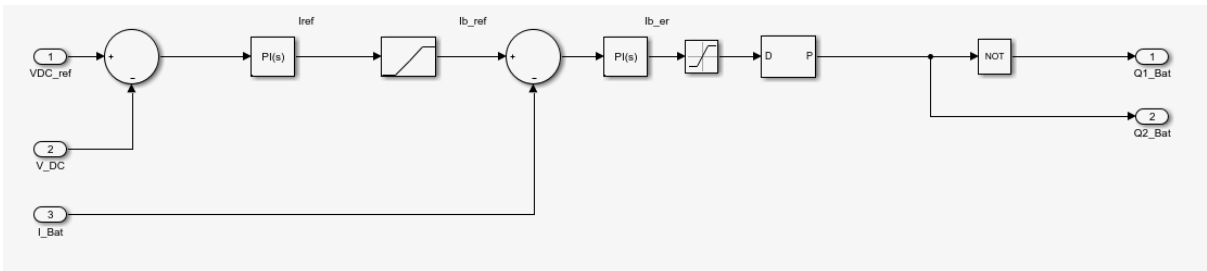

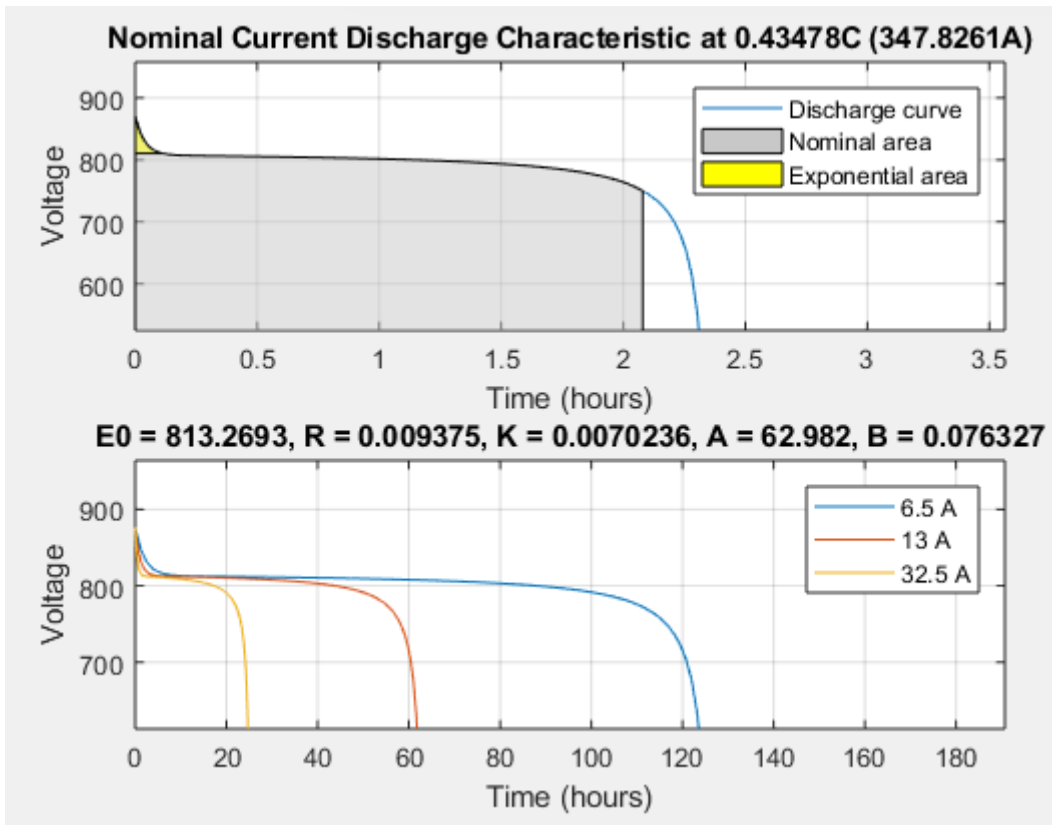Figure 4-22: Battery DC-DC Bidirectional converter control

Figure 4-23: Battery current discharge characteristics

4.12 Energy Management

Continuous power flow is of prime importance hence it requires the need to have system controls that dictates when to store energy when there is excess and when to dispatch from the storage where the deficit occurs. When the power from the MHP system and the PV array is more than the load demand, the excess needs to be stored. When MHP system power and PV array is less than the load demand then the Battery bank needs to dispatch power to the grid. The battery charging or discharging is further dependent on the SOC of the battery during fluctuations. It is, therefore, crucial to provide energy security by having an energy management system that control, operate and organize battery storage system, renewable energy sources and power electronic converters(Luta, 2019).

4.12.1 Fuzzy logic Control

Fuzzy logic is a computational paradigm that mimics the way a human brain works, takes information then responds with precise action. It is utilized in a variety of applications, including control systems. Fuzzy logic controllers are known for being resilient and simple to build since they do not need perfect knowledge of the model of the system to be managed. They are made up of three parts: an input, a processing phase, and an output(Luta & Atanda K. Raji, 2019).
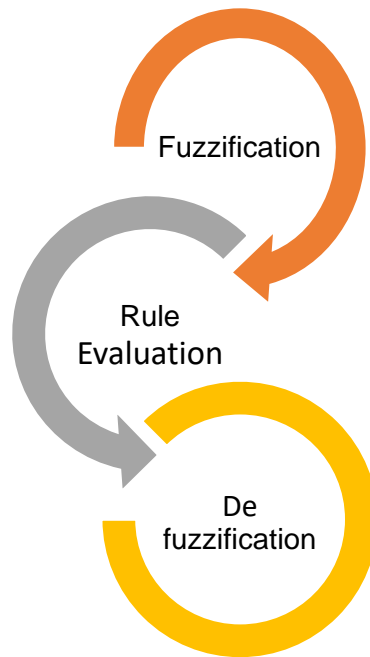
94

Figure 4-24: Fuzzy Inference Progress

The processing phase of the input is known as inference engine process and is based on logical rules that entails IF-THEN statement.

Fuzzification	Rule Evaluation	De fuzzification
Translate input to truth values	Compute output to truth values	Transfer truth values into output
Input variables are assigned degrees of membership in different classes	The inputs are applied to a set of IF/THEN control rules	Fuzzy outputs are combined into discrete values needed to drive control mechanism
Fuzzification maps the outputs from set sensors to values from 0 to 1 using set of input membership functions	The results of various rules are added together to generate a set of fuzzy outputs	

1. If (Error is BNE) and (SOC is SSOC) then (BatteryControl is not Discharge) (1)
2. If (Error is BNE) and (SOC is MSOC) then (BatteryControl is Discharge) (1)
3. If (Error is BNE) and (SOC is LSOC) then (BatteryControl is Discharge) (1)
4. If (Error is MNE) and (SOC is SSOC) then (BatteryControl is not Discharge) (1)
5. If (Error is MNE) and (SOC is MSOC) then (BatteryControl is Discharge) (1)
6. If (Error is MNE) and (SOC is LSOC) then (BatteryControl is Discharge) (1)
7. If (Error is MPE) and (SOC is SSOC) then (BatteryControl is Charge) (1)
8. If (Error is MPE) and (SOC is MSOC) then (BatteryControl is Charge) (1)
9. If (Error is MPE) and (SOC is LSOC) then (BatteryControl is not Charge) (1)
10. If (Error is BPE) and (SOC is SSOC) then (BatteryControl is not Charge) (1)
11. If (Error is MPE) and (SOC is LSOC) then (BatteryControl is Charge) (1)
12. If (Error is BPE) and (SOC is SSOC) then (BatteryControl is Charge) (1)
13. If (Error is BPE) and (SOC is SSOC) then (BatteryControl is Charge) (1)
14. If (Error is BPE) and (SOC is SSOC) then (BatteryControl is Charge) (1)
15. If (Error is BPE) and (SOC is SSOC) then (BatteryControl is Charge) (1)
16. If (Error is BPE) and (SOC is LSOC) then (BatteryControl is not Charge) (1)
17. If (Error is Zero) and (SOC is SSOC) then (BatteryControl is not Charge) (1)
18. If (Error is Zero) and (SOC is MSOC) then (BatteryControl is not Charge) (1)
19. If (Error is Zero) and (SOC is LSOC) then (BatteryControl is not Charge) (1)
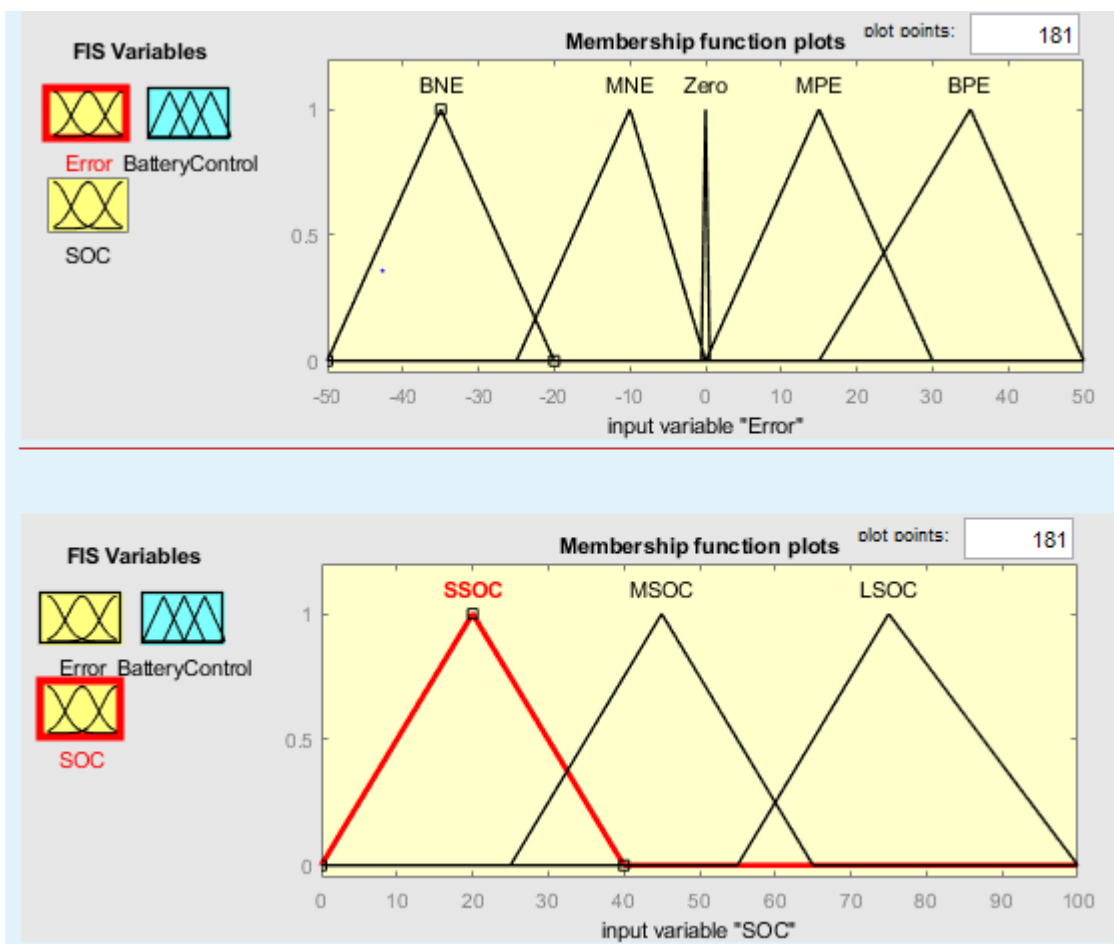
Figure 4-25: Fuzzy rules

Figure 4-26: Input membership functions

96

Table 4-4: Input Membership function in full

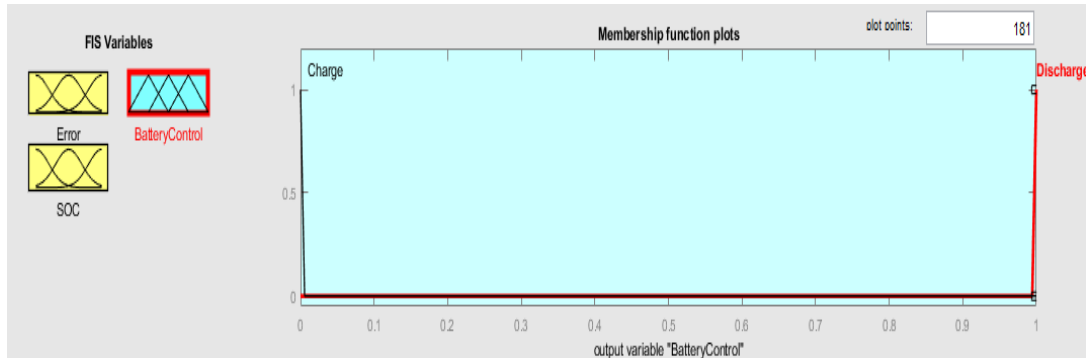| Error	SOC
BNE : Big Negative Error	SSOC : Small State of Charge
MNE : Medium Negative Error	MSOC : Medium State of Charge
Zero : No Error	LSOC : Large State of Charge
MPE : Medium Positive Error	
BPE : Big Positive Error	

Figure 4-27: Output membership function

The equation governing the energy management system can be

$$P_{NET} = P_{MHP} + P_{PV} - P_L \qquad (5.1)$$

where

P_{NET}, = difference between the supply of power $P_{MHP} + P_{PV}$ and the demand P_L

P_{MHP} and P_{PV} are the power generated from the MHP and photovoltaic,

P_L = Total demand

If the P_{NET} is either greater than one or less, then the battery bank will either charge or discharge depending on the SOC to maintain the battery in good conditions to prolong the lifespan of the storage system

SOC_{min} <=20%

SOC_{max} >=80%

97

The battery can only dispatch power when the SOC bigger than the SOC_{min} and it can only charge if the SOC less than SOC_{max}.

This control is operated by employing fuzzy logic control to the charging and discharging of the battery. This is based on the SOC and the error presented in figure 4.24 between the Load and the renewable energy supply. Figure 4.25 illustrates how the blocks are set up to determine if power is dispatched or absorbed by the battery.
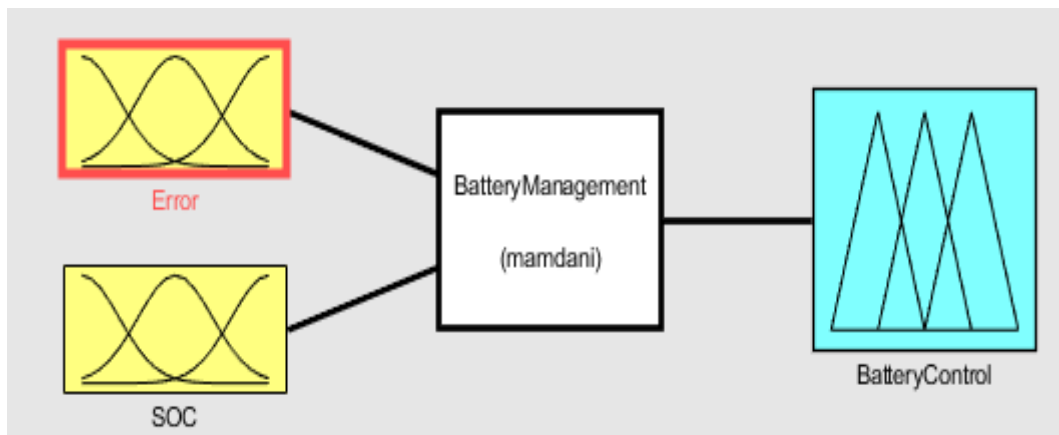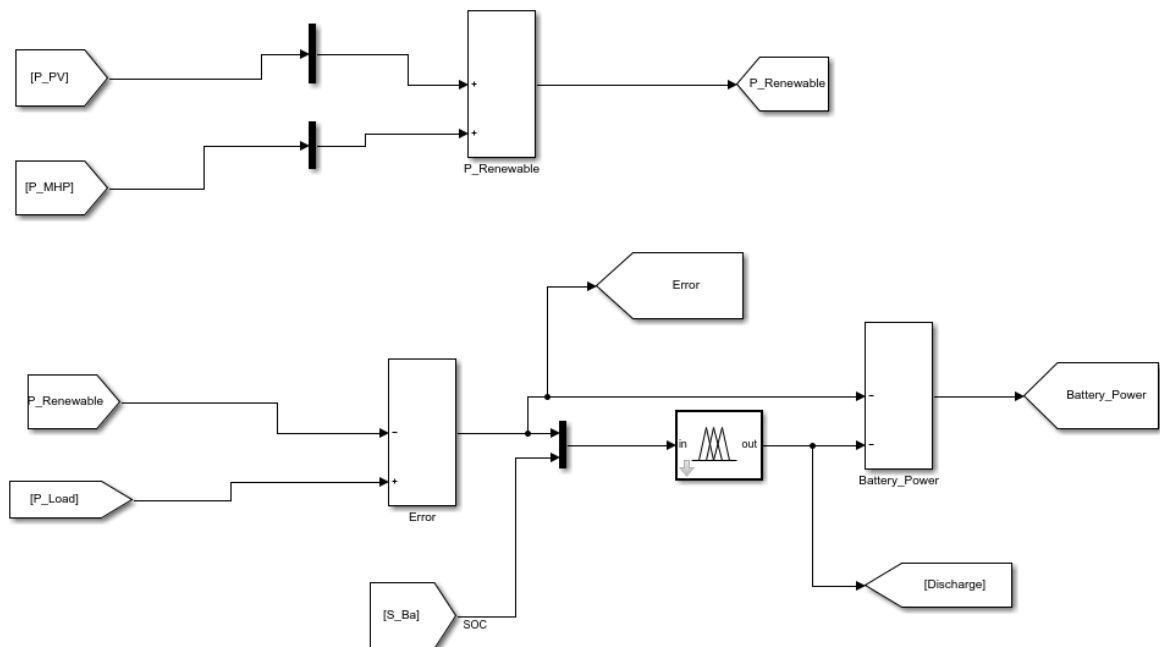

Figure 4-28: Fuzzy logic inputs and output

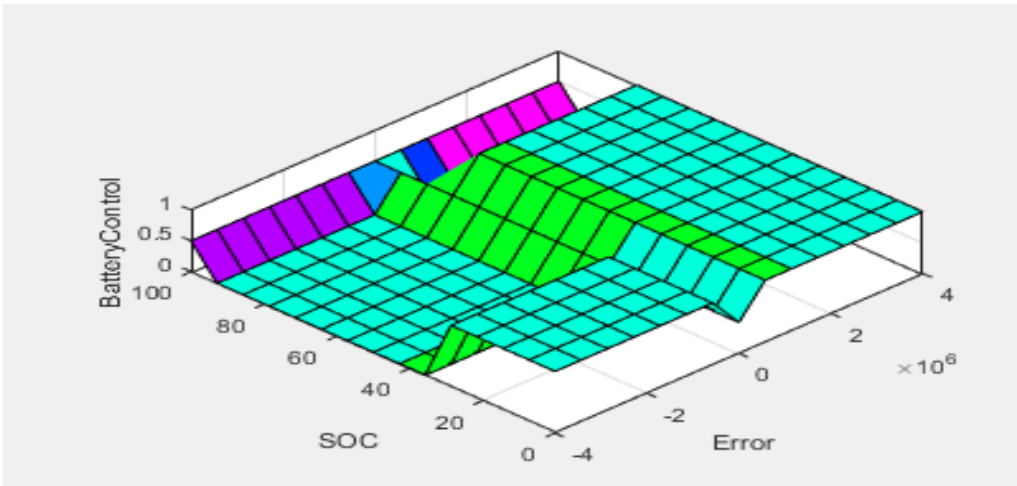Figure 4-29: Simulink blocks for battery control
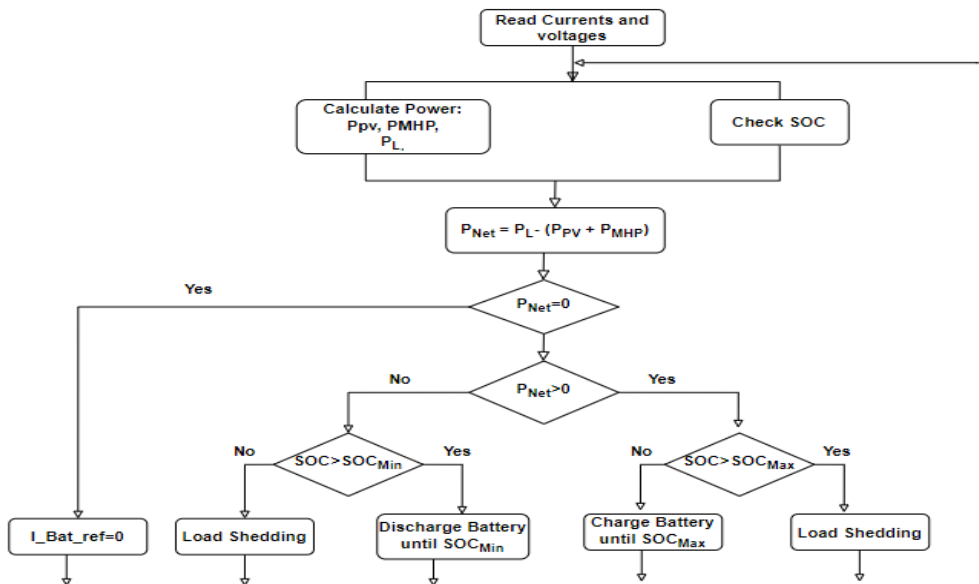
Figure 4-30: Fuzzy logic surface view

Figure 4-31: Energy Management algorithm

5 Chapter five: Simulation Results and discussion

5.1 Introduction

The need to electrify rural areas, reduce greenhouse emissions, and increase energy demand due to population growth and increased standard of living has prompted the world to renewable generators. The conventional power systems are predominantly closer to the load which is located mostly in the urban area thus, employing a hybrid standalone system is crucial for rural electrification. This is caused by the terrain and the scattered nature of those settlements and reduces the burden on the grid. It further reduces operating expenses due to network costs reduction. A hybrid system that is composed of an MHP plant, PV array, and battery storage is modelled and simulated in MATLAB/Simulink environment. This chapter discusses the results obtained after the simulation. Four scenarios are tested to ascertain the energy management of the system. The system has a 180 kW AC peak load for 50 households which is interfaced by the three-phase inverter from the DC supply. The MHP with a capacity of 95kW connected to the rectifier to the DC bus. The PV array with the 102kW capacity with a DC-DC boost converter that boosts the voltage to 750 V to the DC bus. The lithium-ion battery bank is also connected to the DC bus through a DC-DC bidirectional converter.

This chapter discusses the results of a model in MATLAB/Simulink using simpower toolbox and fuzzy logic control. The irradiance will be varied to mimic the real-life scenario of the fluctuation of solar power since it is dependent on weather patterns. The results are divided into four smaller sections. Firstly, in section 5.2 scenario 1 results will be discussed where the irradiance is kept constant at 1000W/m^2. The system is producing more than required while the MHP is producing consistent power. Section 5.3 deals with scenario 2 where the irradiance is 400W/m^2 and the total power from renewable energy is less than the demand. This is where the battery needs to dispatch. Furthermore, section 5.4 focuses on the varying irradiance from 1000W/m^2 to 400W/m^2 then back to 1000W/m^2 .The battery will then charge and discharge depending on the renewable power produced. Finally in Section 5.5 explores the conduct of the system where the battery SOC is less than 20% and less power is generated than the demand. It further looks at when there is more power produced but the SOC is more than 80%. All this is to test the energy management of the system and how it responds to different instances that are highly possible in real-life instances.
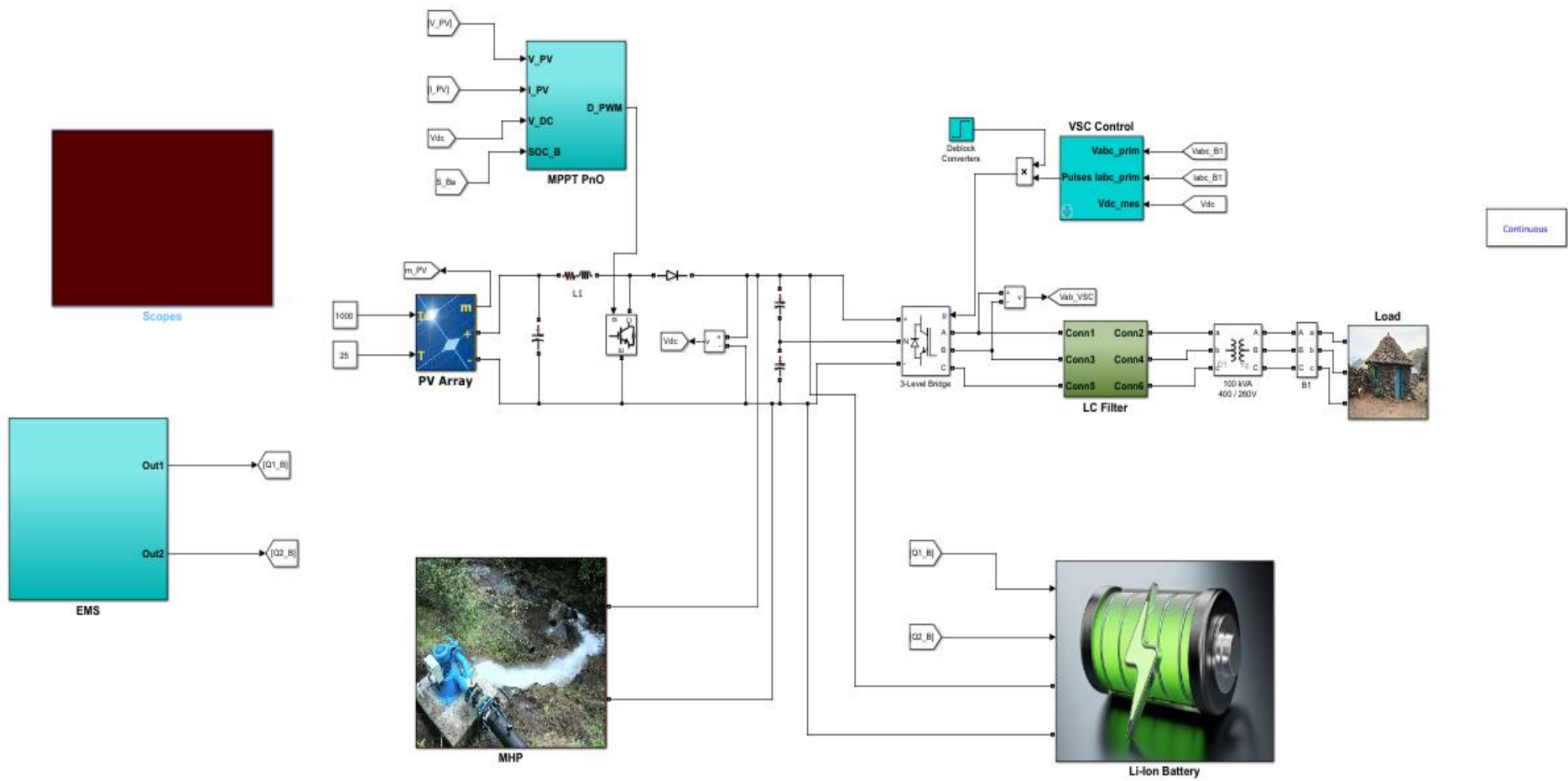
Figure 5-1: System model

5.2 Scenario 1

Firstly, the irradiance will be kept at 1000W/m², and the PV array is made up of 28 modules in parallel and 16 in series with each module producing 228Wp such that it provides about 102.2kW. The PV array is connected to the DC-DC boost converter with a duty cycle of 0.362 to stabilize the random PV input voltage from 478.40 V to 750 V. The array is connected to the DC-DC boost converter via a DC link capacitor to minimize voltage ripples on PV terminals. The P&O MPPT algorithm is employed to extract power from the array. The system is built up utilising physical electronic components like diodes, capacitors, resistors, current sources to build solar cell equivalent circuit. The 102.2kW produced under normal test conditions of irradiance of 1000 W/m² and the temperature of 25⁰C . The power output from the PV array is shown in figure 5.2 below.

The power generated by the PV plant is 102.20kW when the irradiance is 1000W/m² as seen in figure 5.2 below and the temperature is 25⁰C. The calculated value is 102.47kW and this results in a 0.003% error which makes the simulated results very accurate. The transient time for PV power to stabilize is 15ms in the system depicted in Figure 5.3.
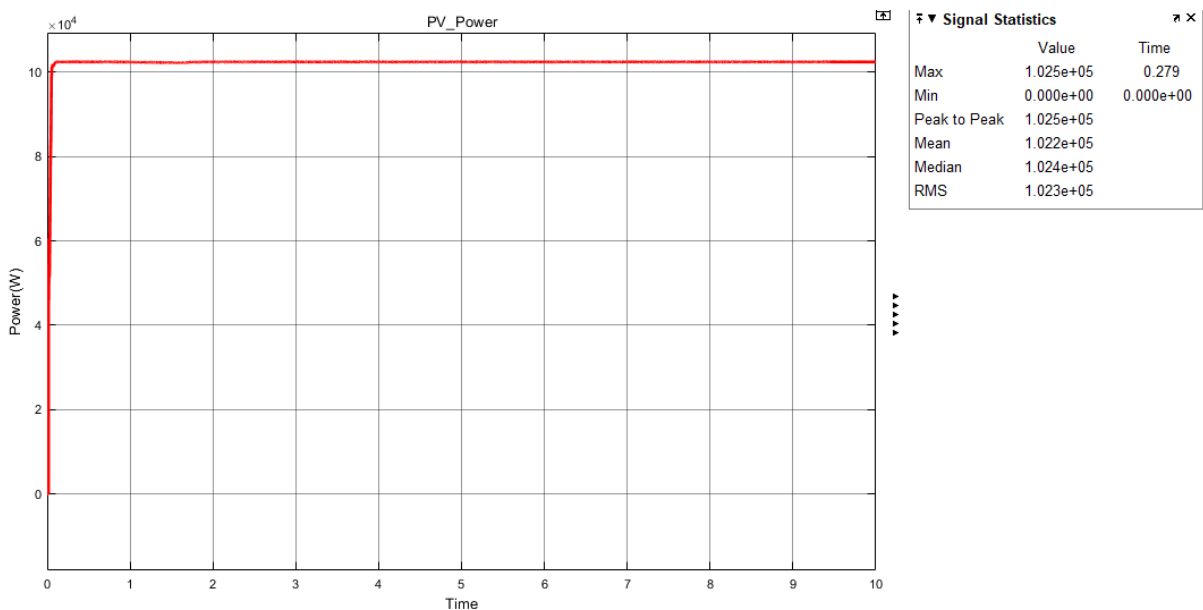

Figure 5-2: PV power output in constant irradiance
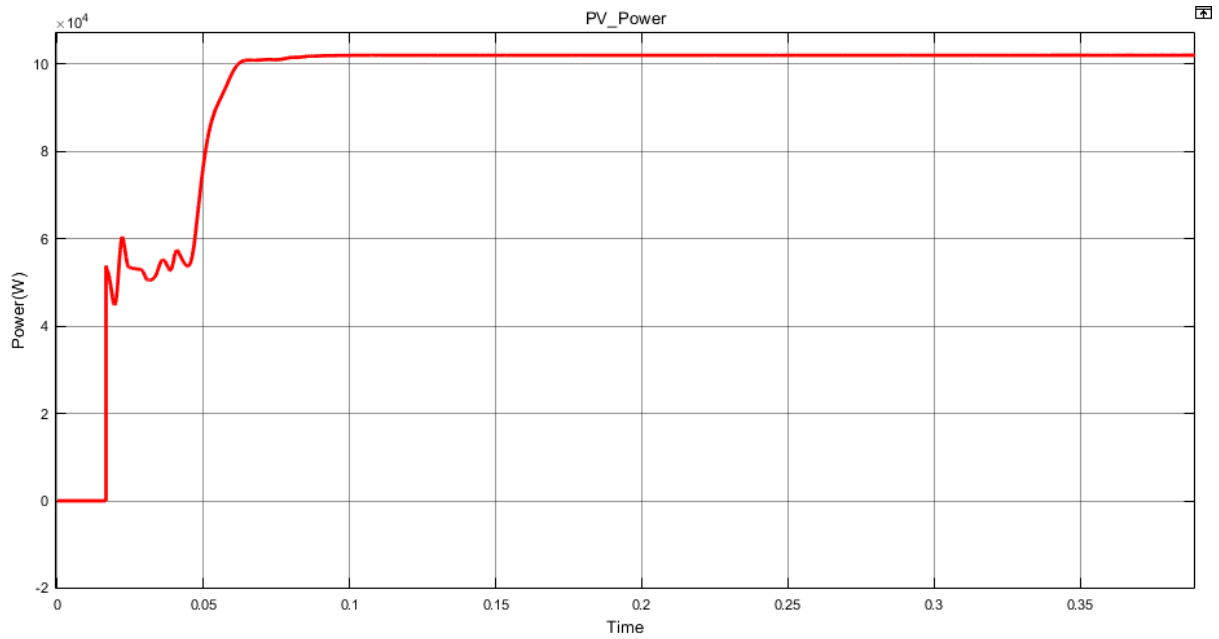
Figure 5-3: PV output power transient time

The voltage output shown in Figure 5.4 below illustrates PV voltage from the array before being boosted which is 476 V_{dc} while the calculated one is 478.40 V_{dc} which is 99.4% accuracy, and it signifies how accurate simulated results are. Furthermore, the duty cycle is varied with 0.362 being an average to provide 750 V_{dc} of voltage to the DC bus. The transient state for stabilization of both the input and output voltage is 20ms.
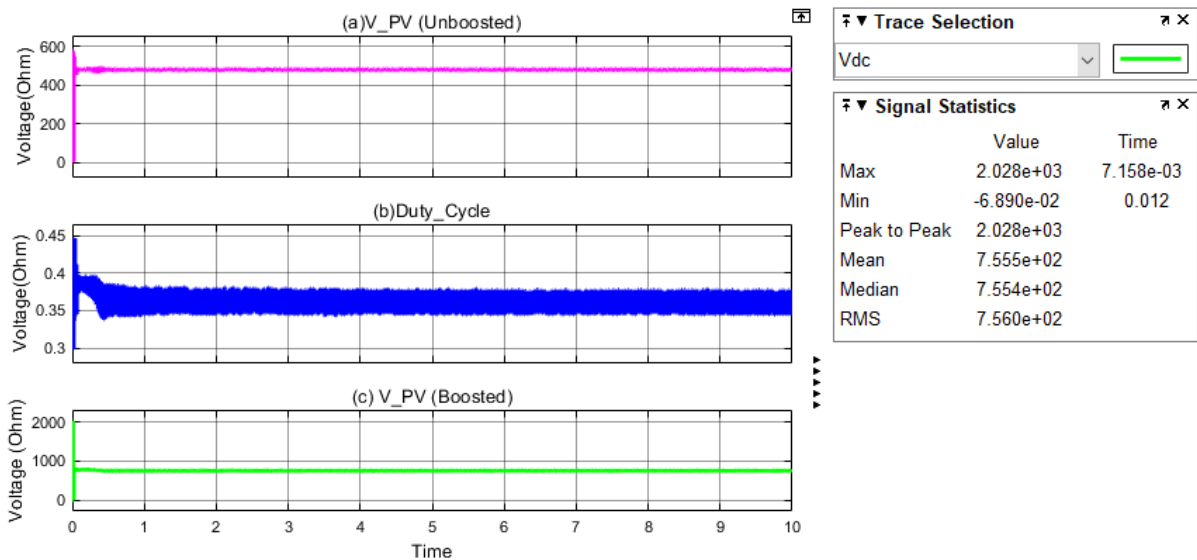
Figure 5-4:PV Voltage (a) Unboosted (c) Boosted and (b) Duty cycle
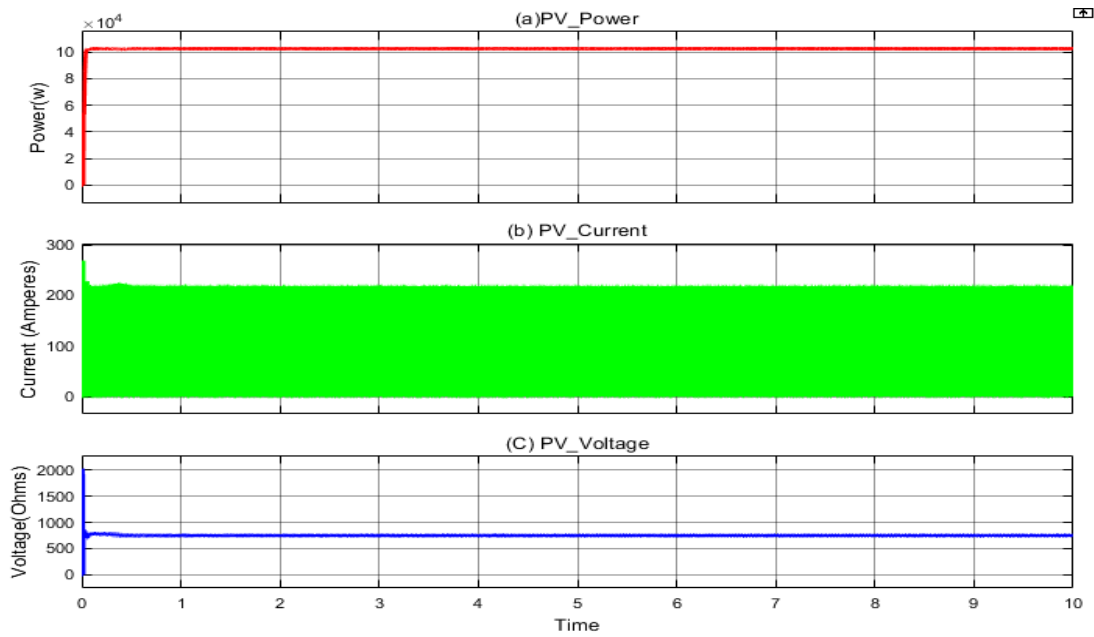
Figure 5-5: PV array (a) Power, (b) Current, (C) Voltage

The MHP will generate around 96.18kW in contrast with the calculated one which gives 95.66kW shows that the accuracy is 99.4%. It is seen that between 0 s to 400ms is a transient state and from 400 ms to 800 ms the steady-state is then reached. This is due to the sudden mechanical torque because of the kinetic energy of water on the blades, there is a spike in shaft speed hence the exponential power from the initial start of the simulation to 800 ms. The oscillations are eventually damped and the steady-state is reached at t=1 sec as illustrated by figure 5.6 and figure 5.7 below.
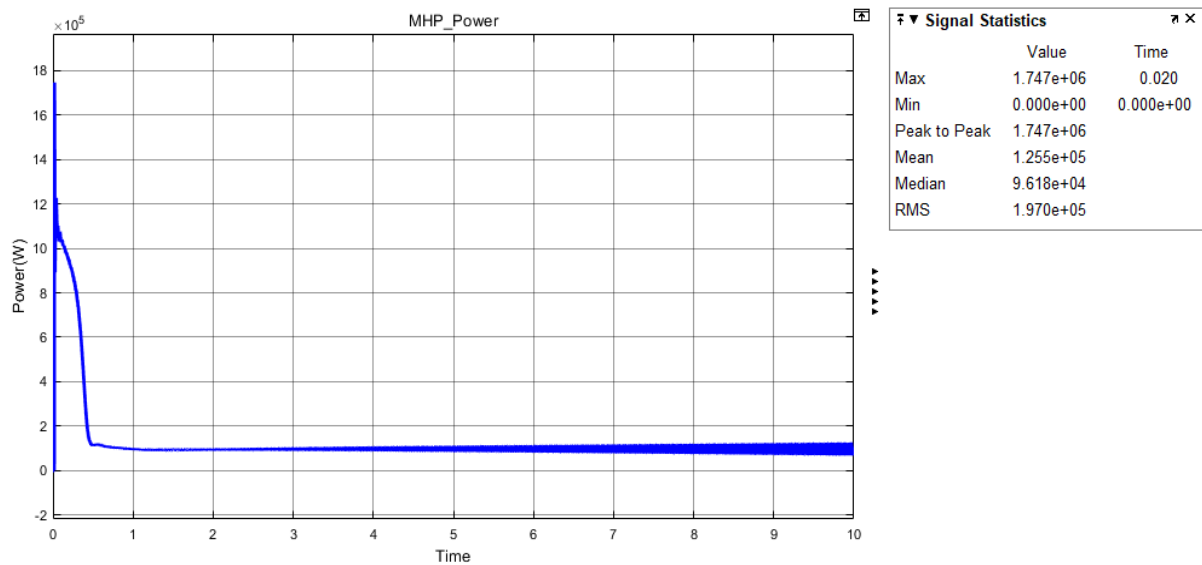
Figure 5-6: MHP Power output
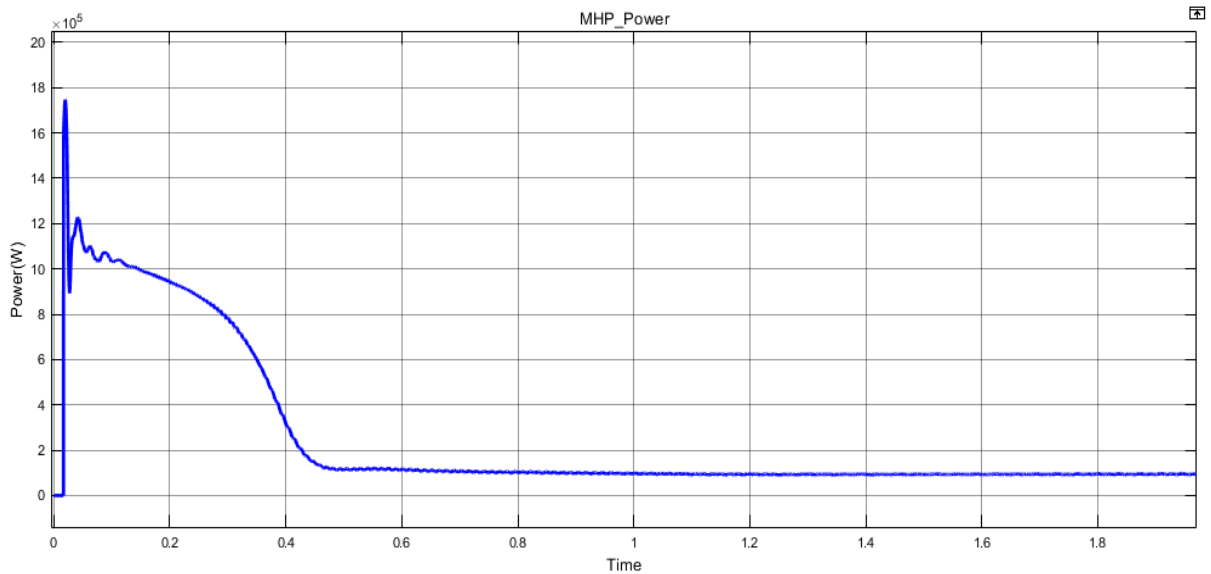
Figure 5-7:MHP transient time

Under constant irradiance of 1000W/m², the total renewable power generated is 198.38kW which is more than the demand. The excess power produced is then absorbed by the Li-ion battery storage to charge the battery. This is illustrated in figure 5.8 where the SOC changes from 50% which is the initial state of charge to 50.19%. The initial charging is high because of the spike in MHP and due to the exponential power because of the high rotational speed before the dumping. The SOC changes from 50% to 50.10% in 320 ms. This, however, slows down when the turbine governor controls the rotational speed of the turbine by regulating the volumetric flow rate by reducing the gate opening. Subsequently, the MHP power reaches a steady state after 400 ms and the charging becomes much lower. The results further show it takes 9 s to move from 50.10% to 50.19% which is a slower charging.
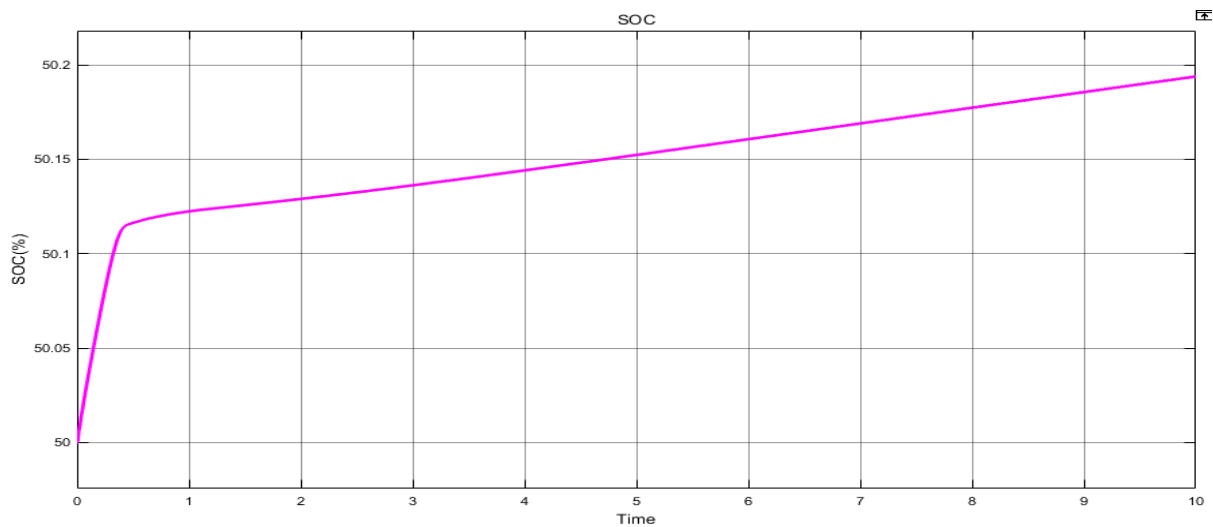
Figure 5-8: Battery charging (SOC increasing)

The Li-ion battery characteristics are depicted in figure 5.9 which are voltage, current, SOC, and power output. When the irradiance is 1000W/m² more energy than the demand is generated hence the battery is absorbing power. This is demonstrated by increasing SOC and the negative value of the battery current. The load is also kept constant at 180kW and the battery is in charging mode.
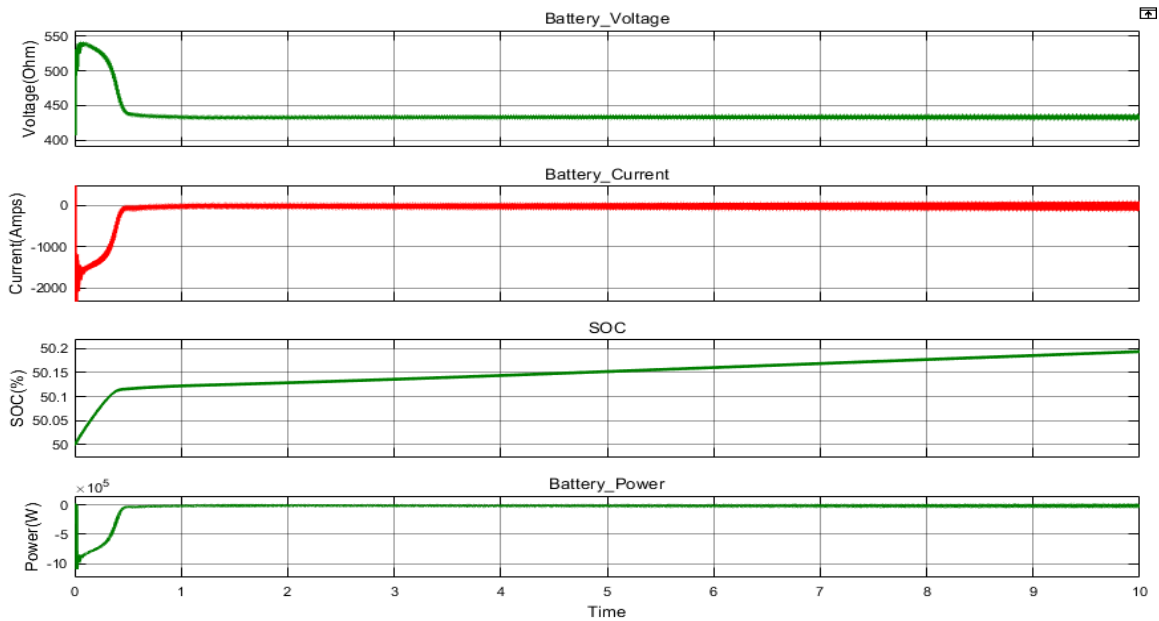
Figure 5-9:Battery (a) Voltage, (b) Current, (c) SOC, (d) Power

Figure 5.10 depicts the system characteristics under constant irradiance with the load being kept constant at 180kW. The system is producing more energy than the demand, so the battery is being charged hence increasing SOC. The power from the MHP is kept constant with a flow rate of 0.27 m³/s to generate about 96.18kW and the demand is well catered for.
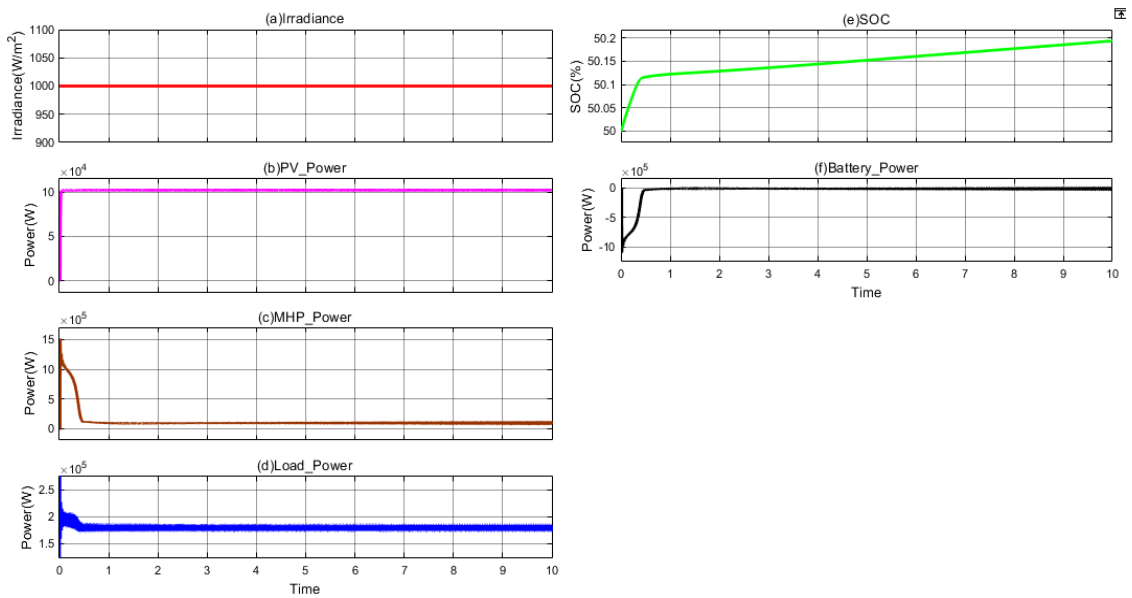
Figure 5-10: System Characteristics(a) Irradiance, PV power, (c) MHP power (d) Load power (e) SOC and (d) Battery power
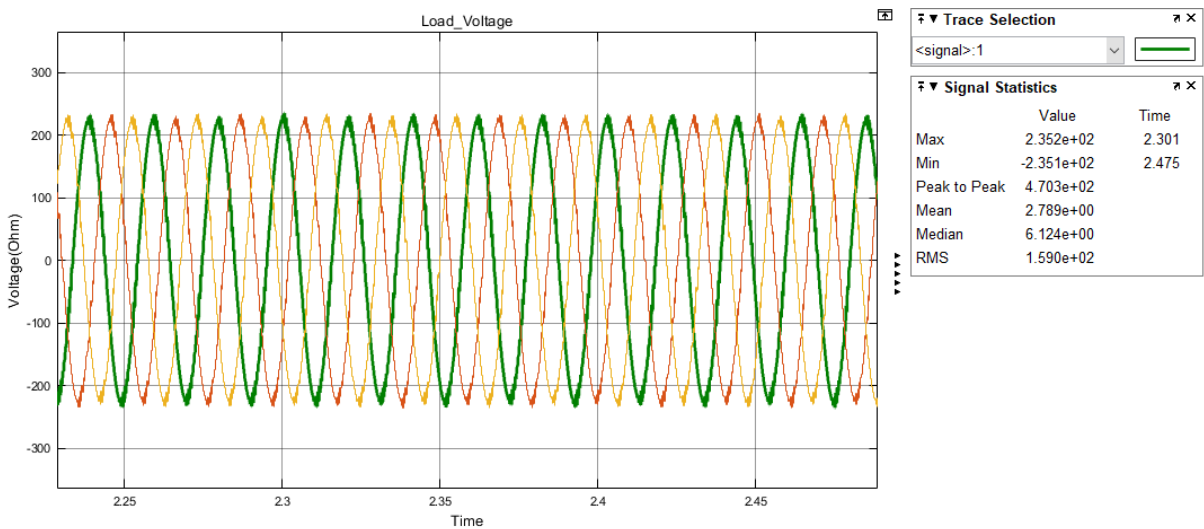
Figure 5-11: Load voltage

The load voltage is not affected, and it is maintained at around 235 V despite more power produced from the system and this can be seen in figure 5.11 above.
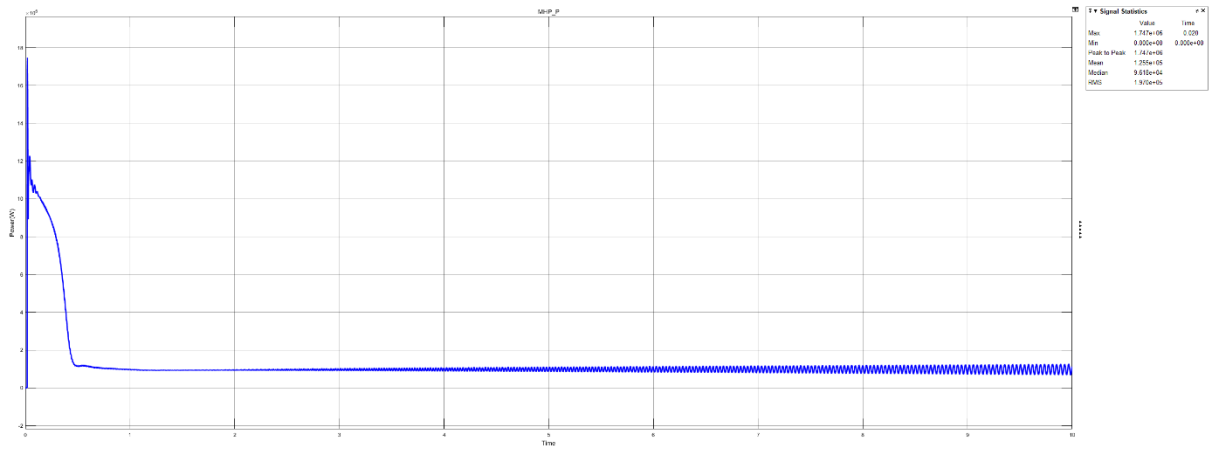
Figure 5-12: MHP power

5.3 Scenario 2

Conversely from the first scenario where it shows ideal weather conditions, this is not always the case. Renewable energy sources are undoubtedly volatile so there are certainly going to be power fluctuations due to weather conditions. The solar irradiance will be decreased as input to the PV array instead of 1000W/m^2 to 400W/m^2. The power generated from the PV array is about 41.22kW shown in figure 5.13 which then added to MHP power the system generates around 123.60kW of power illustrated in figure 5.14(a). This is certainly below what the load requires. According to the energy management algorithm in figure 4.27 the battery needs to dispatch power to meet the load demand. In this state, the battery will be in discharging mode as depicted in figure 5.14(b) by the SOC decrease. Therefore, the Li-ion battery storage system provides about 42.6kW to compensate for power deficits since their power generated is less than the demand.

Figure 5.14 depicts the characteristics of the system, in this scenario since SOC is kept at 50% and the MHP power is kept constant. The battery SOC changes from 50% charges for 0.80 s to 50.1% that is due to high initial power from MHP then the battery discharges hence the SOC moves from 50.10% to 49.84%.
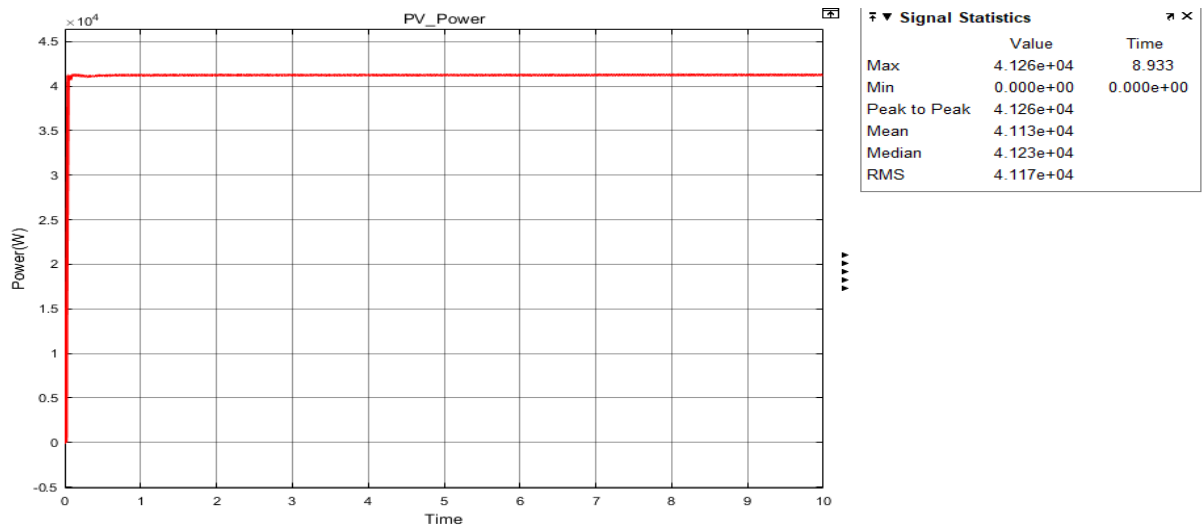
Figure 5-13: PV Power under 400W/m2
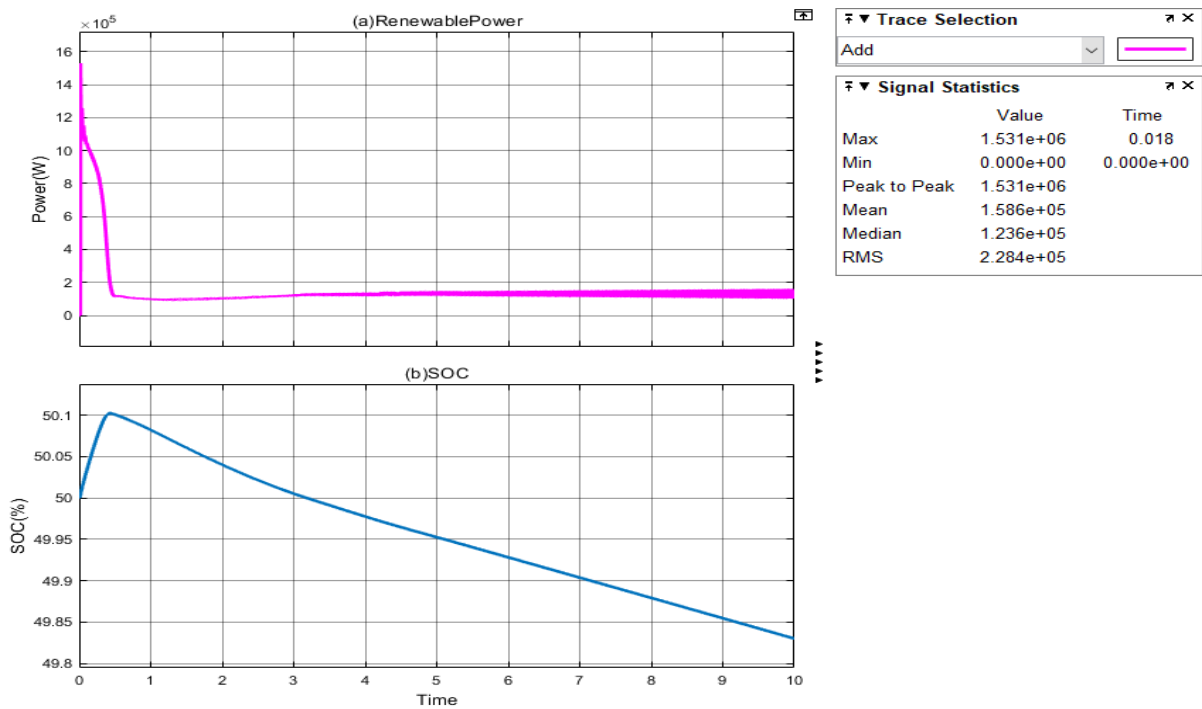
Figure 5-14: System (a) Total Power and (b) SOC

When the irradiance is kept at 400W/m² the power from the PV is 41.22kW and figure 5.15(c) indicates battery power and how it compensates for the power shortage. The battery dispatches around 55.28kW and the load power become 179.50kW which is less than the demand by 0.27%.
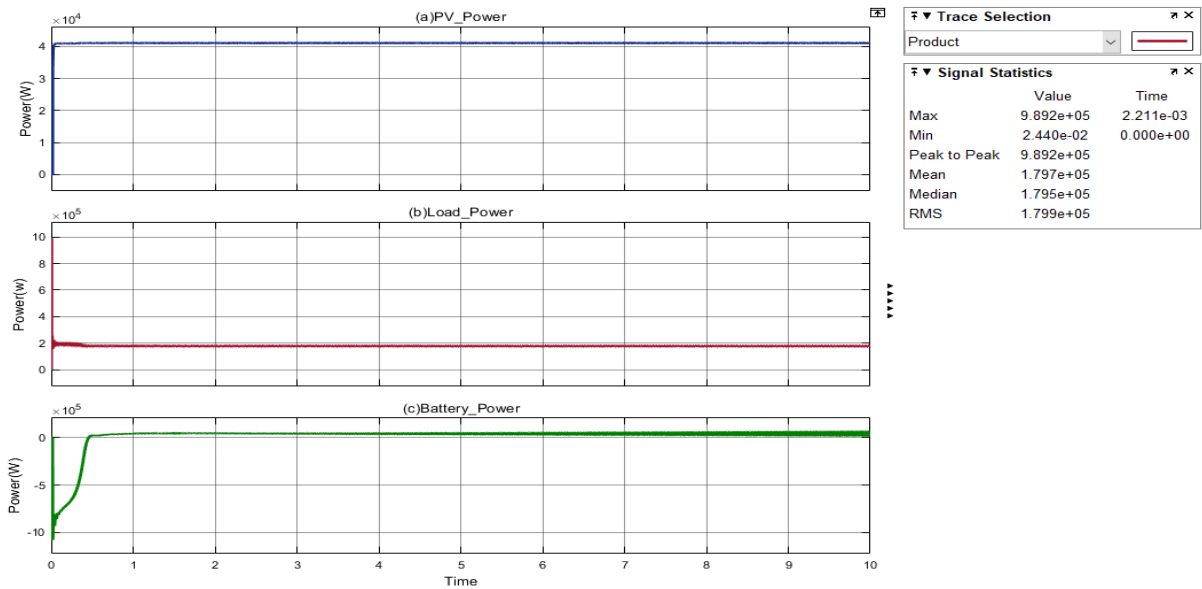
Figure 5-15: (a) PV_Power (b) Load_Power and (c) Battery_Power
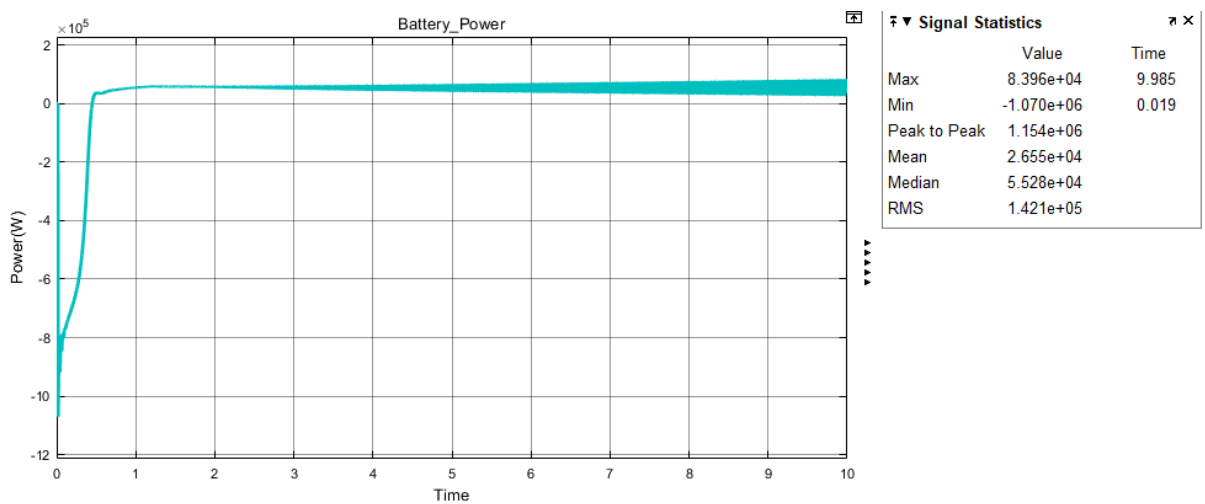
Figure 5-16: Battery Power

Scenario 3

In this scenario, the irradiance will be 1000W/m^2 for the first four seconds. The power generated in this instance exceeds the demand hence the battery will charge this can be seen by the improvement in SOC in figure 5.17(e). The SOC increases from 50% to 50.15% in those first four seconds. The irradiance then drops to 400W/m^2 from four seconds to seven seconds. The power generated from the renewable sources is certainly lower than what is needed by the load so, the battery will dispatch power to the load to compensate for the mismatch shown by figure 5.17(f). The SOC of the battery storage system then drops from 50.15% to 50.08% as illustrated in figure 5.17(e) below. The battery power is kept at 0 for most of four seconds.

This however changes between four seconds to seven seconds where the battery dispatches power to the load. The irradiance swiftly goes back to 1000W/m² and then the sudden change of power causes little fluctuations in load power. The battery then needs to charge again since the power generated is now more than the demand. The SOC improves from 50.08% to 50.11% from seven seconds to ten seconds where the simulation is terminated.
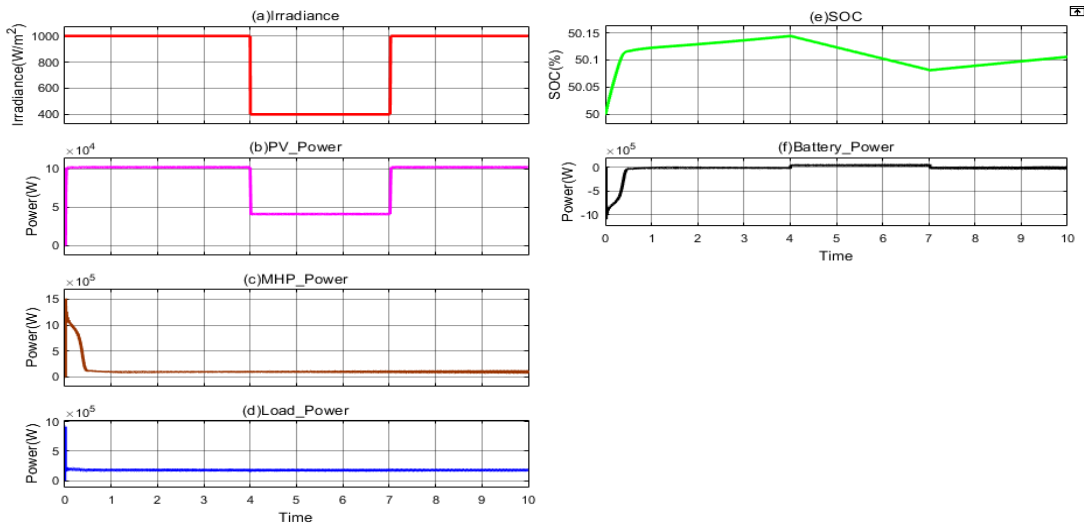
Figure 5-17: System Characteristics (a) Irradiance, (b) PV power, (c) MHP power, (d) Load power, (e) SOC and (f) Battery power

The battery current is negative in the first four seconds and this signals that the battery is charging in figure 5.18 (b). The current then becomes positive when the PV power drops the battery dispatches the power and the current becomes positive. This indicates the battery discharging mode.
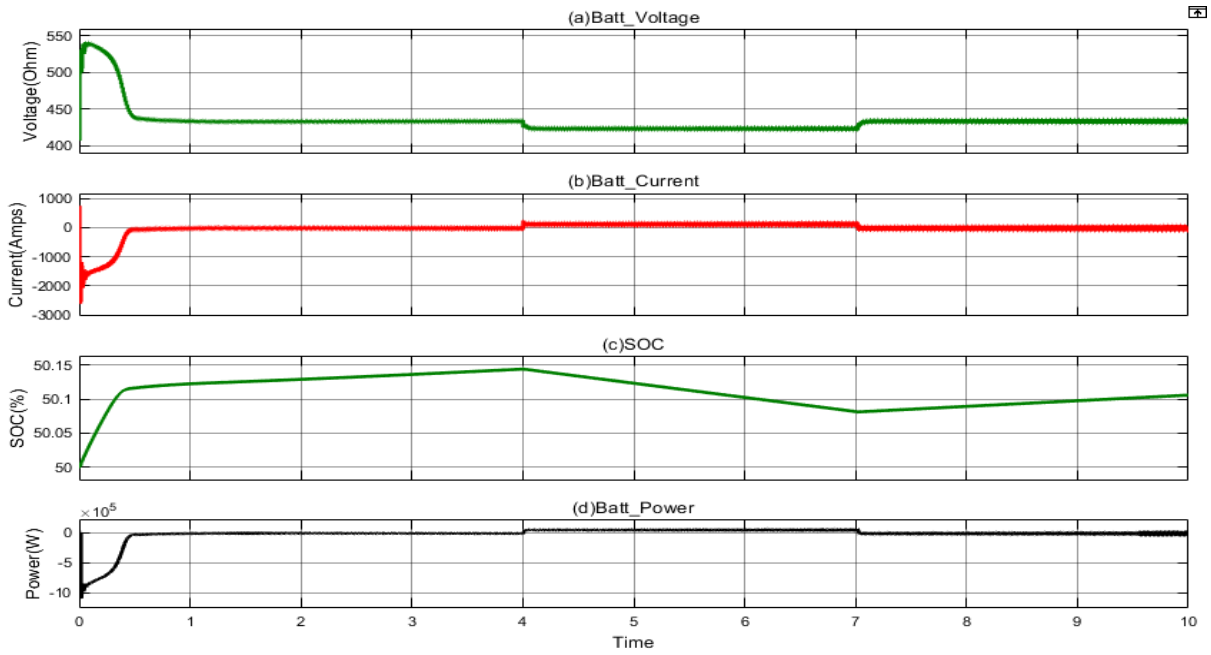
Figure 5-18: Battery Characteristics (a) Voltage, (b) Current, (c) SOC and (d) Power

The power to the load is kept constant at about 180.20kW depicted in figure 5.19(b) despite the fluctuation in PV power which leads to the decrease in the total power generated.
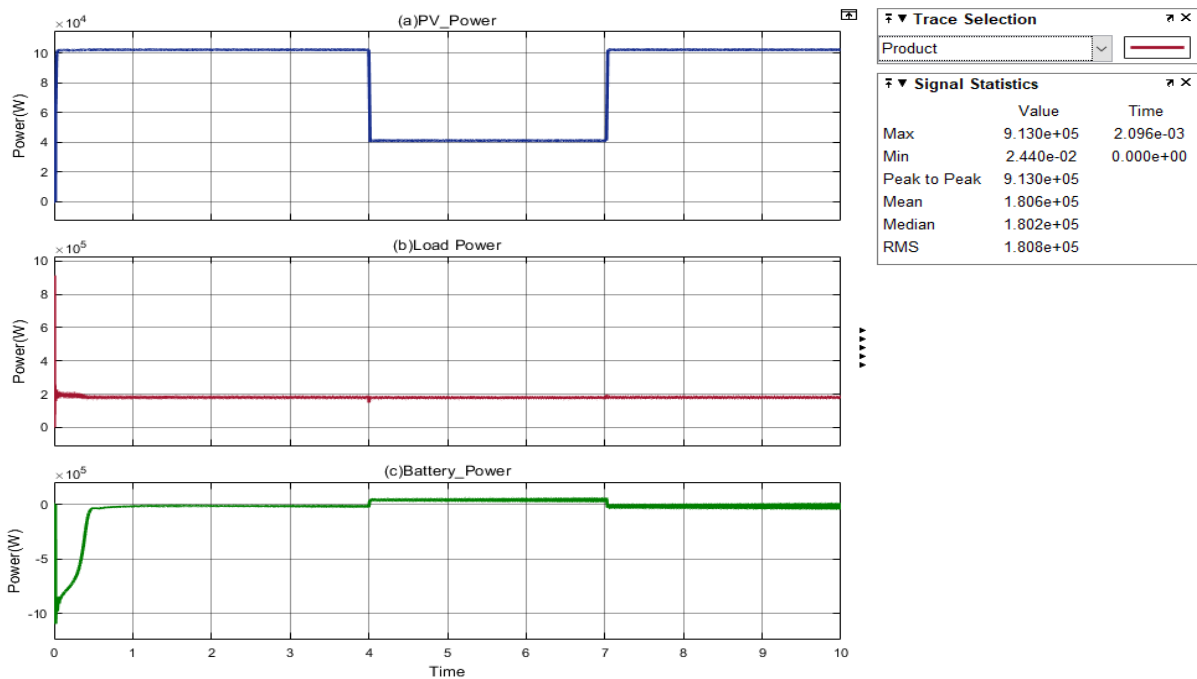
Figure 5-19: System (a) PV power (b) Load power (c) Battery power

Scenario 4

Energy storage has a high initial cost and shorter lifespan so it is critical to keep them in good condition to prevent overcharging and deep discharging. The last scenario is where irradiance is varied from 400W/m² to 600W/m² in both cases the PV power fluctuates between 41.22kW to 62.42kW. The total renewable power generated is around 149.40kW as depicted in figure 5.20(b) which below 180kW which is the demand. In instances where the SOC is more than 20%, the battery would dispatch power to meet the load but now it is 18% but it is not dispatching power to prevent deep discharge. In figure 5.20(c) and 5.20(d) illustrates that SOC stays constant and battery power is 0kW.
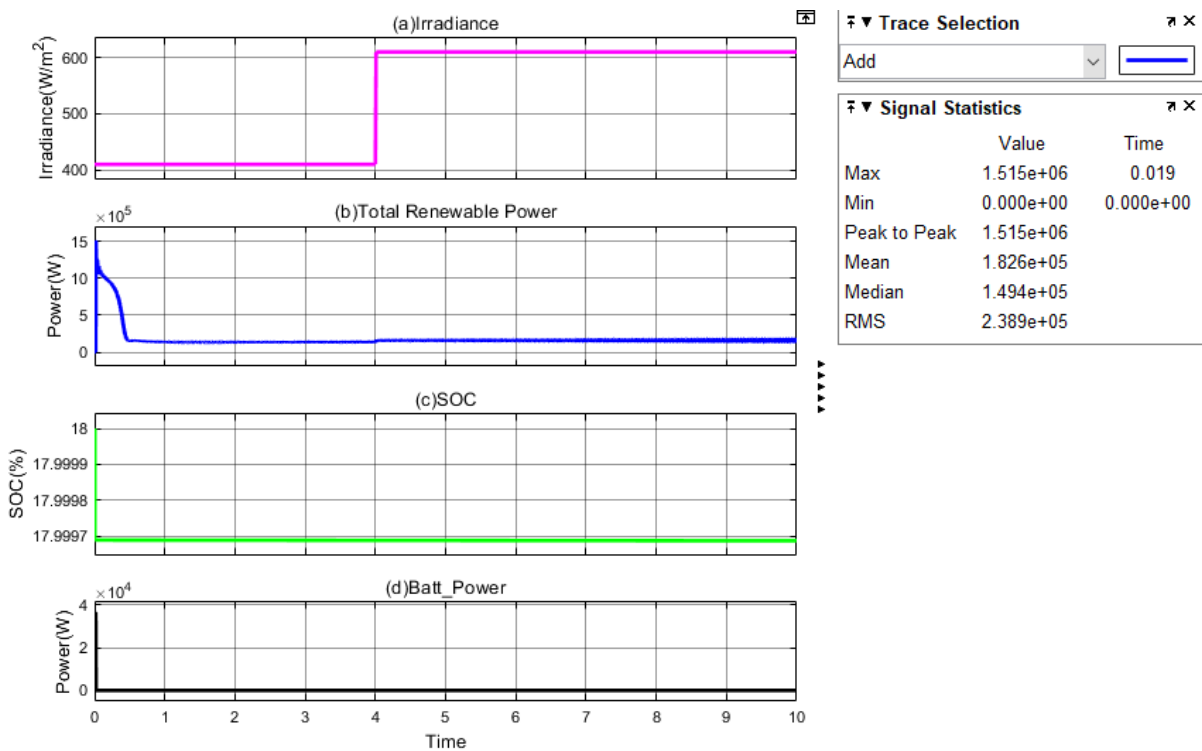
Figure 5-20: (a) Irradiance (b) Renewable power (c) SOC<20% and (d) Battery power

Figure 5.21(b) the generated power is more than the load requirement but the SOC is more than 80%. The battery system does not charge to prevent overcharging. The battery power remains 0kW in figure 5,21(d) and the SOC remains constant at 82% illustrated by figure 5.21(c). This is to keep the battery in good condition and prolong its lifespan.
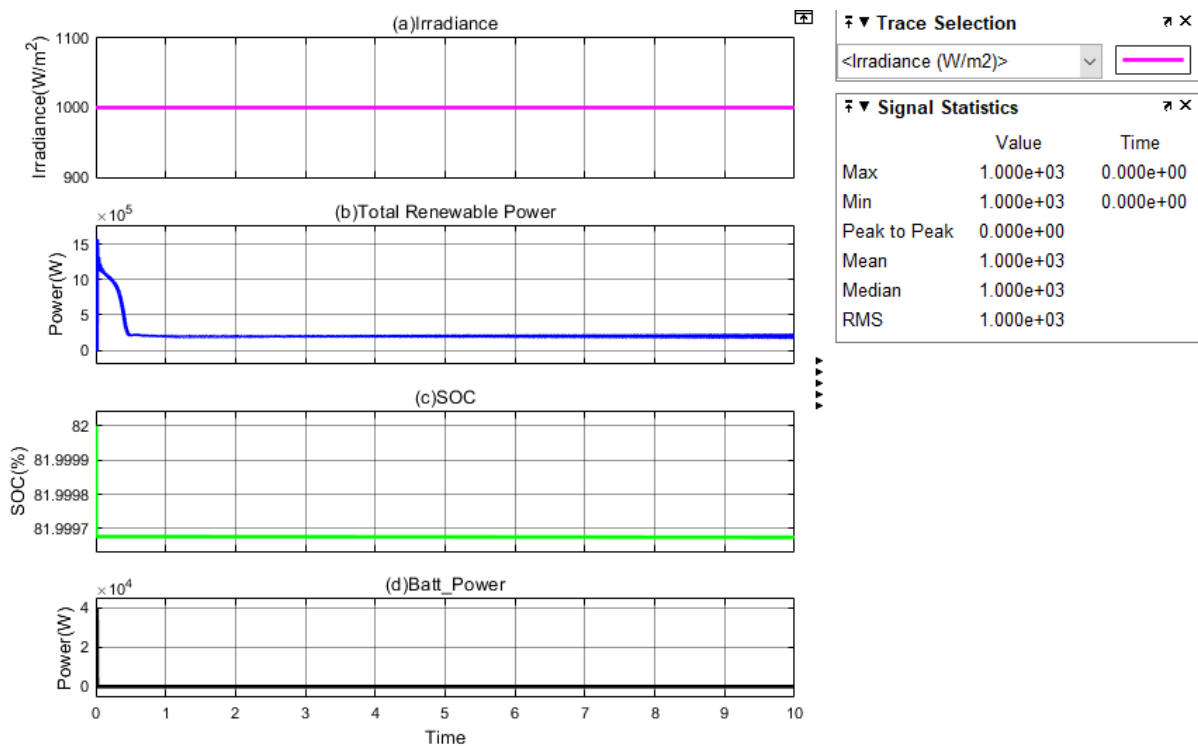
Figure 5-21:(a) Irradiance (b) Renewable power (c) SOC> 80% and (d) Battery power

5.4 Results Analysis

Firstly, the when comparing the power generated during the simulation and the calculated are all over 99% in terms of accuracy and how precise the system is as illustrated in table 5.1 below.

Table 5-1 : Accuracy of calculated power and voltage Vs Generated power and voltage from Matlab/Simulink

Sourcce	Calculated Power	Generated power from Matlab/Simulink	Accuracy(%)
PV	102.47 kW	102.20 kW	99.7
MHP	95.66 kW	96.18	99.4
PV Voltage	478.4 V_{dc}	476 V_{dc}	99.5

Secondly, the system perfoms very well in terms of stabilization of power where in PV system it takes only 15ms for power to stabilize.The MHP system takes a bit longer to stabilize which results from high mechanical torgue from ke kinetic energy on the turbine blades. This yields to exponential power being generated before the dumping by the governor becomes fully effective.It takes a total of 0.8s for MHP to reach steady state

Thirdly, the overall operation of the system with regards to energy management is very efficient and provides great results.The energy management employs fuzzy logic control mechanism to control whether the battery charges or discharges through a bi-directional converter.The input variable to the inference engine is the Error generated from power produced and the load, also from the SOC. . The inputs are applied to the set os IF/THEN control rule, then fuzzy outputs are summed into discrete values required to drive the control mechanism.

The output decides if the battery charges or discharges depending on the inputs or whether to neither charge nor discharge.In *scenario 1* the battery charges because more power is produced and the SOC is less than 80% as explained by the algorithm depicted on figure 4.31. The voltage at the AC bus is kept 235 V and on the DC bus is 750 V_{dc} after being boosted. *Scenarion 2* continous power is maintained to the load despite irradiance fluctuation and the battery dispatches 55.28 kW of power to compasate for the mismatch.

Scenario 3 is testing when the system is generating more power than the load then generated power drops after four seconds after irradiance fluctuation then suddenly more power is generated again.This shows by the charging hence the improving SOC for four seconds then SOC is reduced as battery is dispatching power then charges again after seven seconds as irradiance improves. The results means the energy management control in energy sharing.*Scenario 4* is focus on two extremes where SOC is beyond SOC_{max} and below SOC_{min} how the system will behave.The energy management control prevents the battery from over charging and from deep discharge.

Finally, its takes the battery bank 5ms to respond to any fluctuations so to mitigate the mismatch between the load and the supply.

5.5 Summary

This chapter discussed the operation of the designed model of a standalone hybrid microgrid. The energy management algorithm was developed to suit the research objectives. The system was implemented on Simulink and the results attained correlate with the calculated parameters from the design. The findings of the simulation with different scenarios to mimic real-life situations illustrate that an energy management system assists with power-sharing, protecting the battery from under and overcharging, and handling the load.

6   Chapter six: Conclusion and future work

6.1 Conclusion

The purpose of this research was to develop a hybrid microgrid system with backup energy storage for rural areas. The multitude of energy sources requires an energy management strategy so to mitigate any mismatch between supply and demand. This strategy also needs to keep the battery in good condition in terms of regulating the charging and discharging to prolong the lifespan. The system needs to cater to 180kW for 50 households. In this study, a hybrid microgrid system is proposed that comprises of a 100kW PV array, DC-DC boost converter, 95kW MHP system using the synchronous generator, excitation system, turbine, and a governor, a lithium-ion battery storage system, DC-DC bidirectional converter, and a three-phase inverter. The tussle with the renewable energy-based systems is the volatility of power supply hence the need for the energy management system. The robustness of the system is tested during different scenarios. The bidirectional converter is utilized to allow power in both directions either by charging or discharging the battery storage system. This is possible through the communication of renewable sources and the battery through signals to facilitate a quick response whether to operate on buck or boost mode. The system was based on the mathematical modelling of several components then assembled with an energy management strategy on Matlab/Simulink environment. In chapter 5 the robustness of the system is investigated using four different scenarios to check the capability of maintaining continuous power flow to the load. In the first scenario, the irradiance is kept at 1000Wm^2 and the PV power becomes 102.40kW. The MHP contributes around 96.18kW which yields 198.58kW however this is more than 180kW load demand. The battery then absorbs excess power produced by going to charging mode and the SOC increases from 50% to 50.19%. In the second scenario on contrary to the first scenario the irradiance is kept at 400W/m^2 and the combined power from the PV and the MHP is 123.60kW which is less than the 180kW demand. The drop in power is been sensed and the battery dispatches power amounting to 56.4kW(include battery power in results) to cater for the mismatch between supply and demand. The battery is now in discharging mode and the SOC decreases from 50% to 49.84% and the response to the change in irradiance is 0.01 of a second. The third scenario is where the irradiance is varied between 1000Wm^2 to 400W/m^2 then back to 1000W/m^2.In instances where the irradiance is at 1000W/m^2 for the first four seconds, the battery goes to charge mode since the power produced is more than the load, and SOC increases from 50% to 50.15%. The irradiance is then dropped to 400W/m^2 after four seconds to six seconds. The mismatch is sensed then the battery injects power into the system hence the positive current and the SOC decreases from 50.15% to 50.08%. The irradiance then goes back to 1000W/m^2 from seven seconds till ten seconds and the current becomes negative which signifies that the battery is in charging mode hence the SOC increases from 50.08% to 50.11%. Regulation of charging and discharging of the battery is pivotal in preserving the lifespan as energy storage

has a high capital cost. The mitigation of overcharging and discharging below the DOD reduces the lifespan of the battery. When the SOC is above 80% the battery will not charge to prevent overcharging even when there is more power generated and when the battery SOC is below 20% the battery will not discharge even when there is a deficit in power to supply the load. The scenarios prove that the energy management strategy employed is capable to protect the battery by controlling the charging and discharging. Furthermore, there is a continuous power flow to meet load demand even through the fluctuations in supply.

6.2 Future work

Several variables can not be all be tested using the model. To validate the precision of the system, hardware or a prototype needs to be built. The dump load would be beneficial if more power is produced and the SOC is more than 80% to absorb that excess power. The challenge in analysing microgrids with software simulations is they cannot test all interconnection issues. The real-time(RT) simulations have a great ability to validate complex control strategies and debugging them. Therefore, to validate the energy management strategy of the microgrid the RT simulation needs to be employed.

7 Bibliography

Abdulkadir, R. 2015. Modelling and Simulation of Micro Hydro Power Plant Using Matlab Simulink. , (January): 260–272.

Abu-sharkh, S., Arnold, R.J., Kohler, J., Li, R., Markvart, T., Ross, J.N., Steemers, K., Wilson, P. & Yao, R. 2006. Can microgrids make a major contribution to UK energy supply ? , 10: 78–127.

Acakpovi, A., Hagan, E. Ben & Fifatin, F.X. 2015. Review of Hydropower Plant Models Review of Hydropower Plant Models. , (December 2014).

Alramlawi, M., Gabash, A., Mohagheghi, E. & Li, P. 2018. Optimal operation of hybrid PV-battery system considering grid scheduled blackouts and battery lifetime. , 161(January): 125–137.

Amrollahi, M.H. & Bathaee, S.M.T. 2017. Techno-economic optimization of hybrid photovoltaic/wind generation together with energy storage system in a stand-alone micro-grid subjected to demand response. *Applied Energy*, 202: 66–77. http://dx.doi.org/10.1016/j.apenergy.2017.05.116.

Anderson, P.. & Fouad, A.. 2002. *Power system control and stability*. second. S. Kartalopoulos, ed. Hoboken: John Wiley & sons.

Anitha, M. & Krishma, R. 2015. A fuzzy logic based battery management system for a microgrid. *ARPN Journal of Engineering and Applied Sciences*, 10(6): 2663–2669. www.ijert.org 13 October 2020.

Ashraf, I. & Mallick, M.A. 2009. *Electrical Machines*. 1st ed. New-Delhi: I.K. International Publishing House.

Ayasun, S., L, U.G.E. & Sönmez, F. 2014. Computation of Stability Delay Margin of Time-Delayed Generator Excitation Control System with a Stabilizing Transformer. , 2014.

Badal, F.R., Das, P., Sarker, S.K. & Das, S.K. 2019. A survey on control issues in renewable energy integration and microgrid. *Protection and Control of Modern Power Systems*, 4(1). https://www.researchgate.net/publication/331951891_A_Survey_on_Control_Issues_in_Renewable_Energy_Integration_and_Microgrid 29 March 2020.

Battersby, S. 2019. The solar cell of the future. , 116(1): 7–10.

Bellini, E. 2017. South Africa ' s PV capacity reaches 1 . 47 GW , new PV installations for 2016 total 509 MW. *PV Magazine*: 1–7. https://www.pv-magazine.com/2017/03/17/south-africas-pv-capacity-reaches-1-47-gw-new-pv-installations-for-2016-total-509-mw/ 29 May 2020.

Bonthuys, G.J. 2016. *SMALL-SCALE HYDROPOWER DEVELOPMENT FOR RURAL ELECTRIFICATION IN SOUTH AFRICA © University of Pretoria SMALL-SCALE HYDROPOWER DEVELOPMENT FOR RURAL ELECTRIFICATION IN SOUTH AFRICA*. University of Pretoria.

Curley, M. 2014. *Financial Policy for Renewable Energy and a Sustainable Environment*. A. Ghassemi, ed. New York: Taylor & Francis.

Dijk, M. Van, Loots, I. & Barta, B. 2016. *ENERGY GENERATION USING LOW HEAD*. Pretoria. http://www.wrc.org.za/wp-content/uploads/mdocs/2219.pdf.

Eker, I. 2004. Governors for hydro-turbine speed control in power generation : a SIMO robust design approach. , 45: 2207–2221.

Eltawil, M.A. & Zhao, Z. 2013. MPPT techniques for photovoltaic applications. *Renewable and Sustainable Energy Reviews*, 25: 793–813. http://dx.doi.org/10.1016/j.rser.2013.05.022.

Fahad, M., Elbouchikhi, E. & Benbouzid, M. 2018. Microgrids energy management systems : A critical review on methods , solutions , and prospects. *Applied Energy*, 222(May): 1033–1055. https://doi.org/10.1016/j.apenergy.2018.04.103.

Fang, J., Tang, Y., Li, H. & Blaabjerg, F. 2018. The Role of Power Electronics in Future Low Inertia Power Systems. *Proceedings - 2018 IEEE International Power Electronics and Application Conference and Exposition, PEAC 2018*: 6–11.

García Vera, Y.E., Dufo-López, R. & Bernal-Agustín, J.L. 2019. Energy Management in Microgrids with Renewable Energy Sources: A Literature Review. *Applied Sciences*, 9(18): 3854. https://www.mdpi.com/2076-3417/9/18/3854 22 January 2021.

Ghorbani, N., Kasaeian, A., Toopshekan, A., Bahrami, L. & Maghami, A. 2017. Optimizing a Hybrid Wind-PV-Battery System Using GA-PSO and MOPSO for Reducing Cost and Increasing Reliability. *Energy*, 154: 581–591. http://linkinghub.elsevier.com/retrieve/pii/S036054421732090X.

Guan, Y., Vasquez, J.C., Guerrero, J.M., Wang, Y. & Feng, W. 2015. Frequency Stability of Hierarchically Controlled Hybrid Photovoltaic-Battery-Hydropower Microgrids. *IEEE Transactions on Industry Applications*, 51(6): 4729–4742.

Gulliver, J. & Arndt, R. 1991. *Hydropower Engineering Handbook.pdf*. New York: McGraw Hill.

Haruni, A.M.O. 2013. *A Stand-Alone Hybrid Power System with Energy Storage*. University of Tasmania. http://eprints.utas.edu.au/16746/ 11 September 2020.

Hirsch, A., Parag, Y. & Guerrero, J. 2018. Microgrids : A review of technologies , key drivers , and outstanding issues. *Renewable and Sustainable Energy Reviews*, 90(April): 402–411. https://doi.org/10.1016/j.rser.2018.03.040.

Iemsomboon, P., Pati, T. & Bhumkittipich, K. 2013. Performance study of micro hydro turbine and PV for electricity generator, case study: Bunnasopit school, Nan Province, Thailand. *Energy Procedia*, 34: 235–242.

iha. 2018. A brief history of hydropower. *international hydropower association*. https://www.hydropower.org/a-brief-history-of-hydropower 25 November 2018.

Jain, S. & Jain, P.K. 2017. The rise of Renewable Energy implementation in South Africa. In *Energy Procedia*. Elsevier Ltd: 721–726. www.sciencedirect.comAvailableonleatwww.sciencedirect.comwww.elsevier.com/locate/procedia1876-6102www.sciencedirect.comwww.elsevier.com/locate/procedia1876-6102 23 March 2021.

Jorde, K. & Hartmann, E. 2009. *Good & bad of Mini Hydropower*. Ritter.Roman, ed. Jakarta: Asean Center of Energy. https://energypedia.info/images/7/77/Good_and_bad_of_mini_hydro_power_vol.1.pdf.

Kabir, E., Kumar, P., Kumar, S., Adelodun, A.A. & Kim, K.H. 2018. Solar energy: Potential and future prospects. *Renewable and Sustainable Energy Reviews*, 82(October 2017): 894–900.

Kaddah, S.S., Abo-al-ez, K.M. & Diab, S.A. 2018. Performance Deviation of PV Water Pumping System under Different Ambient Factors. , (April).

Karimi, Z.M. 2014. *Modelling, implementation and performance analysis of a hybrid wind solar power generator with battery storage*. Universidade De Coimbra.

Kaunda, C.S., Kimambo, C.Z. & Nielsen, T.K. 2014. A technical discussion on microhydropower technology and its turbines. *Renewable and Sustainable Energy Reviews*, 35: 445–459. http://dx.doi.org/10.1016/j.rser.2014.04.035.

Keyhani, A. 2011. *Design of Smart Power Grid Renewable Energy Systems*. New Jerseey: John Wiley & sons.

Kilama, D. 2013. Review of small hydropower technology. *Renewable and Sustainable Energy Reviews*, 26: 515–520. http://dx.doi.org/10.1016/j.rser.2013.05.006.

Kilimo, A. & Kahn, M. 2012. *Innovative technigues of employing small hydropower plants in distributed electricity generation*. Cape Peninsula University of Technology.

kumar, R. & Singal, S.K. 2015. Operation and Maintenance Problems in Hydro Turbine Material in Small Hydro Power Plant. *Materials Today: Proceedings*, 2(4–5): 2323–2331. http://dx.doi.org/10.1016/j.matpr.2015.07.284.

Kundur, P. 1994. *power system stability and control*. N. Balu & M. Lauby, eds. Califonia: McGraw Hill.

Kunjumuhammed, L.P. 2013. A Power System Dynamic Simulation Program Using MATLAB / Simulink. : 111–118.

Kusakana, K. 2018. Optimal operation scheduling of grid-connected PV with ground pumped hydro storage system for cost reduction in small farming activities. *Journal of Energy Storage*, 16: 133–138. https://doi.org/10.1016/j.est.2018.01.007.

Longe, O.M., Ouahada, K., Ferreira, H.C. & Chinnappen, S. 2014. Renewable Energy Sources Microgrid Design for Rural Area in South Africa. *Innovative Smart Grid Technologies Conference (ISGT)*: 3–7. http://ieeexplore.ieee.org/document/6816378/.

Loots, I., Van Dijk, M., Barta, B., Van Vuuren, S.J. & Bhagwan, J.N. 2015. A review of low

head hydropower technologies and applications in a South African context. *Renewable and Sustainable Energy Reviews*, 50: 1254–1268.

Lopes, J., Madureira, A. & Moreira, C. 2013. A view of microgrids. , 2(February): 86–103.

Luta, D. 2019. *AN ENERGY MANAGEMENT SYSTEM FOR A HYBRID REVERSIBLE FUEL CELL/SUPERCAPACITOR IN A 100% RENEWABLE POWER SYSTEM by DOUDOU NANITAMO LUTA*. Cape Peninsula University of Technology. http://etd.cput.ac.za/bitstream/handle/20.500.11838/2925/Luta_Doudou_212123254.pdf ?sequence=1&isAllowed=y 16 August 2020.

Luta, D.N. & Raji, Atanda K. 2019. Comparing fuzzy rule-based MPPT techniques for fuel cell stack applications. *Energy Procedia*, 156: 177–182.

Luta, D.N. & Raji, Atanda Kamoru. 2019. Energy management system for a remote renewable fuel cell system. In *Proceedings of the 27th International Conference on the Domestic Use of Energy, DUE 2019*. Cape Town: 20–24. https://ieeexplore.ieee.org/stamp/stamp.jsp?tp=&arnumber=8734391 14 September 2020.

Mahmoudimehr, J. & Shabani, M. 2018. Optimal design of hybrid photovoltaic-hydroelectric standalone energy system for north and south of Iran. *Renewable Energy*, 115: 238–251. https://doi.org/10.1016/j.renene.2017.08.054.

Mariam, L., Basu, M. & Conlon, M.F. 2016. Microgrid: Architecture, policy and future trends. *Renewable and Sustainable Energy Reviews*, 64: 477–489.

Marzband, M., Sumper, A., Chindri\cs, M. & Tomoiag\ua, B. 2012. Energy Management System of hybrid MicroGrid with Energy Storage. In 635–642.

Máslo, K., Kasembe, A. & Kolcun, M. 2016. Simplification and unification of IEEE standard models for excitation systems. *Electric Power Systems Research*, 140: 132–138. http://dx.doi.org/10.1016/j.epsr.2016.06.030.

Mataifa, H. 2015. *Modeling and control of a dual -mode grid-intergrated renewable energy system*. Cape Peninsula University of Technology. http://etd.cput.ac.za/bitstream/20.500.11838/2190/1/210265922_Mataifa_H_MTech_Elec_Eng_2016.pdf 12 April 2021.

Messenger, R. & Ventre, J. 2004. *Photovoltaic System Engineering*. 2nd Editio. Boca Raton:CRC Press.

Mokveld, K. & Eije, S. 2018. *Final Energy report South Africa*. Pretoria. https://www.rvo.nl/sites/default/files/2019/01/Final-Energy-report-South-Africa.pdf.

Mortezapour, V. & Lesani, H. 2017. Hybrid AC/DC microgrids: A generalized approach for autonomous droop-based primary control in islanded operations. *International Journal of Electrical Power and Energy Systems*, 93: 109–118. http://dx.doi.org/10.1016/j.ijepes.2017.05.022.

Motapon, S., Louis-A, D. & Al-haddad, K. 2014. A comparative study of energy management schemes for fuel-cell hybrid emergency power system of more-electric aircraft. *IEEE Transactions on Industrial Electronics*, 61(3): 1320–1334. https://ieeexplore.ieee.org/stamp/stamp.jsp?tp=&arnumber=6494629 26 September 2020.

Moubayed, N., El-ali, A.L.I. & Outbib, R. 2014. A comparison of two MPPT techniques for PV system. , (December).

Moussavou, A. 2014. *MODELLING AND ANALYSIS OF MICROGRID CONTROL*. Cape Peninsula University of Technology. http://etd.cput.ac.za/bitstream/20.500.11838/1184/1/208216685_aminou_mtech_elec_eng_2014.pdf.

Muaelou, H., Abo-al-ez, K.M. & Badran, E.A. 2015. Control Design of Grid-Connected PV Systems for Power Factor Correction in Distribution Power Systems Using PSCAD. , (October).

Nababan, S., Muljadi, E. & Blaabjerg, F. 2012. An Overview of Power Topologies for Micro-hydro Turbines. , (June).

Nag, A.K. & Sarkar, S. 2018. Modeling of hybrid energy system for futuristic energy demand of an Indian rural area and their optimal and sensitivity analysis. *Renewable Energy*, 118: 477–488. https://doi.org/10.1016/j.renene.2017.11.047 1 October 2020.

Nasir, B.A. 2014. Design n Consid derations s Of Mic ric Powe er Plant. *Energy Procedia*,

50: 19–29. http://dx.doi.org/10.1016/j.egypro.2014.06.003.

Nazir, R., Laksono, H.D., Waldi, E.P., Ekaputra, E. & Coveria, P. 2014. Renewable energy sources optimization: A micro-grid model design. In *Energy Procedia*. 316–327. www.sciencedirect.com 20 January 2021.

Nihal, K. 2015. *Energy storage devices for electronic systems:Recharchable batteries and supercapacitors*. Chicago: academic press. https://library-books24x7-com.libproxy.cput.ac.za/toc.aspx?site=ML9MZ&bookid=77745.

Nwulu, N.I. & Xia, X. 2017. Optimal dispatch for a microgrid incorporating renewables and demand response. *Renewable Energy*, 101: 16–28. http://dx.doi.org/10.1016/j.renene.2016.08.026.

Okoye, C.O. & Solyalı, O. 2017. Optimal sizing of stand-alone photovoltaic systems in residential buildings. *Energy*, 126: 573–584.

Olabi, A.G. 2017. Renewable energy and energy storage systems. *Energy*, 136: 1–6. http://dx.doi.org/10.1016/j.energy.2017.07.054.

Olivier, C.K., Abo-al-ez, K.M. & Kahn, M.T. 2020. A Proposed Energy Management System (EMS) for a Residential Microgrid A Proposed Energy Management System (EMS) for a Residential Microgrid. , (November).

Øyvang, T., Hegglid, G.J., Øyvang, T., Øyvang, T. & Hegglid, G.J. 2018. ScienceDirect by Models Models of of synchronous with Models of synchronous. *IFAC-PapersOnLine*, 51(2): 91–96. https://doi.org/10.1016/j.ifacol.2018.03.016.

Parida, B., Iniyan, S. & Goic, R. 2011. A review of solar photovoltaic technologies. *Renewable and Sustainable Energy Reviews*, 15(3): 1625–1636. http://dx.doi.org/10.1016/j.rser.2010.11.032.

Patel, M.R. 1999. *Wind and Solar Power Systems*. Boca Raton: CRC Press.

Piagi, P. & Lasseter, R.H. 2006. Autonomous Control of Microgrids. *2006 IEEE Power Engineering Society General Meeting*: 8 pp.

Du Plooy, H. 2016. *Comparative strategies for efficient control and strorage of renewable energy in microgrid*. Cape Peninsula University of Technology. http://etd.cput.ac.za/handle/20.500.11838/2486.

Prakash, R., Meenakshipriya, P.B. & Kumaravelan, R. 2014. Modeling and Design of f MPPT Controller Using Stepped P & O Algorithm in Solar Photovoltaic System. , 8(3): 609–615.

Rai, N. & Rai, B. 2018. Control of fuzzy logic based PV-battery hybrid system for stand-alone DC applications. *Journal of Electrical Systems and Information Technology*, 5(2): 135–143.

Ribeiro, P.F., Member, S., Johnson, B.K., Crow, M.L., Member, S., Arsoy, A., Liu, Y. & Member, S. 2001. Energy Storage Systems for Advanced Power Applications. *Proceedings of the IEEE*, 89(12): 1744–1756.

Roumila, Z., Rekioua, D. & Rekioua, T. 2017. Energy management based fuzzy logic controller of hybrid system wind/photovoltaic/diesel with storage battery. *International Journal of Hydrogen Energy*, 42(30): 19525–19535.

Rousselot, Y. 2015. Upstream Flows of Water: from the Lesotho Highlands to Metropolitan South Africa. *Revue de géographie alpine*, (103–3): 0–16.

Sangal, S., Garg, A. & Kumar, D. 2013. Review of Optimal Selection of Turbines for Hydroelectric Projects. *International journal of emerging technology and advanced engineering*, 3(3): 424–430.

Signal, R.., Signal, M. & Signal, R. 2010. *Hydraulic Machines*. New-Delhi: I.K. International Publishing House.

Singh, G.K. 2013. Solar power generation by PV (photovoltaic) technology : A review. *Energy*, 53: 1–13. http://dx.doi.org/10.1016/j.energy.2013.02.057.

SOLARGIS. 2019. Solar resource maps and GIS data for 180+ countries | Solargis. *Solargis*: All. https://solargis.com/maps-and-gis-data/download/south-africa 29 May 2020.

Spalding-Fecher, R., Senatla, M., Yamba, F., Lukwesa, B., Himunzowa, G., Heaps, C., Chapman, A., Mahumane, G., Tembo, B. & Nyambe, I. 2017. Electricity supply and demand scenarios for the Southern African power pool. *Energy Policy*, 101(December 2015): 403–414. http://dx.doi.org/10.1016/j.enpol.2016.10.033.

Sultan, R.A. 2016. *Renewable Micro Hydro Power Generation*. Military Institute of Science

and Technology.

Sumathi, S., Kumar, L. & Surekha, P. 2015. *Solar PV and Wind Energy Conversion Systems*. Cham: Springer.

Tapia, A., Millán, P. & Gómez-Estern, F. 2018. Integer programming to optimize Micro-Hydro Power Plants for generic river profiles. *Renewable Energy*, 126: 905–914.

Tephiruk, N., Kanokbannakorn, W., Kerdphol, T., Mitani, Y. & Hongesombut, K. 2018. Fuzzy logic control of a battery energy storage system for stability improvement in an islanded microgrid. *Sustainability (Switzerland)*, 10(5): 1–16.

Transport, M., Yaakob, O., Ahmed, Y.M. & Ismail, M.A. 2015. Jurnal Teknologi Hydro Power and Turbine Systems Reviews. , (May).

Tu, C., Xiao, F., Guo, Q. & Lan, Z. 2018. High Voltage Quality Control Strategy of Microgrid Main Inverter for Islanded Microgrid. In *2018 IEEE International Power Electronics and Application Conference and Exposition (PEAC)*. Shenzhen. https://ieeexplore-ieee-org.libproxy.cput.ac.za/stamp/stamp.jsp?tp=&arnumber=8590352 31 March 2021.

Tuballa, M.L. & Abundo, M.L. 2016. A review of the development of Smart Grid technologies. *Renewable and Sustainable Energy Reviews*, 59: 710–725. http://dx.doi.org/10.1016/j.rser.2016.01.011.

Tucci, M. & Ferrari-trecate, G. 2017. ScienceDirect and frequency control in AC Voltage and frequency control in AC a scalable , Voltage and microgrids : *IFAC-PapersOnLine*, 50(1): 13922–13927. https://doi.org/10.1016/j.ifacol.2017.08.2212.

Upadhyay, A. 2012. *Fluid Mchanics*. second. New-Delhi: S.K. Kataria & Sons.

USAID. 2018. South Africa, Power Africa fact shhet. https://www.usaid.gov/powerafrica/south-africa 1 December 2019.

USBR. 2005. Managing Water in the West; Hydroelectric Power. https://www.usbr.gov/power/edu/pamphlet.pdf 21 March 2019.

Vandoorn, T.L., Renders, B., Degroote, L., Meersman, B. & Vandevelde, L. 2010. Voltage Control in Islanded Microgrids by means of a Linear-Quadratic Regulator. , (March).

Varughese, A. & Michael, P.A. 2013. Electrical Characteristics of Micro-Hydro Power Plant Proposed in Valara Waterfall. , (2): 128–131.

Vera, Y.E.G., Dufo-López, R. & Bernal-Agustín, J.L. 2019. Energy management in microgrids with renewable energy sources: A literature review. *Applied Sciences (Switzerland)*, 9(18).

de Villiers, D.. 2009. *Hybrid Energy Harvesting System for a Condition Monitoring Mote*. Cape Peninsula University of Technology.

Vosloo, A. & Raji, K.A. 2015. Intelligent central energy management system for remote community microgrid. *Proceedings of the 23rd Conference on the Domestic Use of Energy, DUE 2015*: 137–140.

Wang, W. & Lu, Z. 2013. Cyber security in the Smart Grid : Survey and challenges q. *Computer Networks*, 57(5): 1344–1371. http://dx.doi.org/10.1016/j.comnet.2012.12.017.

Wang, Y.-X., Qin, F.-F. & Kim, T. 2014. Bidirectional DC-DC converter design and implementation for lithium-ion battery application. In *2014 IEEE PES Asia-Pacific Power and Energy Engineering Conference (APPEEC)*. Hong Kong: IEEE. https://ieeexplore.ieee.org/stamp/stamp.jsp?tp=&arnumber=7066140 26 September 2020.

Xu, B., Chen, D., Venkateshkumar, M., Xiao, Y., Yue, Y., Xing, Y. & Li, P. 2019. Modeling a pumped storage hydropower integrated to a hybrid power system with solar-wind power and its stability analysis. *Applied Energy*, 248: 446–462. https://doi.org/10.1016/j.apenergy.2019.04.125 29 July 2020.

Yildiz, V. & Vrugt, J.A. 2019. Environmental Modelling & Software A toolbox for the optimal design of run-of-river hydropower plants. *Environmental Modelling and Software*, 111(August 2018): 134–152. https://doi.org/10.1016/j.envsoft.2018.08.018.

Zanarini, S. & Ragazzini, G.L. 2005. *HYBRID PV – DIESEL POWER GENERATOR : DESIGN CRITERIA AND PRELIMINARY PERFORMANCE ANALYSIS Sergio Zanarini, Gian Luca Ragazzini*. IFAC. http://dx.doi.org/10.3182/20050703-6-CZ-1902.01795.